Michigan State
University

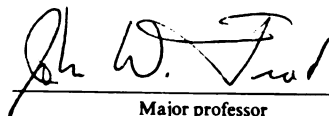This is to certify that the

dissertation entitled

MANIPULATION OF THE GENES AND ENZYMES OF THE

SHIKIMATE PATHWAY

presented by

Sunil S. Chandran

has been accepted towards fulfillment
of the requirements for

_____Ph.D.____ degree in __CHEMISTRY__

_____
Major professor

Date_January 11, 2001_

0-12771

PLACE IN RETURN BOX to remove this checkout from your record.
TO AVOID FINES return on or before date due.
MAY BE RECALLED with earlier due date if requested.

DATE DUE	DATE DUE	DATE DUE

MANIPULATION OF THE GENES AND ENZYMES OF THE

SHIKIMATE PATHWAY

By

Sunil S. Chandran

A DISSERTATION

Submitted to
Michigan State University
in partial fulfillment of the requirements
for the degree of

DOCTOR OF PHILOSOPHY

Department of Chemistry

2000

The

vitamins ha

disposition

diverse ran

manipulate

shikimate p

providing a

prime candi

been atten

Protocatech

element of

allowed ex

DHQ synth

the Zn^{2+} a

attesting to

On

for the mi

ABSTRACT

MANIPULATION OF THE GENES AND ENZYMES OF THE

SHIKIMATE PATHWAY

By

Sunil S. Chandran

The shikimate pathway for the biosynthesis of aromatic amino acids and aromatic vitamins has been the target of intensive research over the last decade. Its central disposition in the life-cycle of a microbial or plant cell has been well established. The diverse range of enzymes and genes responsible for each step in this pathway can be manipulated to suit various purposes. For example, one or more enzymes in the shikimate pathway can be inhibited to render the cell unable to sustain growth, thereby providing an option for antibiotic or herbicidal design. The enzyme DHQ synthase is a prime candidate for this purpose. In the present study, inhibition of DHQ synthase has been attempted by taking advantage of the metal co-factor in the active site. Protocatechuic acid, catechol, and derivatives of these aromatics, sharing the common element of an *ortho* dihydroxylated benzene ring were synthesized. These molecules allowed examination of the role that the metal co-factor plays in the binding properties of DHQ synthase. The results indicated marked differences in binding properties between the Zn^{+2} and Co^{+2} metalloforms of DHQ synthase. These inhibitors provided evidence attesting to the important role that the active site metal played in substrate binding.

On the other hand, instead of inhibiting the shikimate pathway, it can be exploited for the microbial synthesis of industrially applicable chemicals. A major portion of this

thesis inve

shikimic ac

synthetic se

fermentatio

limiting fa

alleviated.

glucose upt

in 27% yield

Atte

formation d

fermentation

most likely

instrumental

thesis investigates the development of a biocatalytic process for the production of shikimic acid, which has recently emerged as a suitable starting material for a number of synthetic schemes. Synthesis of shikimic acid was successfully achieved under fed-batch fermentation conditions, utilizing various recombinant *Escherichia coli* biocatalysts. The limiting factors for obtaining high shikimic acid titers and yields were identified and alleviated. Accounting for low intracellular E4P concentration and loss of PEP due to glucose uptake, proved to be key determinants. Shikimic acid titer of 71 g/L was realized in 27% yield.

Attempts were also made at understanding the mechanism of quinic acid formation during microbial synthesis of shikimic acid. Uptake of shikimic acid from the fermentation broth followed by its in vivo processing to quinic acid was shown to be the most likely source of the contamination. Identifying this role of shikimate uptake was instrumental in developing methods designed to eliminate production of quinic acid.

To my family

For their love and support

The

guidance.

have learn

aggressive

addition. I

Maleczka.

the prepara

I ar

stages in n

which she

gratitude t

Montcham

Satyamahe

Bannon. M

I am fortun

Padmesh V

Las

parents anc

me under a

thesis is de

ACKNOWLEDGMENTS

TABLE OF CONTENTS

BIBLIOG

LIST OF TABLES

LIST OF FIGURES

Ac

ADP

AMP

Ap

ATP

bp

Bu

Cl

ClAP

Cm

COMT

DAH

DAHP

DCU

DEAE

DHQ

DHS

DO

DTT

El

E4p

LIST OF ABBREVIATIONS

Ac	acetyl
ADP	adenosine diphosphate
AMP	adenosine monophosphate
Ap	ampicillin
ATP	adenosine triphosphate
bp	base pair
Bu	butyl
CI	chemical ionization
CIAP	calf intestinal alkaline phosphatase
Cm	chloramphenicol
COMT	catechol-*O*-methyltransferase
DAH	3-deoxy-D-*arabino*-heptulosonic acid
DAHP	3-deoxy-D-*arabino*-heptulosonic acid 7- phosphate
DCU	digital control unit
DEAE	diethylaminoethyl
DHQ	3-dehydroquinate
DHS	3-dehydroshikimic acid
DO	dissolved oxygen
DTT	dithiothreitol
EI	electron impact
E4P	D-erythrose 4-phosphate

EPSP

FAB

FBR

FT

GA

Glu

h

His

HMPA

HRMS

Kan

K_i

K_m

k

kg

LB

M

Me

MGP

MIC

mL

mM

MOPS

EPSP	5-enolpyruvylshikimate 3-phosphate
FAB	fast atom bombardment
FBR	feed back resistant
FT	fourier transform
GA	gallic acid
Glu	glutamate
h	hour
His	histidine
HMPA	hexamethyl phosphoramide
HRMS	high resolution mass spectrometry
Kan	kanamycin
K_i	inhibition constant
K_m	Michaelis constant
k	rate constant
kg	kilogram
LB	luria broth
M	molar
Me	methyl
MGP	methyl α-D-glucopyranoside
MIC	minimal inhibitory concentration
mL	milliliter
mM	millimolar
MOPS	4-morpholinepropanesulfonic acid

MS

min

NAD

NADH

NADP

NMR

OD

PABA

PCA

PEG

PEP

Ph

PHB

PID

PCR

ppm

Pps

iPr

PTS

QA

π

rpm

SA

MS	mass spectrometry
min	minute
NAD	nicotinamide adenine dinucleotide, oxidized form
NADH	nicotinamide adenine dinucleotide, reduced form
NADP	nicotinamide adenine dinucleotide phosphate, oxidized form
NMR	nuclear magnetic resonance
OD	optical density
PABA	*p*-aminobenzoic acid
PCA	protocatechuic aid
PEG	polyethylene glycol
PEP	phosphoenolpyruvate
Ph	phenyl
PHB	*p*-hydroxybenzoic acid
PID	proportional-integral-derivative
PCR	polymerase chain reaction
ppm	parts per million
Pps	PEP synthase
*i*Pr	isopropyl
PTS	phosphotransferase system
QA	quinic acid
rt	room temperature
rpm	revolutions per minute
SA	shikimic acid

SDS

Tc

THF

TMS

TSP

UV

SDS	sodium dodecyl sulfate
Tc	tetracycline
THF	tetrahydrofuran
TMS	trimethylsilyl
TSP	sodium 3-(trimethylsilyl)propionic-2,2,3,3-d_4
UV	ultraviolet

Th

the shikir

microorg

understan

exploitatio

in the me

antimicrob

the other h

relevant c

studying b

The

rampant en

and more

This can be

drug desig

enzyme be

The secon

enzymes.

nicotinami

NADzym

CHAPTER 1

INTRODUCTION

The common pathway for aromatic amino acid biosynthesis, also referred to as the shikimate pathway, is a vital metabolic cascade of events found in plants and microorganisms. Researchers have for long studied this pathway, gaining a better understanding of each enzyme catalyzed reaction. This understanding allowed exploitation of the common pathway to suit a variety of purposes. Given its central role in the metabolism of a cell, scientists have been successful at obtaining potent antimicrobial activity by inhibition of one or more enzymes in this metabolic route. On the other hand, the common pathway has also been manipulated to produce industrially relevant chemicals at a low cost. The work reported in this thesis is an attempt at studying both aspects of the shikimate pathway.

The medical profession is currently facing a formidable adversary with the rampant emergence of antibiotic resistant bacteria. The search is underway to design new and more potent drugs that can combat microbes impervious to present day treatment. This can be achieved by targeting a pathway hitherto underutilized as a possible target for drug design, the shikimate pathway. Chapter 2 of this thesis discusses inhibition of one enzyme belonging to the common pathway, namely 3-dehydroquinate (DHQ) synthase.[1] The second enzyme in this pathway, DHQ synthase belongs to a small, unique family of enzymes. The uniqueness of the enzymes in this family is their catalytic utilization of nicotinamide adenine dinucleotide (NAD).[2] Enzymes in this class, which we will label as NADzymes, also include *myo*-inositol 1-phosphate (MIP) synthase,[3]

S-adenos

diphospha

convenie

investiga

be centere

the active

Th

resulting i

gallic aci

common

describes

The focus

(QA) and

both studie

Th

the biosy

seven enz

(Figure 1

L-phenyl

aromatic

various i

S–adenosylhomocysteine hydrolase,[4] *S*-ribosylhomocysteine hydrolase,[5] and uridine diphosphate galactose 4-epimerase.[6] The catalytic role of NAD has been used as a very convenient tool to achieve inhibition of DHQ synthase in the past. The current investigation will also utilize this aspect of inhibition. However, the major emphasis will be centered around trying to better understand the role that the metal co-factor, present in the active site, plays in binding to substrate and inhibitors.

The shikimate pathway has been a target for metabolic engineering in the past, resulting in strains capable of producing chemicals like 3-dehydroshikimic acid (DHS), gallic acid, vanillin, etc. A major portion of this thesis deals with manipulation of the common pathway in order to biocatalytically produce shikimic acid (SA). Chapter 3 describes studies undertaken to improve the overall titer and yield of SA from D-glucose. The focus of Chapter 4 is on efforts made to better understand the source of quinic acid (QA) and DHS contamination commonly seen in SA fermentations. Results arising from both studies will ultimately result in a more efficient SA producing biocatalyst.

The Shikimate Pathway

The shikimate pathway present in plants and microorganisms is responsible for the biosynthesis of the aromatic amino acids and aromatic vitamins.[7] It is made up of seven enzyme-catalyzed reactions culminating into the biosynthesis of chorismic acid (Figure 1). Chorismic acid is processed further into L-tryptophan, L-tyrosine and L-phenylalanine by three terminal pathways. Besides providing a metabolic route to the aromatic amino acids, the common pathway also provides a means of synthesis of the various isoprenoid quinones, the folic acid family of co-enzymes and enterochelin, via

pathways

lies in el

involved

iron sequ

T

(PEP) wi

acid 7-ph

(Figure 1)

feedback i

aroH enc

isozymes

encoded D

reaction c

reduction

the *aroE*

shikimate

3-phospha

aroK ge

5-enolpyr

synthase.

chorismat

chorismic

pathways branching out from chorismic acid.[7] The primary role of the quinone family lies in electron transport while co-enzymes derived from folic acid are known to be involved in the biosynthetic transfer of one carbon fragments. Enterochelin acts as an iron sequestering agent involved in iron uptake in microorganisms.

The first reaction in the pathway is the condensation of phosphoenolpyruvate (PEP) with D-erythrose 4-phosphate (E4P) resulting in 3-deoxy-D-*arabino*-heptulosonic acid 7-phosphate (DAHP), a reaction catalyzed by the enzyme DAHP synthase (Figure 1).[7] Three isozymes of DAHP synthase exist in *Escherichia coli*, each of them feedback inhibited by one of the three aromatic amino acids. The genes *aroF*, *aroG*, and *aroH* encode the tyrosine-sensitive, phenylalanine-sensitive, and tryptophan-sensitive isozymes of DAHP synthase respectively. DAHP is then converted to DHQ by *aroB*-encoded DHQ synthase. Elimination of a water molecule from DHQ results in DHS, a reaction catalyzed by the *aroD*-encoded enzyme, DHQ dehydratase.[8] Subsequent reduction of DHS by shikimate dehydrogenase affords SA. The enzyme is encoded by the *aroE* gene and it utilizes NADPH to carry out the reaction.[9] Two isozymes of shikimate kinase catalyze the ATP aided phosphorylation of SA to generate shikimate 3-phosphate. The two isozymes of shikimate kinase are encoded by the *aroL*[10] and *aroK*[11] genes. Condensation of shikimate 3-phosphate with PEP to produce 5-enolpyruvylshikimate 3-phosphate (EPSP) is catalyzed by *aroA*-encoded EPSP synthase.[12] The final step in the common pathway is catalyzed by *aroC*-encoded chorismate synthase and involves loss of inorganic phosphate from EPSP resulting in chorismic acid.[13]

CO.

O

OH

DHS

H_2O_3PO''
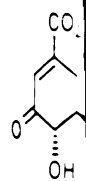
ubiquinon
folic acid

Figure 1.

biosynthe

Genetic lo
aroD. DH
aroA. EPS

Figure 1. The common pathway of aromatic amino acid and aromatic vitamin biosynthesis.

Genetic loci are as follows: *aroF aroG aroH*, DAHP synthase; *aroB*, DHQ synthase; *aroD*, DHQ dehydratase; *aroE*, shikimate dehydrogenase; *aroL aroK*, shikimate kinase; *aroA*, EPSP synthase; *aroC*, chorismate synthase.

<u>Deraili</u>

Di{

and micr{

demonstra

type cells

microbes

necessary

mammalia

DHQ synt

implicatior

against bac

mutations

models as

immune sy

An

availabili

fluoroshik

p-aminobe

against a r

to a numb

could be r

other arom

Derailing the Shikimate Pathway: A Viable Option for Herbicidal and Antimicrobial Agents

Disruption of the shikimate pathway has been proven to be detrimental to plants and microorganisms. Microbes with a disrupted common pathway have been demonstrated to be characterized by severely attenuated growth in comparison to wild type cells when introduced into a mammalian system.[14] This result indicated that microbes deficient in a functional common pathway have a difficult time scavenging the necessary aromatic amino acids and vitamins from the rich growth environment of a mammalian system. More recently, researchers also demonstrated that *aroB* encoded DHQ synthase was required for microbial pathogen virulence.[15] Understanding the implications of this huge body of work has ramifications in terms of developing vaccines against bacterial infections. Live, attenuated strains of *Salmonella typhimurium* carrying mutations in *aroB*[15], *aroD*[14b,16a], *aroA*[16b,c], and *aroC*[14a,b] have been introduced into mouse models as potential vaccines. The effect of the attenuated strains was to stimulate the immune system towards infection caused by the wild type parent strain.

Among all the aromatic amino acids and aromatic vitamins, it appears that availability of *p*-aminobenzoic acid is most critical. The compound (6*S*)-6-fluoroshikimic acid is a potent antimicrobial agent, deriving its activity from inhibition of *p*-aminobenzoic acid biosynthesis.[17] It possesses an MIC value of less than $1 \mu g$ mL^{-1} against a range of bacteria. Mice injected with (6*S*)-6-fluoroSA also exhibited immunity to a number of bacterial infections. However, in vitro inhibition of bacterial growth could be reversed by supplementation with *p*-aminobenzoic acid, but not with any of the other aromatic amino acids or aromatic vitamins.

Figure 2.

P₃

result in [

glyphosat

attributed

in 1998.

Apicompl

effective

falciparu

'severe c

resistant

at a diffe

by either

that cou

combina

enzyme

benefit.

amino a

$$CO_2H$$

(6S)-6-fluoroshikimic acid   **glyphosate**
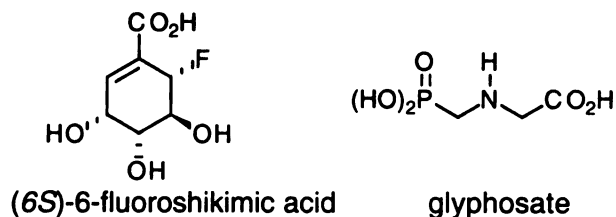
Figure 2. Compounds proven to disrupt the common pathway.

Perhaps the best example to prove that inhibition of the shikimate pathway can result in potent biological activity is the herbicide glyphosate. Marketed as Roundup®, glyphosate is a postemergence, non-selective, broad spectrum herbicide.[18] Its activity is attributed to competitive inhibition of EPSP synthase. An important discovery was made in 1998, indicating the presence of a functional common pathway in the phylum *Apicomplexa*.[19] Agents capable of blocking the common pathway should therefore be effective against parasites belonging to this family which include, *Plasmodium falciparum* (malaria), *Toxoplasma gondii* (toxoplasmosis), and *Cryptosporidium parvum* (severe diarrhea). In fact, glyphosate proved effective against malaria strains that were resistant to an anti-malarial medicine, pyrimethamine, which interrupts folate processing at a different point. But mice injected with lethal doses of *T. gondii* could not be rescued by either glyphosate or pyrimethamine. However, doses of glyphosate or pyrimethamine that could not protect the mice when used alone, rescued infected mice when used in combination even when the mice were allowed to eat diets with folate.

This emphasized the viability of concomitantly targeting either single or multiple enzymes along the common pathway with the goal of deriving medical and commercial benefit. Mammals lack a functional shikimate pathway and rely on their diet for aromatic amino acids and aromatic vitamins. Hence, using herbicides and antimicrobial agents

based on

With th:

understar

3-

catalyzir

carbocyc

acids and

^-O_2C 2

OH

^-O_2C

OH
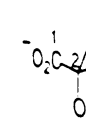
Figure 3

T

DAHP u

oxidatio

inorgani

based on disruption of the shikimate pathway will have minimal side effects on humans. With this aim in mind, it would be of considerable importance to gain a better understanding of the enzymes in this pathway.

Inhibition Studies of DHQ synthase

3-dehydroquinate synthase is the second enzyme of the shikimate pathway catalyzing the conversion of DAHP to DHQ. This step sets into place the six membered carbocyclic unit which will ultimately form the benzenoid portion of the aromatic amino acids and the secondary metabolites derived from the common pathway.
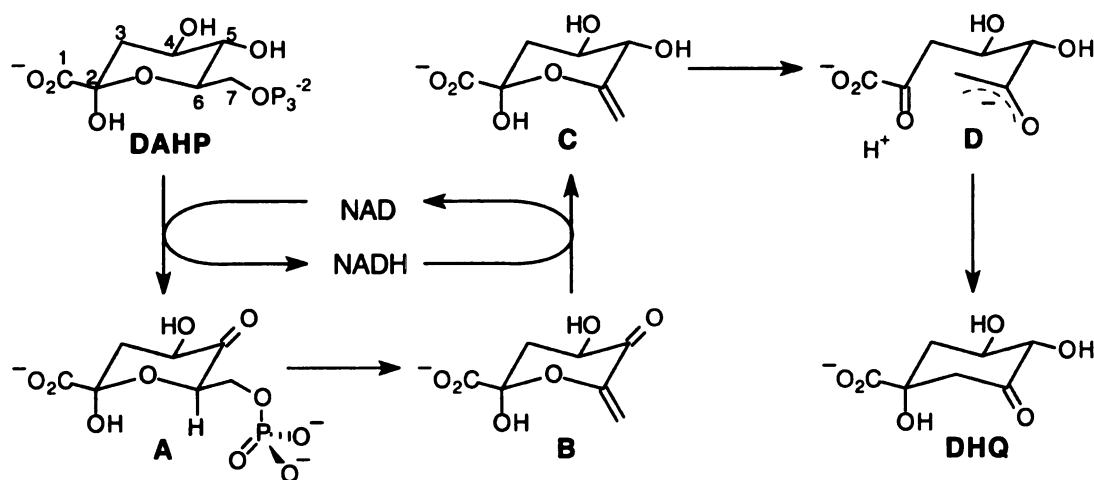
Figure 3. Proposed mechanism of DHQ synthase.

The mechanism[20] for DHQ synthase begins with oxidation of the C-5 alcohol of DAHP utilizing enzyme-bound NAD, resulting in intermediate **A** and NADH. This oxidation results in acidification of the C-6 proton facilitating easy elimination of inorganic phosphate and formation of the enol ether intermediate **B**. Reduction of the

ketone a

NAD. th

unmaski

condens

E

stoichio

catalyze

releases

catalytic

to oxidat

bound tc

is redox

80 nM.

metalloe

absorptic

monome

E

isotope

during t

positions

rate limi

enzyme:

consisten

ketone at C-5 by enzyme-bound NADH results in intermediate **C** and regeneration of NAD, thereby completing the redox cycle. Ring opening of intermediate **C** results in unmasking of the C-2 carbonyl in intermediate **D**, setting it up for an intramolecular aldol condensation to afford DHQ.

Enzymes utilizing NAD as a co-factor in their catalytic cycle normally use it stoichiometrically in the form of a co-substrate. The enzyme binds to the co-factor, catalyzes the oxidation of substrate with concomitant reduction of NAD, and finally releases the product and NAD. DHQ synthase on the other hand utilizes NAD catalytically implying that the initial reduction of enzyme-bound NAD is always coupled to oxidation of the NADH back to NAD during a single turnover. The NAD always stays bound to the enzyme during its lifetime and the overall enzyme catalyzed transformation is redox neutral. DHQ synthase binds to 1 equivalent of NAD with an apparent K_m of 80 nM, the low value reflecting the efficiency of binding.[20a] DHQ synthase is a metalloenzyme requiring either Zn^{+2} or Co^{+2} for its catalytic activity.[20a] Atomic absorption analysis demonstrated that the enzyme requires one divalent metal cation per monomer for activity.[20a]

Evidence for the mechanism (Figure 3) came from several observations : (1) isotope exchange experiments[20b] proved that the C-6 proton was lost to the medium during turnover; (2) kinetic isotope effects[20b,c] were observed at the C-5 and C-6 positions, indicating that NAD oxidation of C-5 and elimination of phosphate at C-6 were rate limiting; (3) NAD was indispensable for maintaining stability and activity of the enzyme;[1,20b,d] (4) a trapping experiment[20d] with tritiated sodium borohydride gave results consistent with formation of a keto group at the C-5 position.

E

synthase

phospha

condens

own elin

indicated

the last tv

to regard

obtained

A

DHQ syr

the activ

the role

absence

did inde

binding

C-6 pro

the C-

mecha

errone

Earlier mechanistic studies led to some suspicion to fall on the role that DHQ synthase played in catalyzing some of the steps in the conversion, especially the phosphate elimination[21a,b,c] and the ring opening followed by intramolecular aldol condensation.[21d] Several results suggested that the phosphate monoester catalyzed its own elimination with the enzyme being a mere spectator. Certain experiments also indicated that DHQ synthase only served as a template to control the stereochemistry of the last two steps, but not to catalyze them. It was therefore considered more appropriate to regard DHQ synthase as a simple oxidoreductase.[21b] However, results were also obtained consistent with theories contradictory to those stated above.[22]

All controversies were put to rest with the elucidation of the crystal structure of DHQ synthase from *Aspergillus nidulans*.[23] A close analysis of the interactions between the active site residues and the substrate analogue carbaphosphonate, served to resolve the role that DHQ synthase played in every step of the catalysis. For example, the absence of basic residues in the vicinity of the C-6 confirmed that the phosphate group did indeed catalyze its own elimination. However, the enzyme provided a phosphate binding pocket to orient the phosphate group in a position suitable for abstraction of the C-6 proton. Interactions between the carboxylate group and active side residues locked the C-2 conformation so as to prevent epimerization during the final two steps in the mechanism. Hence, the labeling of DHQ synthase as an oxidoreductase would be quite erroneous given its active involvement in every step of the transformation.

T

saga. Cu

materials

obtained

Besides

renewab.

feedstock

Abundan

current, a

Chemical

at high te

constitut

environm

T

friendly,

including

cheap an

of orgar

streams

contend

molecul

now be

Biocatalytic Synthesis of Value-Added Chemicals

The search for cleaner, safer, and cheaper chemical processes is a never ending saga. Current chemical production protocols rely on abiotic catalysts and on starting materials derived mostly from petroleum. For instance aromatics are predominantly obtained from the benzene, toluene, xylene (BTX) fraction of petroleum refining. Besides the environmental issue, the cost of isolating these components from a non-renewable feedstock is important to consider. The non-renewability of petroleum feedstock may not be a concern to the current generation or the many more to follow. Abundant stocks of petroleum exist to justify our being indifferent to its use at the current, alarmingly high rate. But we owe it to the future to start probing for alternatives. Chemical processes typically involve use of toxic, corrosive, and carcinogenic materials at high temperatures and/ or pressures. By-products typically find no other use and constitute a waste hazard, the disposal of which has enormous monetary and environmental ramifications.

The use of biocatalysis has the potential to usher in a new age of environmentally friendly, industrial scale processes, capable of producing a wide spectrum of chemicals, including aromatics at a reasonable cost. Biocatalysis relies on the use of renewable, cheap and non-toxic carbohydrate resources. Reactions are typically run in water instead of organic solvents at near-ambient temperatures and atmospheric pressures. Waste streams are generally benign and easily degraded. Biocatalytic processes initially had to contend with problems of low product yields/ titers, paucity in terms of accessible molecules and inconvenient reaction times and volumes. Most of these problems can now be addressed with the advent of improved molecular biology and fermentation

how the

Acrylan

A

starting

currently

floccula

acrylami

Problem

regenera

hydrolys

separatio

transforr

Figure

isot

techniques as well as a better understanding of cellular mechanisms. The remainder of this section will discuss biocatalytic routes to several industrially relevant chemicals and how they compare to their chemical counterparts.

Acrylamide

Acrylamide is one the most important commodity chemicals widely used as starting material in the polymerization industry. Worldwide production of acrylamide currently stands at 200×10^6 kg.[24] Polymers derived from acrylamide find applications as flocculants, stock additives, and in petroleum recovery. Conventional synthesis of acrylamide involves hydration of acrylonitrile using copper salts as catalyst (Figure 4).[24] Problems associated with this process include difficulty in preparing, recycling, and regenerating the catalyst. There is also the danger of polymerization or complete hydrolysis occurring during the reaction because of the heating, which complicates the separation and purification of acrylamide. Industry has now switched to a biocatalytic transformation of acrylonitrile to acrylamide.[25]
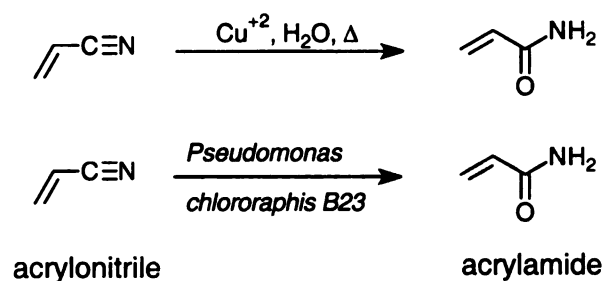
Figure 4. Comparison of chemical and biocatalytic routes to acrylamide.

The strain *Pseudomonas chlororaphis* B23 was isolated from soil as an isobutyronitrile-utilizing bacterium. Under optimized fermentor conditions at 10 °C

quantita

conditio

Lactic a

C

and app

flavorin

recent u

of the n

acid. Po

it could

Lactic a

and L-is

acid hy

of aceta

biocata

biocata

5).[25]

depend

using methacrylate as an inducer, immobilized *P. chlororaphis* B23 converts acrylonitrile quantitatively to acrylamide (Figure 4). There is no purification step, the reaction conditions are very mild and the immobilized cells can be used repeatedly.

Lactic acid

Global lactic acid production is estimated to be more than 100 x 10^8 kg per year, and approximately 75% of the lactic acid produced is used in the food industry as a flavoring acid or baking agent and its glycerol ester is used as an emulsifier.[26a] More recent uses for lactic acid have been driven by ecological interests and include production of the non-chlorinated solvent ethyl lactate as well as the biodegradable plastic, polylactic acid. Polylactic acid is a polymer whose properties are similar to those of polyolefins and it could replace a significant portion of the polyethylene terephthalate-based polymers.[26] Lactic acid can be synthesized chemically but such synthesis results in a mixture of D- and L-isomers with only the L-form being commercially useful. The synthesis entails acid hydrolysis of lactonitrile at 100 °C. Lactonitrile in turn is produced by the treatment of acetaldehyde with hydrogen cyanide under basic conditions (Figure 5).[27]

Chemical synthesis of lactic acid has now been replaced in industry by biocatalytic routes. For example, *Rhizopus oryzae* is a fungus widely used for biocatalytic conversion of carbohydrates to L-lactic acid under aerobic conditions (Figure 5).[28] The fermentations are very efficient and can result in yields higher that 90% depending on the starting carbohydrate used.

Figure 5

A

global s

feedstoc

are prim

being ex

Figure 6

T

synthesi

But in th
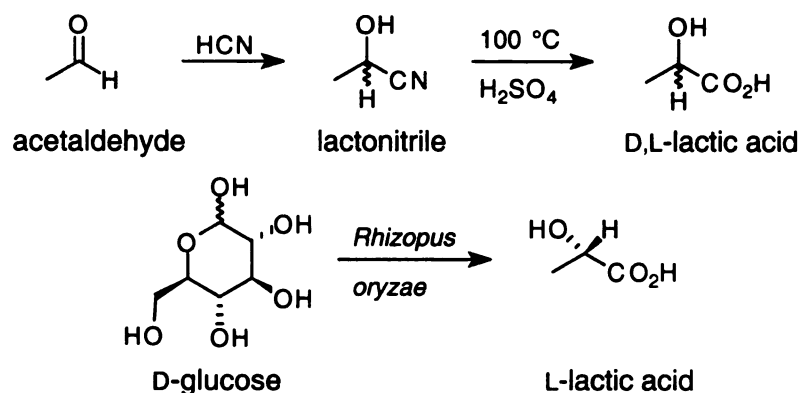
Figure 5. Comparison of chemical and biocatalytic synthesis of L-lactic acid.

Among amino acids, L-lysine commands a huge share of the market with annual global sales of well over 200 x 10^8 kg.[29] Its primary use is as an additive in animal feedstock. Aspartame is the highest selling food additive in the world.[30a] Both molecules are prime examples of compounds previously produced by chemical processes, but now being exclusively manufactured via biocatalytic fermentations (Figure 6).[29,30b]
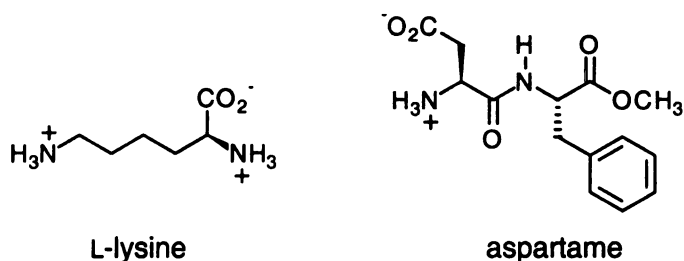
Figure 6. Structures of L-lysine and aspartame.

The sequence of events leading to the crossover from chemical to biocatalytic synthesis for either of the aforementioned compounds is very engaging in its own right. But in the context of the subject of this thesis, it would now be pertinent to discuss how

the shikimate pathway can be manipulated to culminate in the production of industrially relevant value-added chemicals.

The shikimate pathway has proven to be quite prolific in terms of its applicability for biosynthesis of aromatic compounds. Low-cost fermentations have been developed for production of phenylalanine and tryptophan.[31] Chemical and enzymatic routes exist for conversion of the aromatic amino acids to various other value added chemicals (Figure 7).
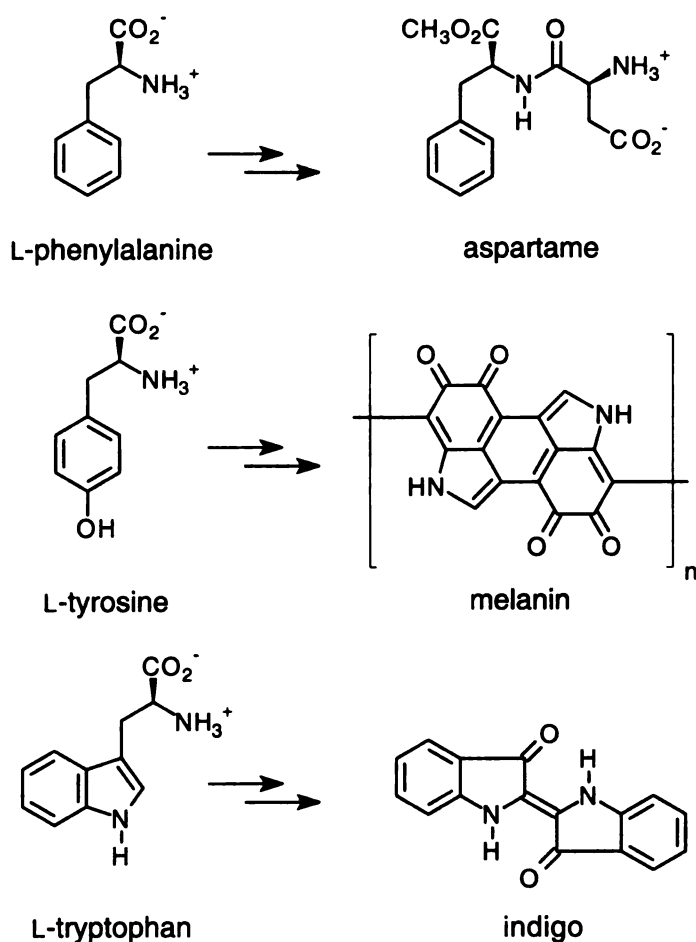
Figure 7. Chemicals accessible from the aromatic amino acids.

Phenylalanine can be chemically or enzymatically converted to aspartame,[30b] tyrosine can be converted to the mammalian pigment melanin,[32] which is widely used in

hair dye

indigo.

Indigo

T

shikima

Indigo.

annual

product:

(Figure

feedstod

presents

Figure 8

hair dyes and in sun screens, while tryptophan can be utilized for the production of indigo.[33]

Indigo

The biocatalytic synthesis of indigo provides an interesting example of how the shikimate pathway can be interfaced with enzymes from other pathways/organisms. Indigo, the dye that imparts the unique blue color to jeans, is a widely used vat dye with annual worldwide production of approximately 1.3×10^7 kg.[34a] Current routes to indigo production involve the use of either aniline or anthranilic acid as starting materials (Figure 8).[34] Not only are these compounds derived from non-renewable petroleum feedstocks, but toxic waste (ammonia, cyanide compounds, formaldehyde, etc.) also presents serious environmental concerns.
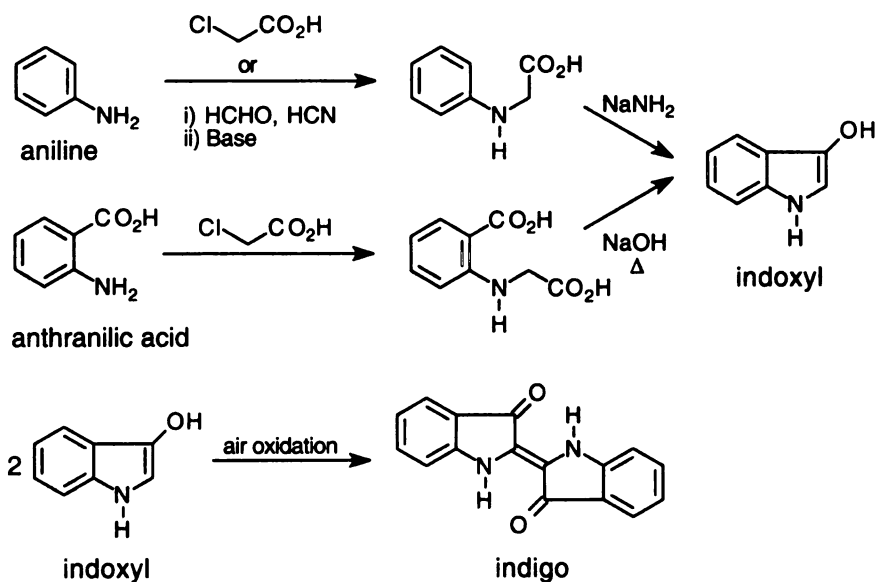
Figure 8. Chemical synthesis of indigo.

A biocatalytic route from a renewable feedstock has now been developed for indigo by overexpressing the tryptophanase and naphthalene dioxygenase enzymes in a

tryptophan-synthesizing microbe (Figure 9).[33] Whether this process will replace current

methods of indigo synthesis remains to be seen, but it highlights the attractive alternatives

that biocatalysis can provide to chemical synthesis.
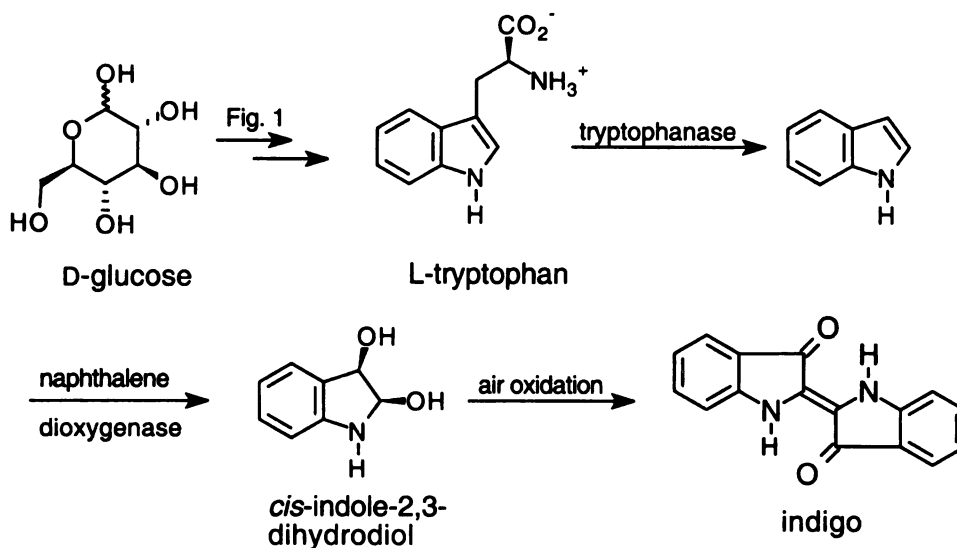
Figure 9. Biocatalytic synthesis of indigo from D-glucose.

Vanillin

As a food flavor, vanillin is second only to aspartame in terms of annual sales.[30a]

About 12 x 10^6 kg of vanillin are produced annually throughout the world.[35] Synthetic

vanillin can either be obtained from waste sulfite lye in wood pulping operations or from

catechol (Figure 10).[36] Both methods are fraught with huge amounts of toxic waste

streams and use of toxic, carcinogenic materials.

Figur

Figur

recom
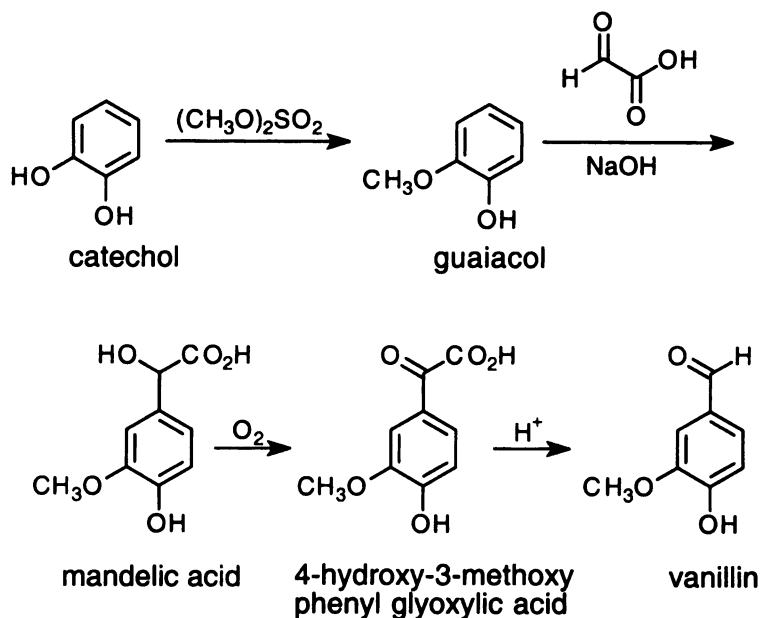
Figure 10. Chemical production of vanillin from catechol.
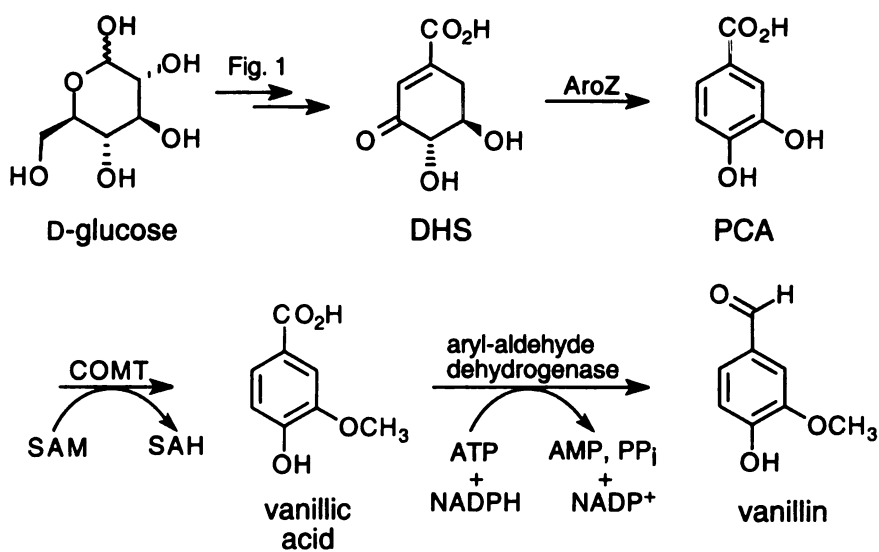
Figure 11. Biocatalytic synthesis of vanillin from D-glucose.

Recently a synthesis of vanillin from glucose has been elaborated by using a recombinant *E. coli* strain (Figure 11).[37] The conversion was accomplished by synthesis

by aryl

though

towards

p-hydr

These

also use

reaction

(Figure

Problem

the use

petrole

choris

choris

aroB,

into th

produc

encod

of DHS from glucose via the common pathway followed by conversion of DHS to vanillic acid by the action of *aroZ* encoded DHS dehydratase and catechol-*O*-methyl transferase (COMT). The final step involved in vitro reduction of vanillic acid to vanillin by aryl-aldehyde dehydrogenase which was isolated from *Neurospora crassa*. Even though this process afforded less than 5 g/L of vanillin, it is definitely a giant step towards large-scale environmentally-benign manufacture of vanillin.

p-hydroxybenzoic acid (PHB).

The use of PHB in liquid crystal polymers such as Zydar is well documented.[38a] These materials find applications in high performance instruments. Esters of PHB are also used as food preservatives.[38b] Currently, PHB is synthesized via the Kolbe-Schmidt reaction involving treatment of potassium phenoxide with 20 atm dry CO_2 at 180-250 °C (Figure 12). Neutralization of the potassium salt with a mineral acid affords PHB. Problems associated with this process range from the high temperature and pressures, to the use of phenol which is a toxic, corrosive chemical obtained from non-renewable petroleum feedstock.

An *E. coli* strain has been developed incorporating the *ubicC* gene encoding for chorismate-pyruvate lyase (Figure 12). This enzyme catalyzes the conversion of chorismate directly to PHB.[39] The biocatalyst consisted of plasmid-localized *aroA*, *aroL*, *aroB*, and *aroC* along with genome-localized *tktA*, *aroF*[FBR], and *ubicC* The carbon flow into the common pathway was thus optimized leading to increased chorismic acid production which was subsequently processed by chorismate-pyruvate lyase. Genes encoding other chorismate-utilizing enzymes were mutationally inactivated. This

focus of

pctass
phenc

Figure

and D-g

p-amin

problem

out of

methyl

nitro gr

resulted in production of 12 g/L of PHB from glucose.[40] Shikimic acid can also be

converted to PHB by acid catalyzed dehydration.[40] This chemical conversion can be very

profitable provided a cheap, reliable source of shikimic acid can be found, which is the

focus of Chapter 4 in this thesis.
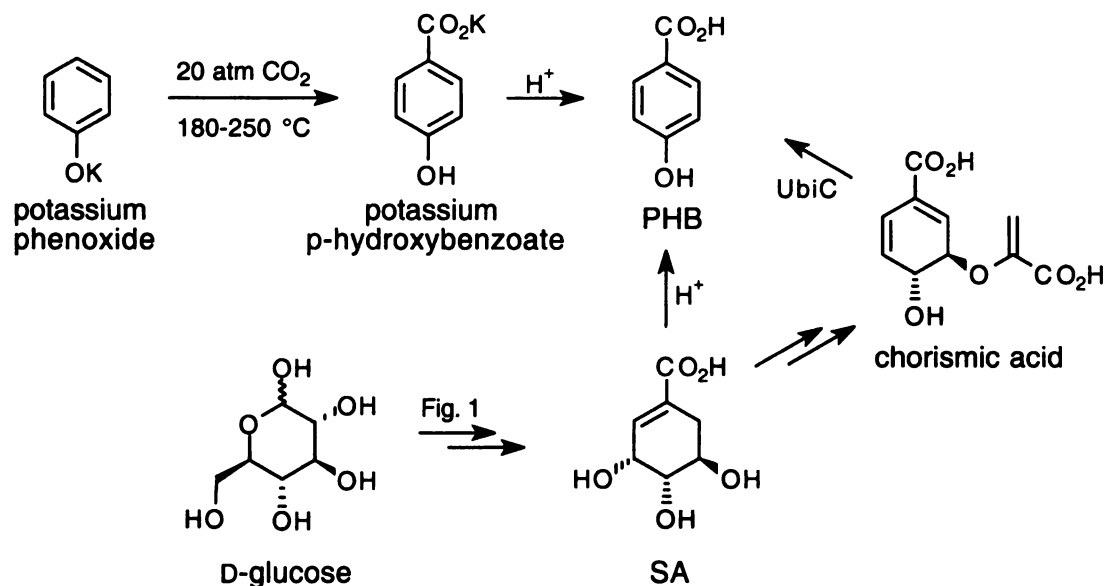
Figure 12. Comparison of the chemical and microbial synthesis of PHB from phenol and D-glucose respectively.

p-aminobenzoic acid (PABA)

The synthesis of PABA is a process that has to deal with health, safety, and waste

problems in every step (Figure 13).[41] Nitration of toluene gives a mixture of compounds

out of which p-nitrotoluene is separated out. Chromic or nitric acid oxidation of the

methyl group to a carboxylate functionality followed by iron catalyzed reduction of the

nitro group results in PABA.

tq

HO

Figure

deoxych

synthas

lyase is

and it w

designe

anaesth

Quinic

shikim

in a nu

cincho
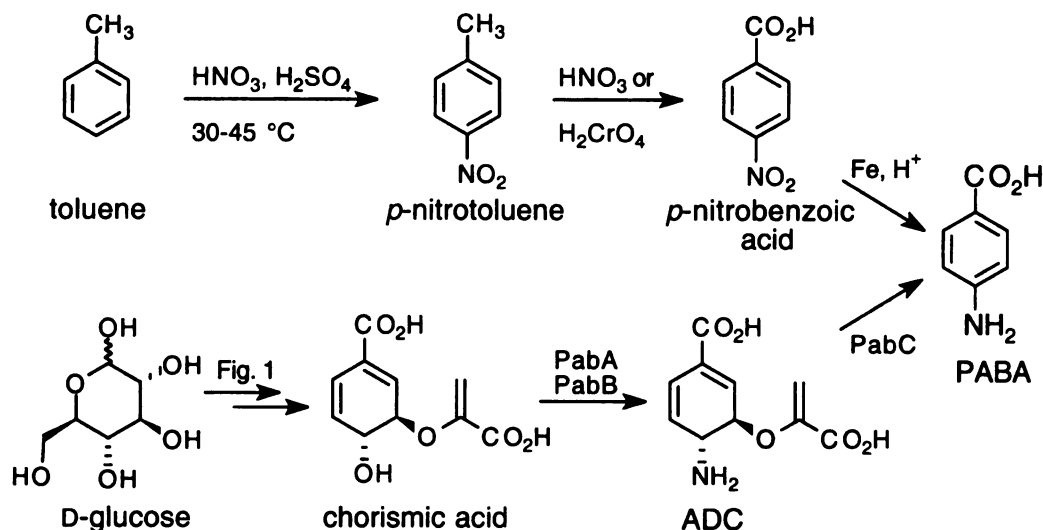
Figure 13. Comparison of chemical and microbial catalyzed synthesis of PABA.

Chorismic acid can be converted to (PABA) via initial formation of 4-amino 4-deoxychorismic acid (ADC) followed by elimination of pyruvic acid (Figure 13).[42] ADC synthase is made up of two subunits encoded by the *pabA* and *pabB* loci, while ADC lyase is encoded by *pabC*. All three genes have been cloned and sequenced from *E. coli* and it will be only a matter of time when a PABA producing biocatalyst is successfully designed. PABA is an ingredient in UV-blocking formulations and its ester is the local anaesthetic benzocaine.[41]

Quinic acid (QA), Hydroquinone, and Benzoquinone

A by-product of the shikimate pathway arising out of reduction of DHQ by shikimate dehydrogenase is QA,[43a] which is a very useful molecule and finds applications in a number of synthetic schemes.[43b-d,21b,22c] It is currently isolated from the bark of the cinchona plant. The Frost group has successfully designed an *E. coli* biocatalyst capable

lackin

benzoqu

product

a phot

Synthe

benzen

derivat

results

explosi

manufa

of benz

excelle

supern

temper

of producing up to 60 g/L QA (Figure 14).[44] This was achieved by overexpression of shikimate dehydrogenase and feedback insensitive DAHP synthase in an *E. coli* strain lacking DHQ dehydratase.
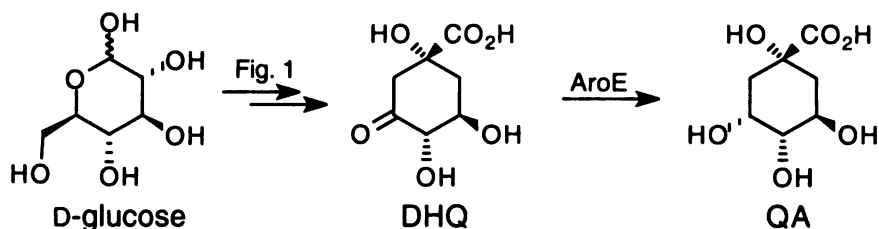
Figure 14. Microbial synthesis of QA.

The largest potential application of QA is in the production of hydroquinone and benzoquinone, both of which are currently synthesized from benzene.[45] Annual global production scales for hydroquinone currently stand at 4.0 x 10^7 kg.[46] It is widely used as a photographic developer. Benzoquinone is used as an organic building block.[45e] Synthesis of hydroquinone[45a-c] involves zeolite catalyzed Friedel-Craft alkylation of benzene to *p*-diisopropyl benzene (Figure 15). Air oxidation of this dialkylated benzene derivative under strong caustic conditions at 90-100 °C along with cobalt or copper salts results in hydroquinone. The air oxidation proceeds via peroxide chemistry, the explosive nature of which cannot be understated. On the other hand, benzoquinone is manufactured by oxidation of aniline with MnO_2 under acidic conditions.[45d,e] Reduction of benzoquinone over iron also affords hydroquinone.

QA produced in fermentations can be easily converted to hydroquinone in excellent yields by the action of industrial bleach (Figure 15).[47] The fermentation culture supernatant is treated to remove protein and cations, acidified and stirred at room temperature for 3 h with bleach. The bleach was neutralized with isopropanol and the

Figure

Dehyd

applica

fact. D

antioxi

econor

strain

This s

resulting solution refluxed for approximately 8 h giving clean hydroquinone. This

reaction sequence represents a process which can be easily manipulated to meet industrial

requirements in terms of yield, purity and waste.
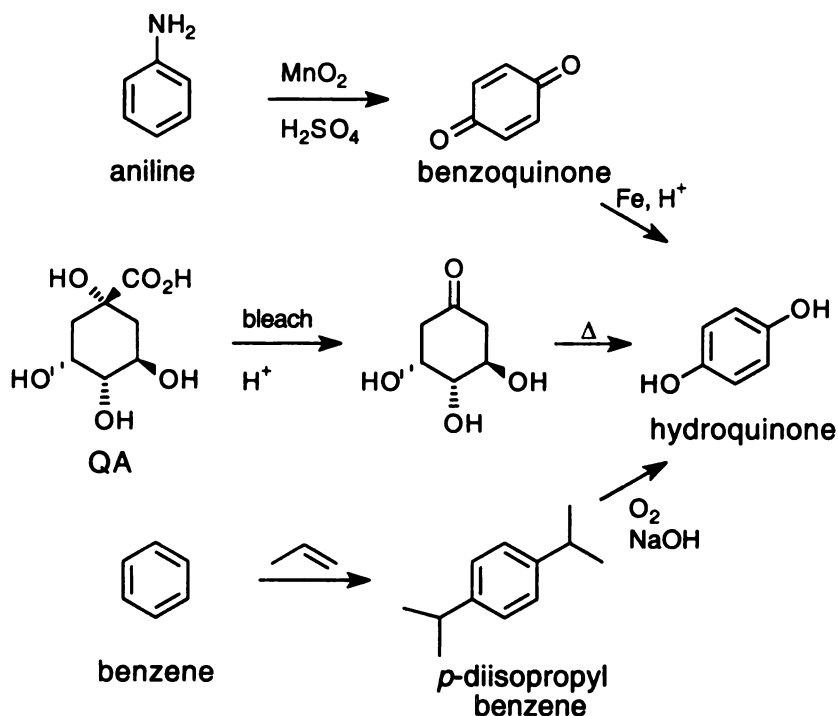
Figure 15. Various synthetic routes to hydroquinone.

Dehydroshikimic acid (DHS)

The shikimate pathway intermediate that has found the most number of

applications to date is DHS.[48] The antioxidant properties of DHS are well known. In

fact, DHS is as good as if not a better antioxidant than many commercially used

antioxidants[49] with the added advantage that DHS can be produced at an industrially

economical scale from glucose. The Frost group has successfully developed an *E. coli*

strain capable of producing up to 88 g/L DHS in a fed-batch fermentor (Figure 16).[50]

This strain was constructed by inactivation of genomic *aroE* encoding for shikimate

HO

D-3

HO

L-d
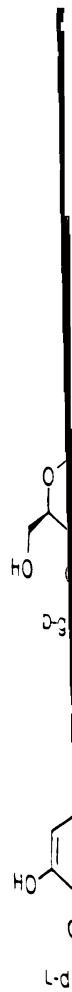
dehydrogenase and overexpression of *aroF*[FBR], *tktA*, and *pps*. Perhaps more important than the properties of DHS itself is its conversion, chemically and biocatalytically, to industrially relevant chemicals (Figure 16).
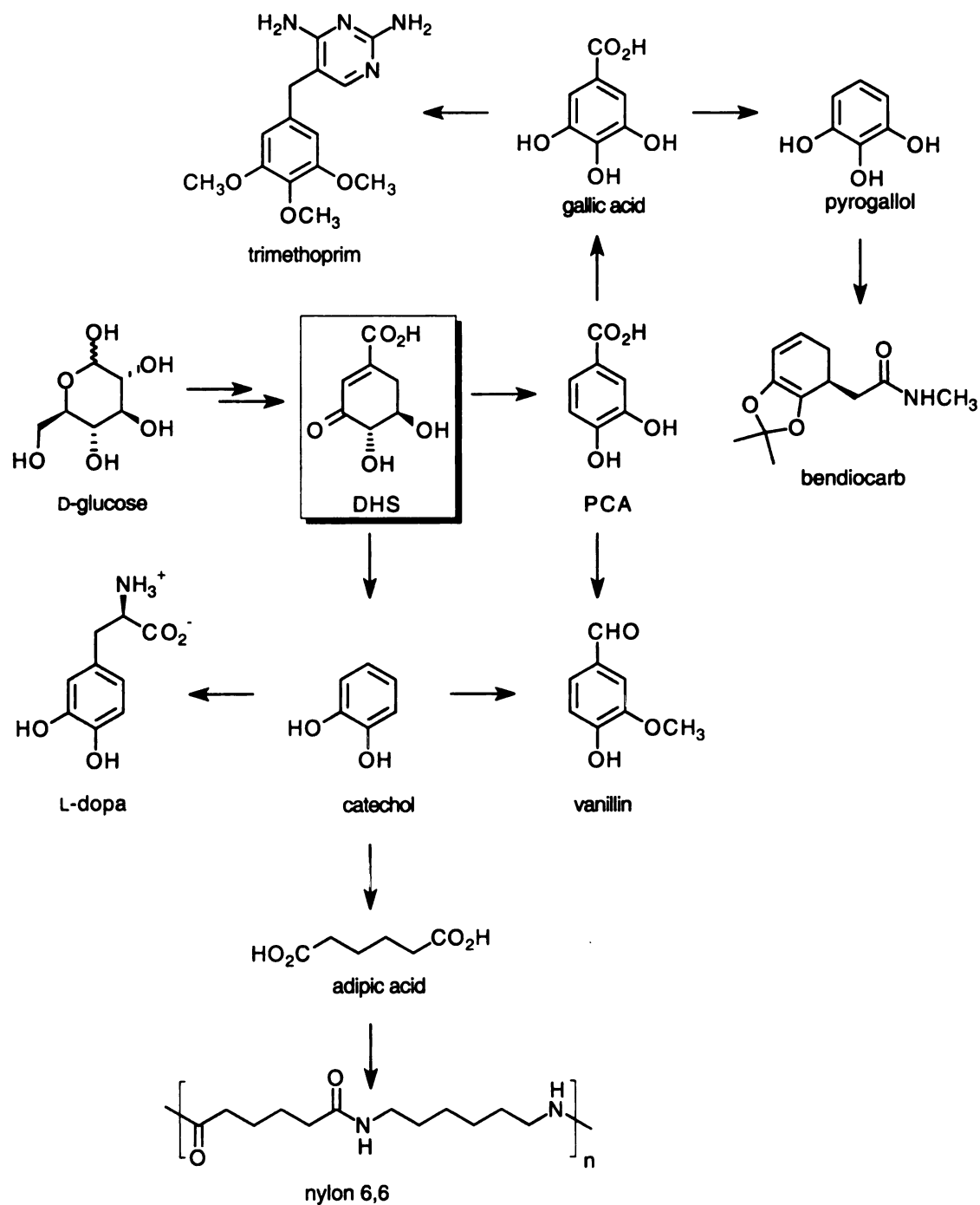
Figure 16. The various synthetic applications of DHS.

pyroga

aroma

relaxar

also fir

well as

encode

dehydr

hydroxy

aerugir

aroZ an

acid fro

catalyze

⊢

Figure

Gallic acid

Gallic acid is a trihydroxy aromatic compound isolated from gall nuts and tara powder.[51] Thermal decarboxylation of gallic acid in copper autoclaves yields pyrogallol.[51] Both compounds are used as building blocks to provide the trihydroxylated aromatic ring of biologically active molecules like the antibiotic trimethoprim, the muscle relaxant gallamine triethiodide and the insecticide bendiocarb (Figure 16).[51] Pyrogallol also finds applications in photographic developing solutions.[52] DHS can be chemically as well as biochemically converted to gallic acid (Figure 17).[49,53] DHS dehydratase, encoded by the aroZ locus and isolated from *Klebsiella pneumoniae*, catalyzes the dehydration of DHS to protocatechuic acid (PCA). A mutant isozyme of *p*-hydroxybenzoate hydroxylase, encoded by pobA*, has been obtained from *Pseudomonas aeruginosa* which is capable of hydroxylating PCA to form gallic acid.[54] Expression of aroZ and pobA* in a DHS-synthesizing microbe resulted in production of 20 g/L gallic acid from glucose.[54] DHS can also be chemically transformed to gallic acid via copper catalyzed oxidation in the presence of zinc (Figure 17).[55]
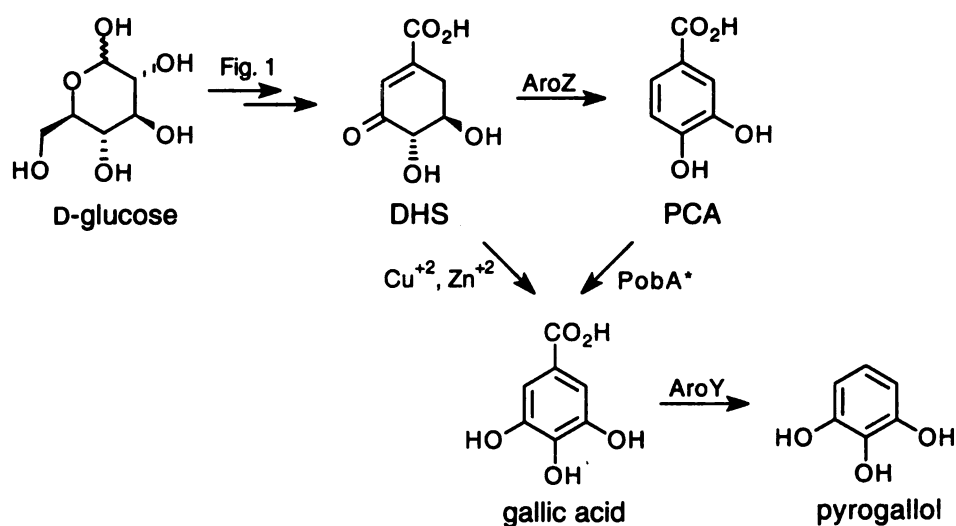
Figure 17. Conversion of D-glucose to gallic acid and pyrogallol.

micr

be c

ferr

of p

acid

Con

with

Cate

finds

prod

adre

(carb

butyl

from

upon

phenc

a mix

by dis

Gallic acid can be decarboxylated to pyrogallol by *aroY*-encoded PCA decarboxylase from *K. pneumoniae*.[56] However, the decarboxylation of gallic acid is slower than that of PCA. Hence *aroY* cannot be overexpressed in a gallic acid producing microbe because PCA occurring as an intermediate between DHS and gallic acid would be converted to catechol.[53,56] The problem was resolved by adding gallic acid to a fermentor containing an *E. coli* strain overexpressing only *aroY*, resulting in a 97% yield of pyrogallol from gallic acid.[53] Thus, even though the biocatalytic production of gallic acid is still not a stage where it can be industrially viable, the outlook is promising. Conversion of gallic acid to pyrogallol though, is already at a stage where it can compete with chemical decarboxylation.

Catechol

Catechol is an example of a simple, dihydroxylated, aromatic molecule which finds applications in a number of industrial chemical processes. The variety of chemical products derived from catechol is staggering and includes pharmaceuticals (L-dopa, adrenaline, papavarine), flavors (vanillin, eugenol, isoeugenol), agrochemicals (carbofuran, propoxur), and polymerization inhibitors and antioxidants (4-*tert*-butylcatechol, veratrol).[43,57] Currently, the primary source of catechol is via synthesis from benzene (Figure 18).[43,57] Friedel-Crafts alkylation of benzene affords cumene which upon oxidation leads to formation of phenol and acetone. Subsequent treatment of the phenol with 70% hydrogen peroxide in the presence of transition metal catalysts leads to a mixture of catechol and hydroquinone. Catechol is purified away from hydroquinone by distillation.

devel

(Figur

HC

(a) pro
60-10(

Figur

Adip

dema

invo

The

culp

acc

As stated before, the enzyme PCA decarboxylase catalyzes the formation of catechol from PCA at a rapid rate. This implies that in theory catechol can be synthesized from glucose via DHS. Akin to gallic acid synthesis, an *E. coli* strain was developed overexpressing *aroZ* and *aroY* to afford catechol via a biosynthetic route (Figure 18).[56]
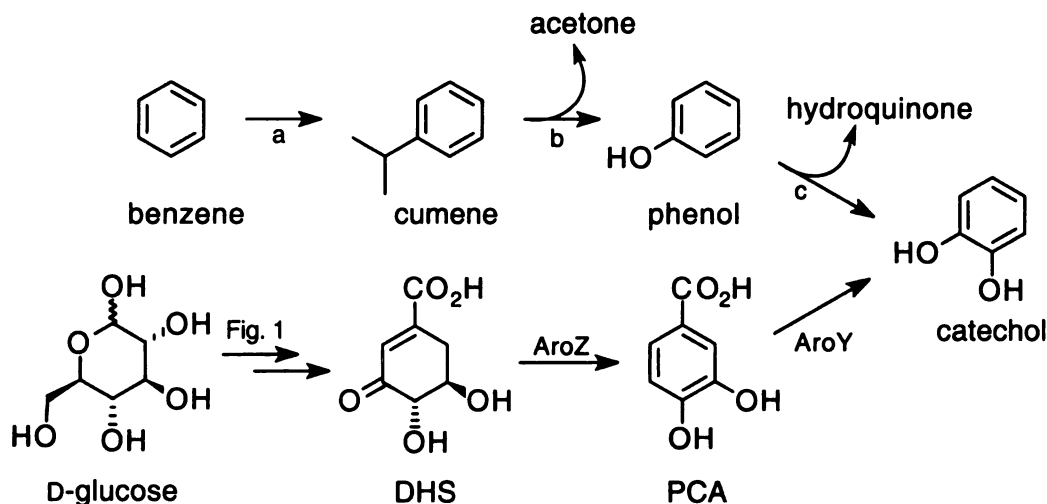
(a) propylene, solid H_3PO_4 catalyst, 200-260 °C, 400-600 psi. (b) O_2, 80-130 °C; SO_2, 60-100 °C. (c) 70% H_2O_2, EDTA, Fe^{+2} or Co^{+2}, 70-80 °C.

Figure 18. Comparison of chemical and biocatalytic routes to catechol.

Adipic acid

Adipic acid makes up one of the 6-carbon units in nylon-6,6. Its annual global demand is about 1.9×10^9 kg.[58a] Adipic acid is currently synthesized via a route involving nitric acid oxidation of a cyclohexanol/ cyclohexanone mixture (Figure 19).[58b] The by-product of this step is nitrous oxide which has been identified as one of the main culprits in depletion of the ozone layer and global warming.[59] This synthetic route in fact accounts for 10% of the annual increase in atmospheric nitrous oxide levels. An

might

catech

catA-e

Acinet

10% P

acid. T

benze

HO

D-g

(a) Ni-

NH₄VO

Figure

eco-fri

The su

environmentally benign biocatalytic synthesis of adipic acid is really called for under such a situation.

Adipic acid may at first glance have nothing in common to catechol, and hence it might be difficult to fathom a biocatalytic route leading from one to the other. But catechol can be biocatalytically transformed to *cis,cis*-muconic acid by the action of *catA*-encoded catechol 1,2-dioxygenase (Figure 19).[56a] The *catA* gene was isolated from *Acinetobacter calcoaceticus*.[60] Catalytic hydrogenation of *cis,cis*-muconic acid using 10% Pt on carbon under 50 psi hydrogen pressure and room temperature results in adipic acid. This would therefore classify as a synthesis of adipic acid from glucose via DHS.
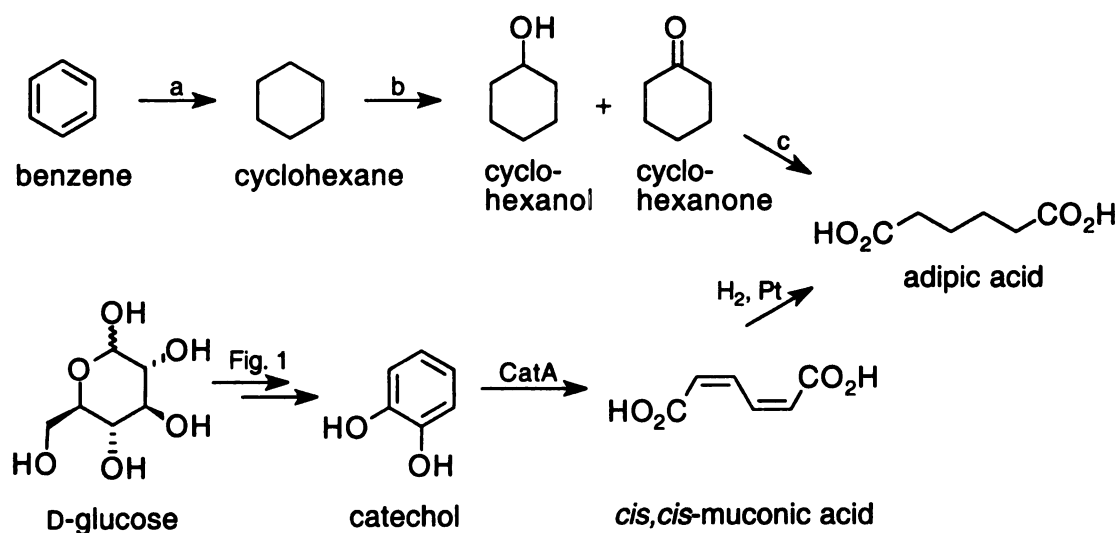
(a) Ni-Al$_2$O$_3$, H$_2$, 370-800 psi, 150-250 °C. (b) Co, O$_2$, 120-140 psi, 150-160 °C. (c) Cu, NH$_4$VO$_3$, 60% HNO$_3$, 60-80 °C.

Figure 19. Chemical and microbial synthetic routes to adipic acid.

These examples prove the versatility of the shikimate pathway in providing safe, eco-friendly, alternative routes for chemicals currently made via hazardous processes. The successful application of genes and enzymes from other pathways and organisms in

to mak

M

industr

biocata

scale, i

amoun

improv

DAHP

catalyti

which

genes

and try

achiev

substra

into th

transcr

conjunction with the *E. coli* shikimate pathway opens the gateway to an entire gamut of compounds. As science heads into the 21st century, and with the chemical industry coming to terms with its role in protecting the environment, the potential for biocatalysis to make an impact is, dare we say, without any boundaries.

Metabolic Engineering of *Escherichia coli* for Optimization of Product Titer and Yield

For any process, be it chemical or biocatalytic, to be successfully applied in industry, it has to fulfill certain criteria in terms of yield and titer. In order for a biocatalyst to produce SA in quantities high enough to justify its use on an industrial scale, it is necessary to improve carbon flow into the common pathway.[61] A considerable amount of research has been expended towards this end. The primary target for improving carbon flow into any pathway is the first enzyme of the pathway, in this case, DAHP synthase. The rate of aromatic amino acid biosynthesis is modulated by the catalytic activity of DAHP synthase. DAHP synthase exists as three isozymes each of which is sensitive to feedback inhibition by one of the three aromatic amino acids. The genes *aroF*, *aroG* and *aroH* encode for the tyrosine-sensitive, phenylalanine-sensitive, and tryptophan-sensitive isozymes respectively. The regulation of the three isozymes is achieved via feedback inhibition, genetic expression levels and availability of their substrates E4P and PEP.

Overexpression of DAHP synthase can be realized by introduction of a mutation into the locus encoding the aporepressor (TyrR) for *aroF* transcription. In lieu of TyrR, transcription of *aroF* is derepressed and the number of molecules of AroF increases.[62]

Repla

give :

polyr

Ampl:

aroF

cannot

This is

DAHP

syntha

techni

improv

amplifi

synthe

increas

Several

Chief a

carbohy

(PTS) s

however

T

co-work

synthase

Replacing the native promoter (P_{aroF}) of *aroF* with a strong promoter like a P_{tac} can also give the same result. The TyrR repressor protein does not influence binding of RNA polymerase to the P_{tac} promoter resulting in a higher degree of transcription. Amplification of DAHP synthase activity can also be accomplished by localization of the *aroF* gene on a multi-copy plasmid. However, the in vivo activity of DAHP synthase cannot be increased beyond a certain point irrespective of the level of gene amplification. This is because of the powerful role played by feedback inhibition in the regulation of DAHP synthase activity.[63] Feedback insensitive mutants of all three isozymes of DAHP synthase have been isolated.[62,64,65] Application of any of the gene amplification techniques to a feedback insensitive version of DAHP synthase can now result in improved in vivo catalytic activity.

Ultimately, DAHP synthase catalytic activity attains a point where further amplification of feedback resistant DAHP synthase has no incremental effect on the synthesis of aromatic amino acids or their precursors. Attempts were then made to increase availability of the substrates required by DAHP synthase namely, PEP and E4P. Several cellular processes and enzymes compete with DAHP synthase for available PEP. Chief among them are pyruvate kinase, PEP carboxylase and the PEP-dependent native carbohydrate uptake system, the phosphoenolpyruvate-carbohydrate phosphotransferase (PTS) system. Mutational inactivation of pyruvate kinase[66] and PEP carboxylase[61c,67] however did not give any significant improvement in aromatic amino biosynthesis.

The focus was then placed on in vivo concentrations of E4P. In 1990, Frost and co-workers reported that availability of E4P was an important factor limiting DAHP synthase activity when glucose was used as the carbon source.[61a,68] Levels of E4P were

reporte

for thi

Transf

Condit

high c

mainta

howev

requir

involv

enzym

cataly

glycer

to be

sedoh

cataly

increa

with

heptu

ampli

the co

substr

reported to be low even in the absence of amplified DAHP synthase activity.[69] A reason

for this could be its rapid dimerization, trimerization, and polymerization in solution.[70]

Transformation of these polymeric forms back to monomeric E4P is quite slow.

Conditions disfavoring the monomeric E4P form include low temperature, basic pH, and

high concentration. By matching the rate of E4P production with E4P utilization, the cell

maintains a low concentration of E4, ensuring its stability as a monomer. This strategy

however meant that steady state concentrations of E4P were insufficient to satisfy

requirements of an amplified DAHP synthase activity level. Analysis of processes

involving E4P as a substrate or a product led to the pentose phosphate pathway and the

enzyme transketolase encoded by the *tktA* gene (Figure 20). The transketolase enzyme

catalyzed formation of E4P from the coupling of D-fructose 6-phosphate with either D-

glyceraldehyde 3-phosphate or D-ribose 5-phosphate. Formation of E4P was also found

to be catalyzed by a second enzyme, transaldolase. This enzyme however utilized D-

sedoheptulose 7-phosphate, which was generated as a by-product during the transketolase

catalyzed formation of E4P. Amplification of transketolase expression levels resulted in

increased channeling of E4P into the common pathway.[68] Coupling *tktA* overexpression

with that of *aroG*[FBR] in an *E. coli aroB* strain led to increased 3-deoxy D-*arabino*

heptulosonic acid (DAH) accumulation relative to that observed when only *aroG*[FBR] was

amplified.[68] Accumulation of DAH can be considered as a measure of carbon flow into

the common pathway. Formation of DAH results from dephosphorylation of DAHP, the

substrate of DHQ synthase which is the enzyme mutationally inactivated in *E. coli aroB*.

Figur

worke

The si

PEP.

which

carbo

regula
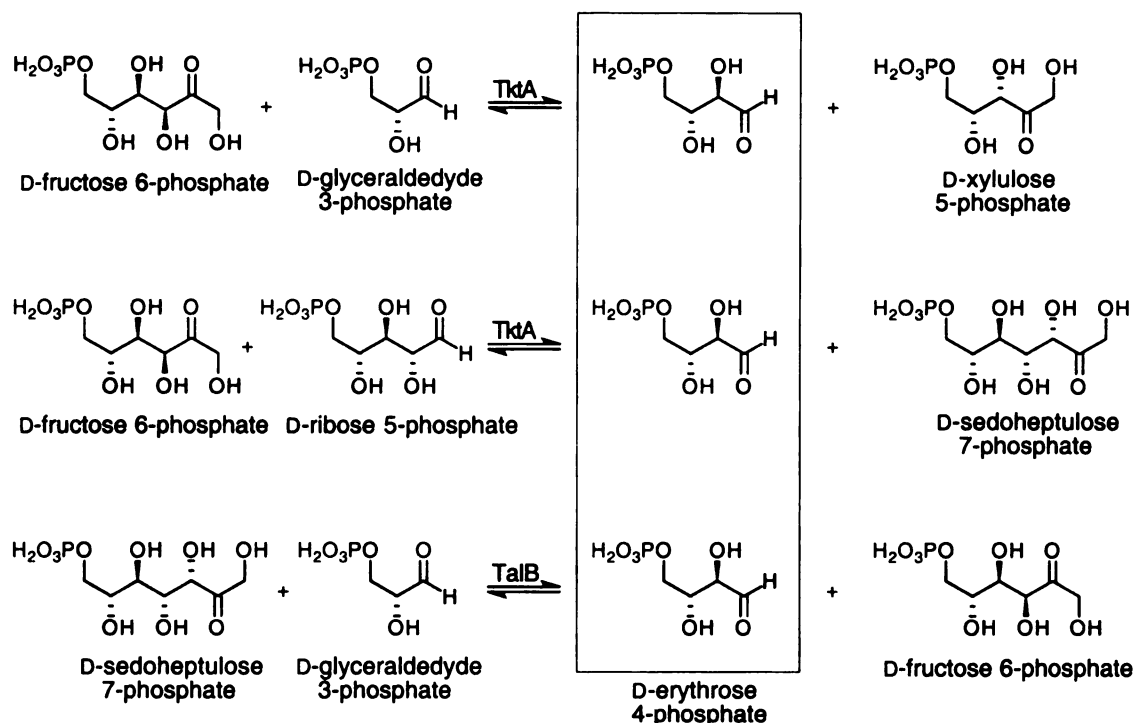
Figure 20. Reactions catalyzed by transketolase (TktA) and transaldolase (TalB).

With the problem of E4P availability no longer being a factor, Liao and co-workers re-examined the role of PEP availability in increasing aromatic biosynthesis.[61d,e] The shikimate pathway and glucose uptake compete for the same intracellular levels of PEP. Glucose uptake in *E. coli* is mediated by the PTS transport system (Figure 21), which is responsible for the transport and phosphorylation of a large number of carbohydrates, movement of cells towards these carbon sources (chemotaxis), and in the regulation of a number of metabolic pathways.[71]

pyruva

Figur
Genet
glucos

interm

encod

of all

encod

as IIC

PTS-

even

for s

imp

shik

enz

pyr

(Fig

glucose 6-phosphate

PEP — (P)—EI — (P)—HPr — (P)—IIAᵍˡᶜ — (P)—EB

pyruvate — EI — HPr — IIAᵍˡᶜ — EB

C — glucose

cytoplasm   periplasm
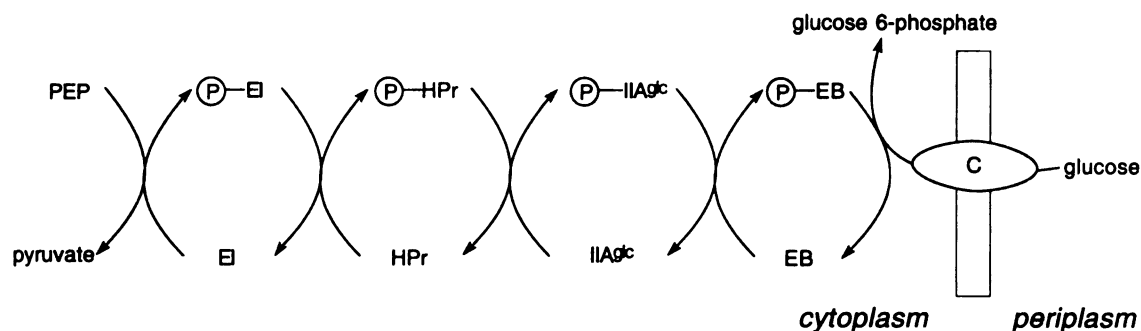
Figure 21. The PTS-system for glucose uptake.
Genetic loci are as follows: *ptsI*, Enzyme I (EI); *ptsH*, Histidine protein (HPr); *crr*, glucose specific Enzyme IIA (IIA^{glc}); *ptsG*, Enzyme B and C (EB and C).

The phosphate group is transferred to the glucose via obligatory phospho-intermediates of proteins EI, HPr, IIA^{glc}, EB and C. The *ptsI*-encoded EI and *ptsH*-encoded HPr proteins are soluble cytoplasmic proteins that participate in phosphorylation of all PTS carbohydrates. Protein IIA^{glc} is a soluble enzyme specific for glucose and is encoded by the *crr* locus. The two membrane bound proteins EB and C, also designated as IICB^{glc}, comprise the *ptsG*-encoded II^{glc} domain which is specific for glucose. The PTS-system relies on phosphoryl group transfer from PEP to initiate the cascade of events leading to glucose uptake (Figure 21).[71] The pyruvic acid by product is then used for sustaining cell growth. As a result three carbon atoms are lost for every six carbons imported by the cell (Figure 22). One strategy to nullify the competition between the shikimate pathway and the PTS-system for glucose, is to overexpress PEP synthase. The enzyme PEP synthase, encoded by the *pps* locus, catalyzes the phosphorylation of pyruvate in the presence of ATP, resulting in PEP, AMP, and inorganic phosphate (Figure 23).

Figur

conve

pathw

benefi

overex

carbor

observ

biosyr

availa

limitar

aroma
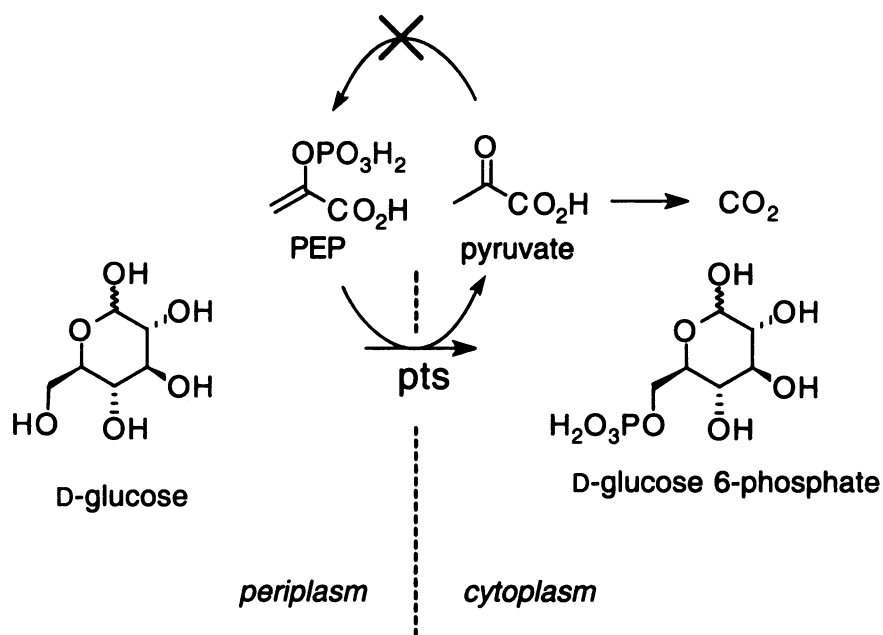
overex

Figure 22. Phosphorylation of D-glucose during its uptake.

Overexpression of PEP synthase will hence enable PTS-generated pyruvate to be converted back to PEP. However, no improvement in carbon flow into the shikimate pathway was detected in *E. coli aroB* with amplified expression of *pps* and *aroG*[FBR]. The benefits of enhanced PEP availability was realized only when *pps* and *aroG*[FBR] overexpression was coupled to that of *tktA*. The result was a twofold improvement in carbon flow as measured by the yield of DAH produced by *E. coli aroB*.[61d,e] These observations indicate that E4P is the first limiting metabolite in aromatic amino acid biosynthesis. Once this limitation is removed, the full benefits of increased PEP availability are realized. Amplified expression of transaldolase also relieves E4P limitation in the presence of amplified PEP synthase, but no further improvements in aromatic amino acid biosynthesis are observed relative to when transketolase is overexpressed.[72]

prob|

expr

is to

An u

mob.

affin

area

(glf)

larg

and

coli
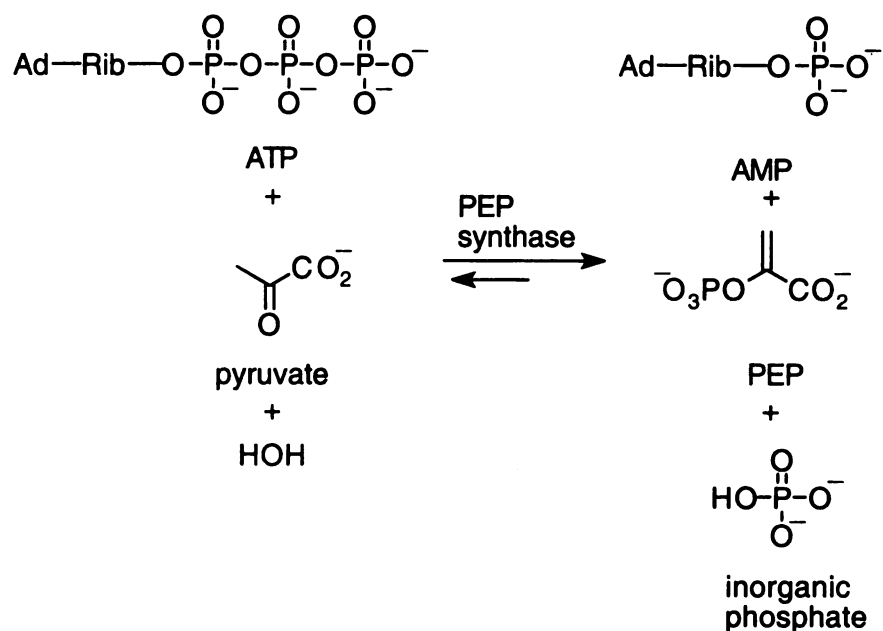
Figure 23. Reaction catalyzed by PEP synthase.

Alleviation of PEP deficiency by overexpression of PEP synthase can be problematic. PEP synthase is reported to be a heavily regulated enzyme and its amplified expression is known to be detrimental to the health of the microbe.[61d] A better alternative is to channel the glucose into the cell via a mechanism which is not dependent on PEP. An uptake system fulfilling this criteria is facilitated diffusion (Figure 24). *Zymomonas mobilis* is known to transport glucose by a facilitated diffusion process which is a low-affinity, high-velocity, non-energy dependent system.[73] A large amount of interest in this area has resulted in the cloning and sequencing of a putative glucose transporter gene (*glf*).[74] The deduced amino acid sequence of the *glf* gene product is closely related to a large family of glucose transporters.[75] Most importantly, expression of the *Z. mobilis glf* and glucose kinase (*glk*) genes was able to provide for glucose transport capability in *E. coli* strains lacking a native PTS system.[73c-e]

c

fa
g
o

Fig

upt

we

an

co

ur

co
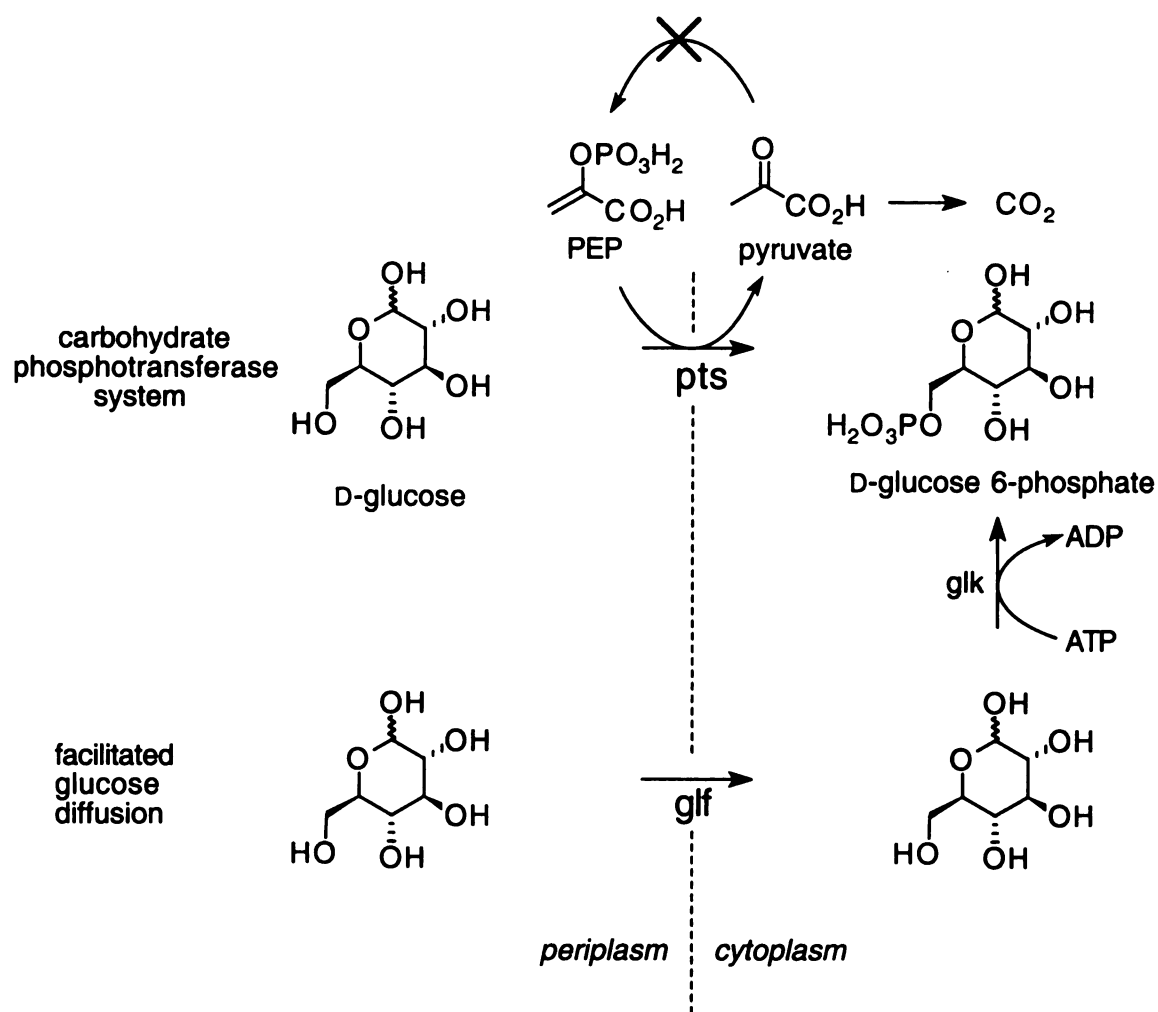
Figure 24. **Comparison of the PTS and facilitated diffusion systems for glucose uptake.**

The initial results concerning DAHP synthase, transketolase and PEP synthase were obtained under shake-flask conditions. Evaluation of the impact of $aroF^{FBR}$ and $tktA$ amplification have now been performed and confirmed under fed-batch fermentor conditions.[48,76] Results reported in this thesis for SA synthesis have all been obtained under fed-batch fermentor conditions. This is an important consideration because contrary to results from fed-batch fermentations, calculated yields from shake-flask

cultiv

impor

gluco

conce

cultivations do not really reflect the percent conversion of glucose to product. It is also important to consider that under shake-flask conditions, it is not easy to maintain constant glucose, oxygen, and pH levels which is not the case where fed-batch fermentations are concerned.

IN

better

a sing

reduc

produ

synth

consi

the th

role

intra

labe

DH

but

of

div

wi

ap

CHAPTER 2

INHIBITION OF DHQ SYNTHASE VIA UTILIZATION OF METAL-DIOL INTERACTIONS

Background

Inhibition studies on DHQ synthase have made significant contributions towards better understanding the intricacies of this enzyme. It was considered inconceivable that a single enzyme could catalyze an alcohol oxidation, phosphate elimination, carbonyl reduction, and an intramolecular aldol condensation in a single turnover of substrate to product. Initial results did support the mechanism outlined in Figure 3 resulting in DHQ synthase being considered as a mechanistic marvel. However, conclusions from a considerable body of work performed in the 1980's and early 1990's seemed to debunk the theory of DHQ synthase being an extraordinarily diverse and efficient catalyst.[21] The role of DHQ synthase in catalyzing the elimination of the phosphate and the intramolecular aldol condensation came into scrutiny, and some studies even hinted at labeling it as an oxidoreductase. The recently solved crystal structure of the active site of DHQ synthase finally provided evidence that the enzyme was not a mere oxidoreductant, but did indeed play a catalytic role in the conversion of DAHP to DHQ.[23]

The main focus of the work discussed in this chapter deals with studying the role of the metal co-factor. DHQ synthase has been proven to contain one tightly bound divalent metal cation per monomer by the following observations:[20a] (i) upon treatment with EDTA, the enzyme loses activity and gives rise to a stable but non-functional *apo*enzyme; (ii) reconstitution of the *apo*enzyme with a divalent metal cation restored

activ

catic

the

NAD

has

repor

form.

the a

synth

half l

that D

syster

natur

differ

metal

electr

any g

gene

biolc

coorc

it su

geon

activity back to the enzyme, the level of activity restored depending on the identity of the cation; (iii) EDTA does not cause inactivation in the presence of DAHP, indicating that the metal is less accessible when substrate is bound to the active site; (iii) the rate of NAD$^+$ dissociation varies with the metal ion. Whether the native metal is a Zn^{+2} or a Co^{+2} has been debated in the past. The Co^{+2} form of DHQ synthase from *E. coli* has been reported to be significantly more stable and active than its Zn^{+2} counterpart.[20a] The Zn^{+2} form of DHQ synthase has in the past been prepared from the Co^{+2} form by first stripping the active site of its Co^{+2} and then reconstituting the apoenzyme with Zn^{+2}. DHQ synthase retained some catalytic activity upon reconstitution with Zn^{+2} but had a short half life of approximately 30 min, making kinetic studies difficult. This led to the notion that DHQ synthase existed as a Co^{+2} enzyme in nature.[20a]

This however did not seem very likely given the availability of Zn^{+2} in biological systems.[77] It is second in abundance only to iron among the transition metals found in nature and has been found to be an integral component of more than 300 enzymes in different species.[78] There are several reasons why Zn^{+2} makes an ideal candidate for a metal co-factor, especially for DHQ synthase.[79] It has a completely filled *d-* shell with 10 electrons resulting in no ligand field stabilization energy when coordinated by ligands in any geometry. Zinc is inert to oxidoreduction especially in the divalent state and does not generate reactive radicals. The lack of redox activity allows Zn^{+2} to remain stable in biological systems whose potential is in a constant flux. Properties like its flexible coordination geometry, fast ligand exchange and intermediate hard-soft character makes it suitable for use as a co-factor. The multiplicity of coordination numbers and geometries as well as stereochemical adaptability denotes that Zn^{+2} submits readily to the

dem
activ
prod
ioniz
a var
is the

beyor
termin
involv
three
group
the ac
enzyr
facili
group
intern
rotati
the C
thus

demands of its ligands. The ability to exchange ligands at a fast rate is essential for an active site co-factor to be able to bind and activate substrate followed by rapid release of product. The Lewis acidity of Zn^{+2} enables it to polarize carbonyl groups and promote ionization of water molecules at physiological pH. It is known to interact very well with a variety of amino acid residues including histidine, glutamate, aspartate and cysteine. It is the combination of these factors that makes Zn^{+2} so attractive.

Elucidation of the crystal structure[23] of DHQ synthase from *A. nidulans* proved beyond doubt that the enzyme existed as a Zn^{+2} enzyme in vivo (Figure 25). The C-terminal domain of the enzyme contains the Zn^{+2} binding site and many of the residues involved in catalysis and substrate binding. The penta-coordinate Zn^{+2} ion interacts with three ligands from the protein, Glu^{195}, His^{271} and His^{287} as well as the C-4, C-5 hydroxyl groups of the substrate analogue inhibitor carbaphosphonate. The positioning of Zn^{+2} in the active site allows speculation about the role that it might be playing during the enzyme catalysis (Figure 26). For example, given its polarizable nature, Zn^{+2} can facilitate oxidation of C-5 hydroxy group in DAHP and reduction of the C-5 carbonyl group in intermediate **B**. At the same time, it serves to immobilize the C-4, C-5 edge of intermediate **D** during the intramolecular aldol condensation. This chelation will allow rotation in intermediate **E** only about the C-5, C-6 carbon-carbon bond but immobilizes the C-4, C-5 bond. The stereochemistry of the intramolecular aldol condensation may thus be controlled.
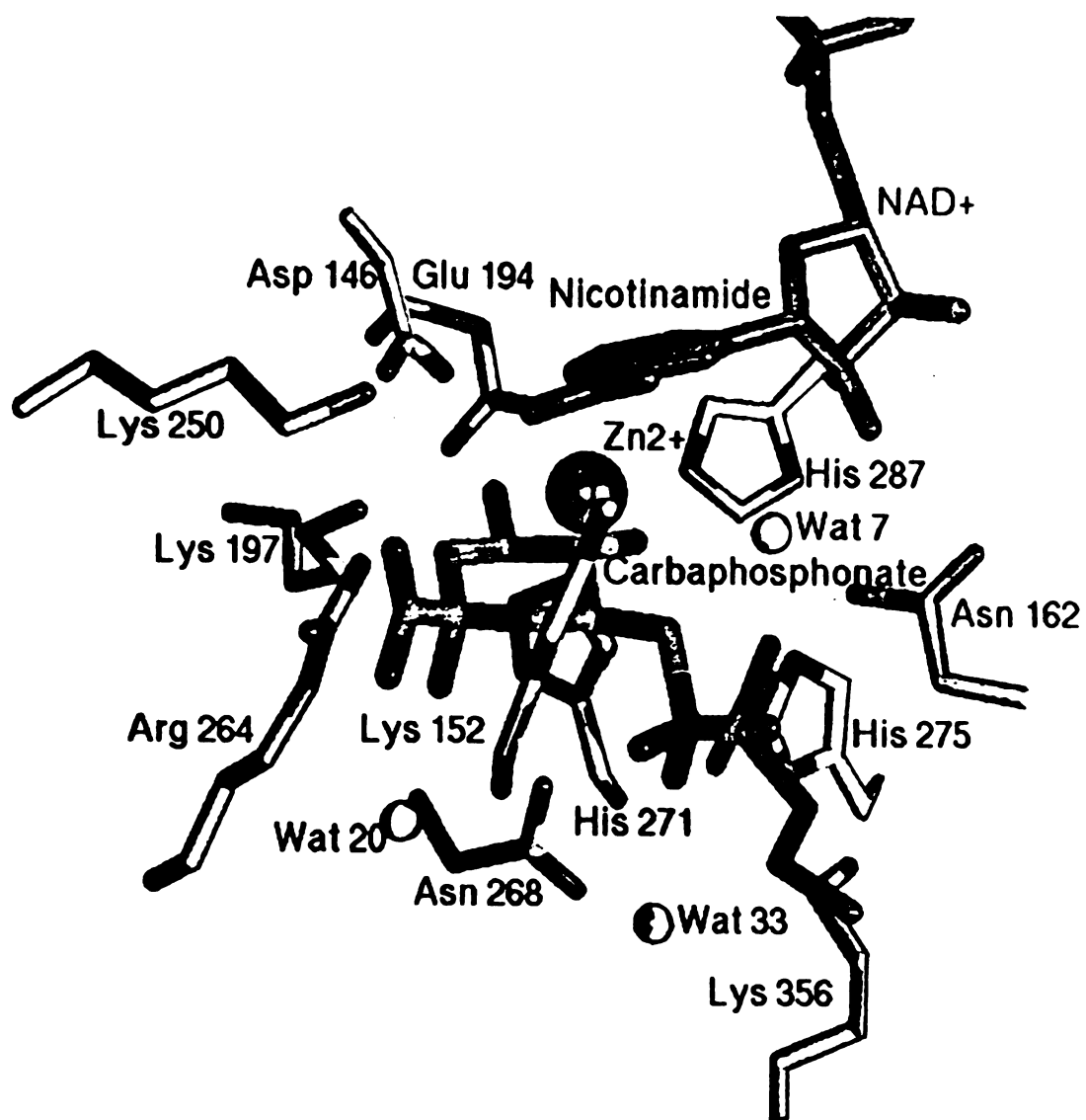
Figure 25. Active site of DHQ synthase.

DA

cat

NA

③

Figu

cis-

syn

con

ver

sin

the

oth

the

Zn

bu
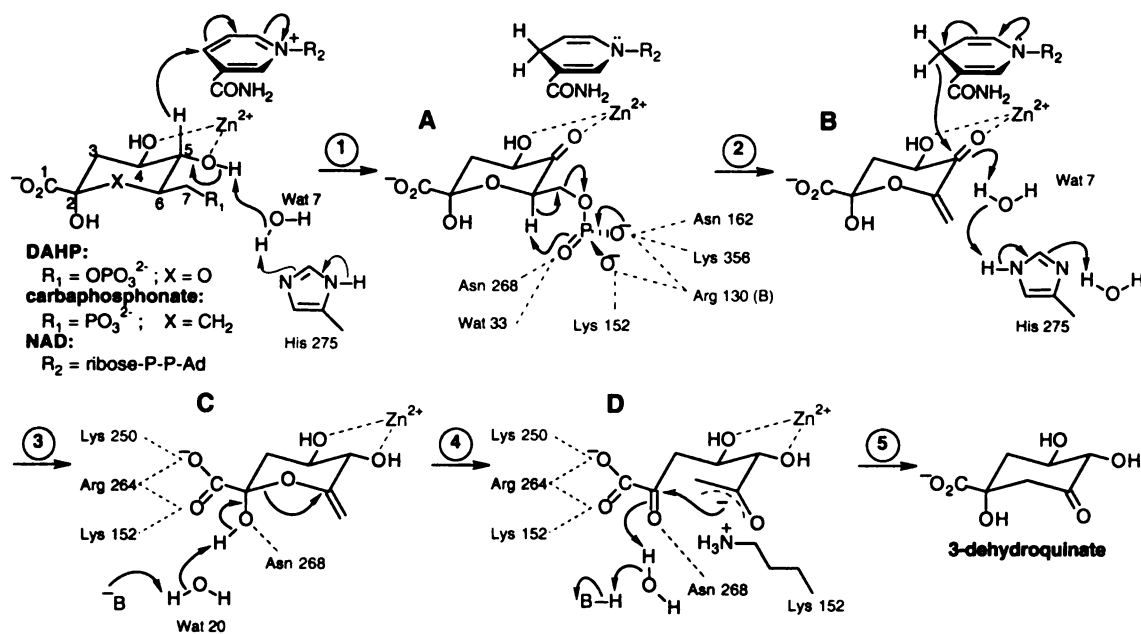
Figure 26. Interactions postulated to occur at the active site of DHQ synthase.

Rationale Behind Inhibitor Design

This study attempts to investigate the inhibition of DHQ synthase based on simple *cis*-vicinal diol complexation to a metal co-factor. Past inhibition studies with DHQ synthase have always been performed with the Co^{+2} enzyme due to practical considerations. The Frost group has now successfully purified *E. coli* DHQ synthase in a very stable Zn^{+2} form by simply replacing Co^{+2} in the purification buffers with Zn^{+2}. The similarity of k_{cat} and K_m for the Co^{+2} and Zn^{+2} enzymes suggests that no major changes in the nature of mechanism of catalysis occur when one metal is substituted with the other.[20a] However, that doesnt mean that subtle differences in active site interactions for the two metals do not exist. It has been proven that NAD^+ dissociates slower from the Zn^{+2} enzyme by a factor of about 10. Also, the presence of excess Zn^{+2} in the assay buffer leads to decreased rates showing mixed-type inhibition kinetics. This seems to

- 41 -

sugg

effec

role

form

cons

DHQ

subst

Zn^{2+}

metal

was

metal

succe

active

enzyr

comp

desig

inclu

synth

suggest that the Zn^{+2} may be binding to a second lower affinity inhibitory site. The same effect is not seen with Co^{+2}.[20a] It would therefore be quite interesting to investigate the role that metal co-factors played in binding of inhibitors to the enzyme and whether one form of the enzyme was more susceptible to inhibition over the other.

While designing potential inhibitors of DHQ synthase, two factors were taken into consideration; the crystal structure of DHQ synthase and the structures of the most potent DHQ synthase inhibitors. The crystal structure of DHQ synthase was resolved using the substrate analogue inhibitor carbaphosphonate. The crystal structure indicated that the Zn^{+2} is tightly nestled with the C-4 and C-5 hydroxyl groups of carbaphosphonate with a metal to oxygen distance of 2.3 Å and 2.2 Å respectively (Figure 25). This interaction was utilized in the designing of new DHQ synthase inhibitors. Inhibition of Zn^{+2} metalloenzymes by utilization of functionalities capable of Zn^{+2} complexation has been successfully achieved. For example, captopril, with its thiol group complexing to the active site Zn^{+2} in a monodentate fashion is a potent inhibitor of angiotensin converting enzyme (ACE).[80] Substrate based alcohol inhibitors of ACE such as 1 employ bidentate complexation of the hydroxyl and the amino group to the Zn^{+2} (Figure 27).[81] Of course, design of these inhibitors also takes into account other active site interactions but inclusion of Zn^{+2} complexation is of equal importance. Hence inhibition of DHQ synthase via inhibitors designed to bind to the metal co-factor is a viable option.
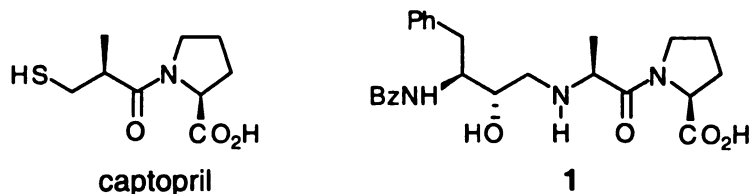
Figure 27. Inhibitors functioning via complexation of Zn^{+2}.

tran-

3 ar

and

Figu

transi

The

perha

carbo

woul

Prot

inhil

requ

diffe

Inhibition of DHQ synthase has been achieved using various substrate and transition state analogues. Cyclohexylidene phosphonate **2** and cyclohexenyl phosphate **3** are the most potent inhibitors *of E. coli* DHQ synthase with K_i values of 2.9×10^{-10} M and 1.2×10^{-10} M respectively (Figure 28).[22c]
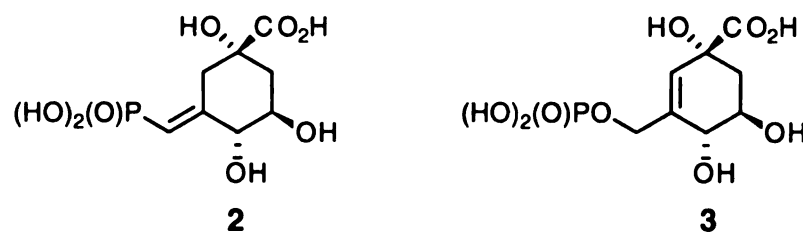
Figure 28. Unsaturated inhibitors of DHQ synthase.

These inhibitors were designed to mimic an E1cb intermediate or E1cb–like transition state during the transformation of intermediate **A** to intermediate **B** (Scheme 1). The results obtained indicated that the unsaturation at C-6 was not only tolerated but perhaps also contributed to the overall binding.

Based on the crystal structure of DHQ synthase and the inhibitory capabilities of carbocyclic inhibitors **2** and **3**, it was decided that any new inhibitor of DHQ synthase would have to incorporate a cis-vicinal diol at C-4 and C-5 and an sp^2 center at C-6. Protocatechuic acid (PCA) **7** was chosen as a suitable starting template leading towards inhibitors **4** and **5** (Figure 29). The substituted PCA derivatives **4** and **5** fulfill the requirements stated above even though they constitute a structural class radically different from that of the enzyme substrate/transition states (Figure 29).

Figu

subst

Deri

of th

and

has

phos

isost

isost

and

dete

on a

dihy

site
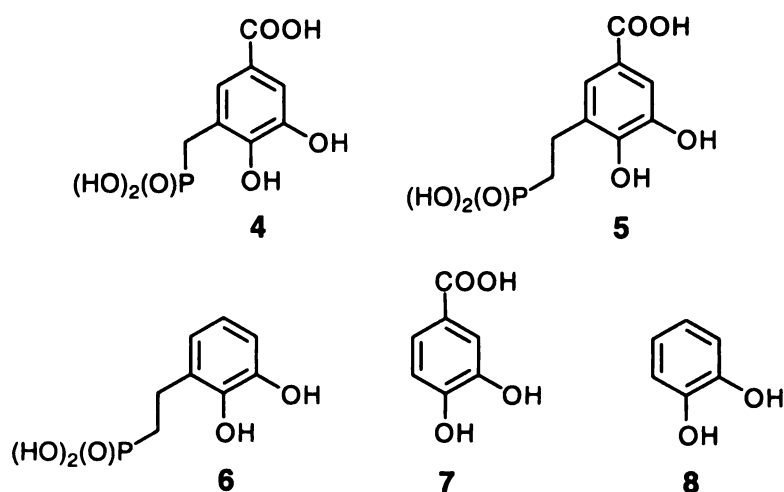
Figure 29. Aromatic compounds designed for inhibition of DHQ synthase.

The cis-vicinal diol complexation of the active site metal co-factor in carbocyclic substrate analogues is now replaced by the *ortho* dihydroxyl complexation of a catechol. Derivatives **4** and **5** still provide a trianionic ionization state and the relative orientation of the phosphonomethyl and phosphonoethyl groups relative to the backbone hydroxyls and carboxylate functionalities is maintained. Maintaining a trianionic ionization state has been proven to be important for binding to the active site of DHQ synthase.[82] The phosphonomethyl group in **4** is isosteric and the phosphonoethyl group in **5** is non-isosteric to the phosphate functionality of substrate DAHP. Inhibitors with a non-isosteric phosphate monoester are often but not always better inhibitors of DHQ synthase and hence, both **4** and **5** will be examined.[21c,22b,82,83] Compound **6** was designed to determine the contribution of the carboxylate to the overall binding. Its binding will rely on active site interactions of the phosphonoethyl group and the metal binding of the *ortho* dihydroxyl groups. PCA **7** on the other hand will derive its binding affinity via active site interactions to the carboxylate and metal interactions with the *ortho* dihydroxyl

fur

hor

car

the

of J

3.4-d

brom

The

give

meth

with

Ren

foll

pho

met

upo

inte

sarr

functionality. Differences in the inhibition of DHQ synthase by catechol homophosphonate **6** and PCA **7** will provide a good measure of the importance of the carboxylate relative to the phosphate for active site binding. Finally, catechol **8** will test the efficacy of utilizing binding of metal to the *ortho* dihydroxyl group as the sole means of achieving inhibition.

Synthesis of Phosphonate 4 and Homophosphonates 5-6

The synthesis of the PCA analogues **4** and **5** exploited commercially available 3,4-dimethoxy benzoic acid **9** (Figure 30). Fischer esterification of **9** followed by bromination of the resulting ester **10** gave 5-bromo-3,4-dimethoxy methylbenzoate **11**.[84] The substitution of the bromide with a vinylic group was achieved via a Stille coupling to give **12**. Subsequent ozonolysis of the olefin **12** resulted in 3-formyl-4,5-dimethoxy methylbenzoate **13**. Reductive iodination[85] of **13** followed by treatment of the iodide **14** with triisopropyl phosphite under reflux afforded the phosphonate intermediate **15**. Removal of the methoxy groups by treatment with an excess of boron tribromide followed by acidic removal of the carboxylate and phosphonate esters furnished PCA phosphonate **4**. The reaction of **13** with the lithium anion of tetraisopropyl methylenediphosphonate yielded the olefinic homophosphonate intermediate **16**, which upon hydrogenation under 10% Pd on carbon cleanly produced the homophosphonate intermediate **17**. Removal of the protecting groups in **17** was performed in exactly the same manner as for PCA phosphonate **4**, to afford PCA homophosphonate **5**.

Figu

dime

tetra

inter

redu

tribr
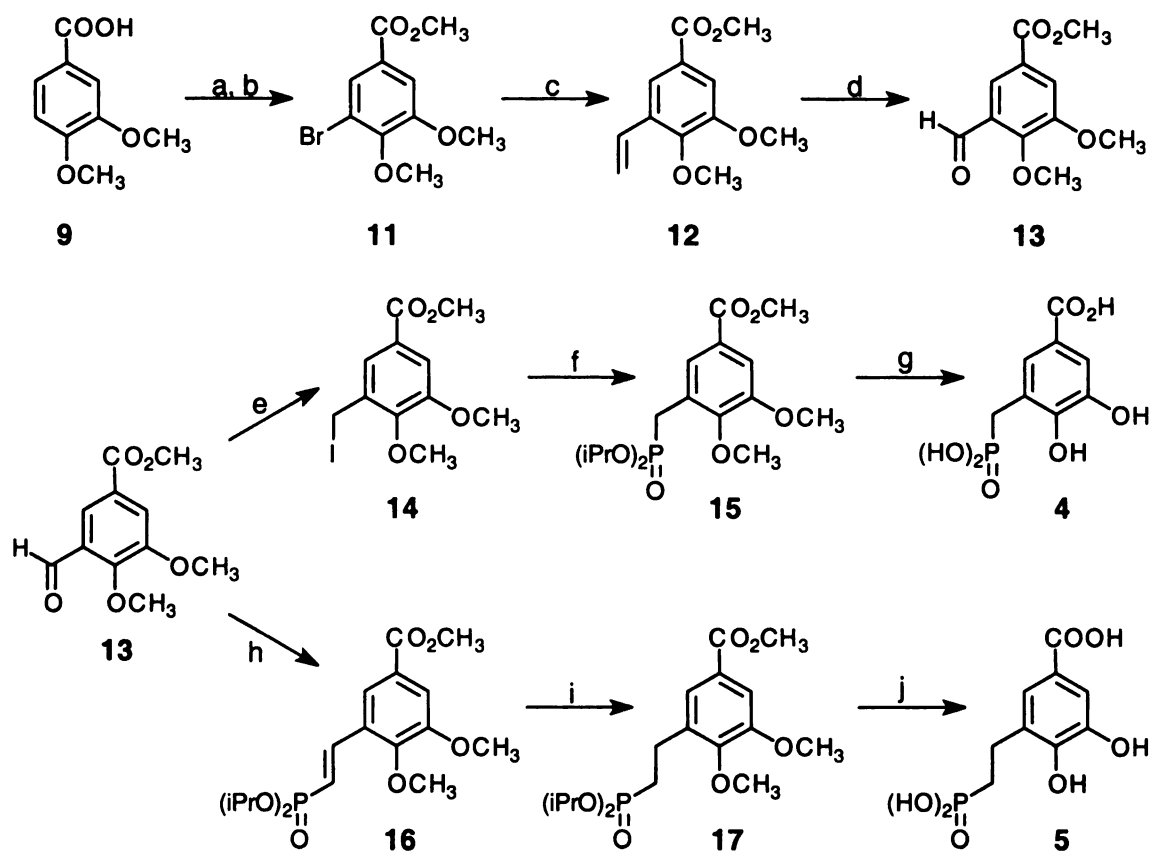
Key: (a) MeOH, H₂SO₄, 98%; (b) Br₂, AcONa, AcOH, 70 °C, 97%; (c) Bu₃Sn(CH=CH₂), Pd(PPh₃)₄, HMPA, 65 °C, 63%; (d) O₃, CH₂Cl₂, -78 °C, 91%; (e) [(CH₃)₂HSi]₂O, TMSCl, NaI, AcCN, reflux; (f) P(OiPr)₃, toluene, reflux, 23%; (g) (i) BBr₃, CH₂Cl₂, -78 °C to rt; (ii) conc. HCl, 62%; (h) n-BuLi, [(iPrO)₂P(O)]₂CH₂, THF, -78 °C to rt, 34%; (i) H₂, 10% Pd/C, MeOH, 76%; (j) (i) BBr₃, CH₂Cl₂, -78 °C to rt; (ii) conc. HCl, 88%.

Figure 30. Synthesis of PCA phosphonate 4 and PCA homophosphonate 5.

Catechol homophosphonate **6** was synthesized using commercially available 2,3-dimethoxy benzaldehyde **18** (Figure 31). Wadsworth-Emmons reaction of **18** using tetraisopropyl methylenediphosphonate yielded the required catechol homophosphonate intermediate **19**, which upon hydrogenation using catalytic 10% Pd on C resulted in reduced homophosphonate intermediate **20**. Subsequent deprotection with excess boron tribromide and hydrochloric acid afforded the catechol homophosphonate **6**.

H

Key
75

Figu

dehy

conv

spec

quan

Co

this w

DHQ

comp

comp

show

deter
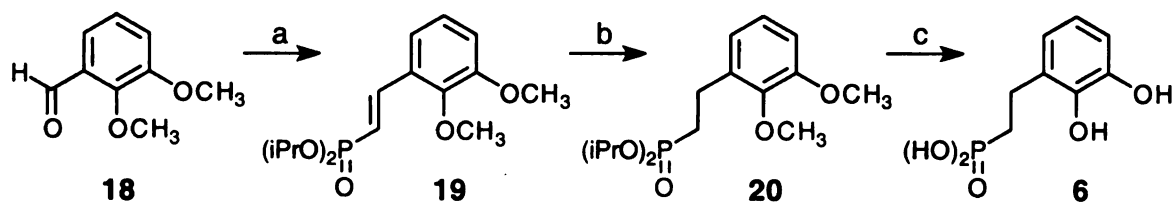
Key: (a) n-BuLi, [(iPrO)₂P(O)]₂CH₂, THF, -78 °C to rt, 95%; (b) H₂, 10% Pd/C, MeOH, 75%; (c) (i) BBr₃, CH₂Cl₂, -78 °C to rt; (ii) conc. HCl, 97%.

Figure 31. Synthesis of catechol homophosphonate 6.

Inhibition Studies of 4-8 with DHQ synthase

Inhibition of DHQ synthase was studied using a coupled enzyme assay with DHQ dehydratase being used as the coupling enzyme.[86] DHQ dehydratase catalyzes the conversion of DHQ to 3-dehydroshikimate (DHS), the formation of which can be spectrophotometrically detected at 234 nM, thus providing a means for continuous quantitation of DHQ formation.[8] The Michaelis constant (K_m) for DAHP binding to the Co^{+2} form of DHQ synthase has been reported to depend on the assay method[20a] and for this work has been taken as 18 μM. The K_m for the binding of DAHP to the Zn^{+2} form of DHQ synthase was measured to be 16 μM. Inhibition constants (K_i) were measured for compounds **4-8** and are reported in Table 1. Compounds **4-7** exhibited classical competitive inhibition of both forms of DHQ synthase. Surprisingly, catechol **8** also showed some level of inhibition although its K_i value could be estimated only from an I_{50} determination.

Ta

syr

ver

repl

Fi

Table 1. Inhibition constants (μM) for binding to the Co^{+2} and Zn^{+2} forms of DHQ synthase.

Enzyme	Inhibitor				
	4	**5**	**6**	**7**	**8**
DHQ synthase-Co+2	21	5	200	44	880
DHQ synthase-Zn+2	0.35	1.7	90	65	630

K_i values were obtained from the Dixon plot of the reciprocal initial velocities versus inhibitor concentrations at fixed substrate concentrations (Figure 32). The Dixon replot gave a line passing through the origin indicating competitive inhibition.[87]
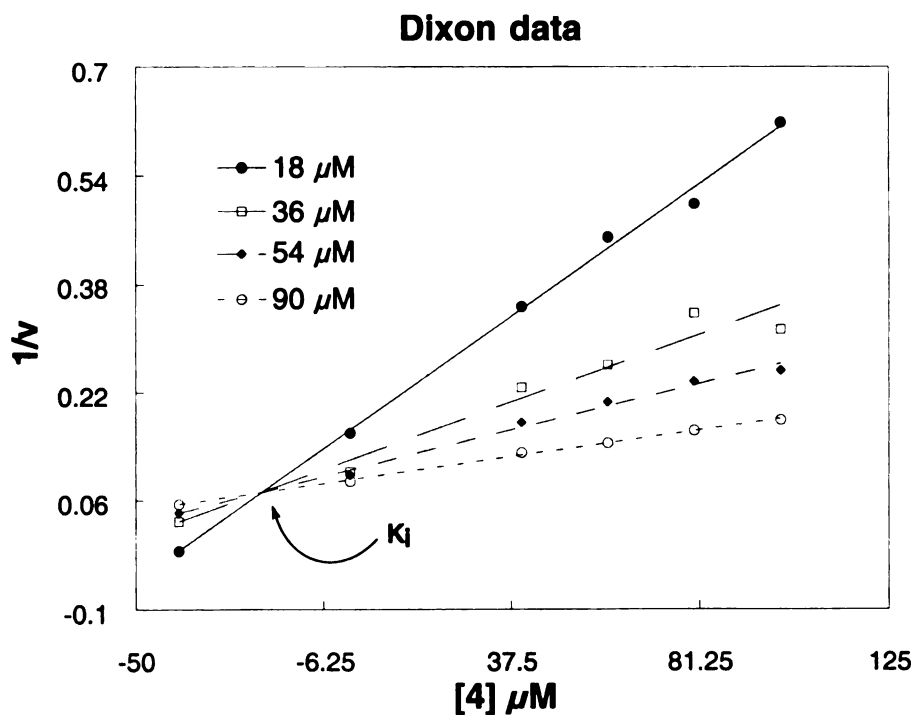
Figure 32. Dixon plot for PCA phosphonate 4.

com
velo
DA
the

Zn^{2}
the
sub
wa
tre
dis
sin
rel
bia
di
6
v
di

Lineweaver-Burke and Hanes-Woolf plots also gave results consistent with competitive inhibition. I_{50} determinations were done by plotting the reciprocal initial velocity versus inhibitor concentrations at 18 μM DAHP for the Co^{+2} enzyme or 16 μM DAHP for the Zn^{+2} enzyme. The x-intercept gave the value for the I_{50}, half of which was the K_i.

Interpretation of the Inhibition Pattern Exhibited by Aromatic Inhibitors 4-8

The first piece of information that could be gleaned from these results was that the Zn^{+2} form of the enzyme was more susceptible to inhibition than the Co^{+2} form except in the case of PCA 7. The results obtained with inhibitors 4 and 5 also highlighted the subtle differences between the two forms of DHQ synthase. PCA homophosphonate 5 was a better inhibitor of the Co^{+2} enzyme than PCA phosphonate 4, while the reverse trend was observed in case of the Zn^{+2} enzyme. The Zn^{+2} enzyme evidently did not discriminate between a carboxylate and a homophosphonate group as indicated by the similar reduction in enzyme inhibition for catechol homophosphonate 6 and PCA 7 relative to PCA homophosphonate 5. The Co^{+2} form of the enzyme however exhibited a bias between binding to a carboxylate or a homophosphonate functionality based on the different extents to which enzyme inhibition was reduced for catechol homophosphonate 6 and PCA 7 relative to PCA homophosphonate 5. These observations indicate the slight variations that exist in the binding interactions between the two enzymes. The inhibition displayed by catechol 8 does indicate the minimal level of inhibition that can be obtained

wh

av

fac

fu

to

Th

str

ar

ac

aci

ga

as

Ap

the

whi

inte

aci

ela

sy

uni

fur

when all other functionalities are missing on an inhibitor and the only interactions available are those between the C4-C5 diol and the metal co-factor.

This is the first inhibition study performed with DHQ synthase utilizing a Zn^{+2} co-factor as opposed to a Co^{+2} co-factor. DHQ synthase has also been reported[88] to be functional with metals like Ni^{+2}, Cd^{+2}, Eu^{+3} and Sm^{+3} and this study makes it worthwhile to consider how various metal co-factors might influence binding of substrate/ inhibitors. The activity observed with the PCA analogues is quite important considering their novel structural simplicity, mode of inhibition and ease of synthesis. Results discussed with the aromatic inhibitors of DHQ synthase assume significance because of the ability to account for the accumulation of DAH as a by-product in the microbial synthesis of gallic acid.[53] This was true even when *aroB*-encoded DHQ synthase was overexpressed in the gallic acid synthesizing recombinant *E. coli*. As was illustrated in Figure 17, PCA occurs as an intermediate in the microbe catalyzed conversion of glucose to gallic acid. Apparently, the PCA is inhibiting DHQ synthase resulting in accumulation of DAHP in the cytosol. Dephosphorylation of DAHP results in its export from the cell as DAH, which appears as the contaminant in the fermentation broth. PCA also occurs as an intermediate in the biocatalytic synthesis of vanillin,[37] catechol[56] and *cis,cis*-muconic acid.[56a] Its inhibition of DHQ synthase therefore constitutes a major impediment in the elaboration of high yielding microbial synthesis of these compounds.

In conclusion, PCA phosphonate **4** and PCA homophosphonate **5** were synthesized and successfully tested as inhibitors of DHQ synthase. These compounds are unique given their structural characteristics as well as mode of action and they represent a fundamental departure from previously reported carbocyclic inhibitors. But perhaps their

most important feature is their ability to discriminate between the Co^{+2} and Zn^{+2} forms of

DHQ synthase. These compounds can act as valuable templates on which future and

hopefully better inhibitors of DHQ synthase can be based upon.

int

ste

ch.

Illi

m

ve

(Fi

Figu

infl

sca

The

CHAPTER 3

BIOCATALYTIC SYNTHESIS OF SHIKIMIC ACID USING RECOMBINANT *ESCHERICHIA COLI*

Introduction

Shikimic acid (SA) is a seven-carbon carbocyclic intermediate occurring as an intermediate in the common pathway for aromatic amino acid biosynthesis.[89] The stereochemical disposition of tunable functional groups in SA makes it an attractive chiral synthon for use in various synthetic schemes.[90] It is isolated from the fruits of the *Illicium* plants at a cost of approximately $10,000/kg,[91] precluding its application in moderate to large scale synthetic processes. For example, SA has been reported to be a very convenient starting material in the synthesis of the neuraminidase inhibitor GS4104 (Figure 33).[92]
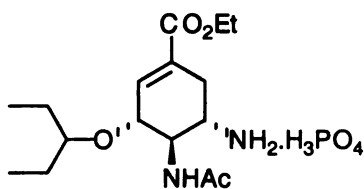
GS-41014

Figure 33. Neuraminidase inhibitor GS4104

This compound is currently being marketed by Hoffman-LaRoche as its new influenza drug, Tamiflu™. Use of SA as the starting material of choice for industrial scale production of GS4104 will depend on identifying a cheap and reliable source for it. The common pathway of *E. coli* has been successfully manipulated for the accumulation

of

w

re

an

ec

ca

pr

of

the

act

Re

act

by

pho

exp

wit

of

am

ph

in

bio

of various intermediates and secondary metabolites. Interfacing the shikimate pathway with enzymes alien to the pathway or to the microbe itself have also met with success. A recombinant *E. coli* biocatalyst can therefore be designed, capable of producing large amounts of SA at a low cost, making the use of SA in industrial scale synthesis economically viable.

The key to achieving high titers and yields of SA is dependent on improving carbon flow into the shikimate pathway. Expression levels of DAHP synthase have proven to be critical for increasing aromatic amino acid biosynthesis. As the first enzyme of the pathway, DAHP synthase dictates the amount of cellular carbon being directed into the common pathway and hence towards shikimate synthesis. Regulation of the in vivo activity of this enzyme is achieved via transcriptional repression and feedback inhibition. Removal of these impediments have helped in achieving respectable DAHP synthase activity levels. However, in vivo DAHP synthase activity is also known to be influenced by intracellular concentrations of the substrates D-erythrose 4-phosphate (E4P) and phosphoenolpyruvate (PEP). Availability of E4P has been reported to hinge on expression levels of the enzyme transketolase. The enzyme transaldolase is also involved with E4P biosynthesis, but its overexpression does not offer any advantage relative to that of transketolase.[72] On the other hand, PEP concentration can be directly improved by amplification of the enzyme PEP synthase. Also, it is known that PEP is involved in the phosphoenolpyruvate-carbohydrate phosphotransferase (PTS) system of glucose transport in *E. coli*. Hence, introduction of a non-PEP dependent glucose uptake system into the biocatalyst can also indirectly alleviate PEP limitation.

K-

in

pr

a.n

ter

itse

util

pro

cor

op

D:

Ex

D.

Rl

A

sy

sh

h.

In this Chapter, the synthesis of SA has been investigated utilizing various *E. coli* K-12 (RB791) biocatalysts under fed-batch fermentor conditions. The effects of increased transketolase, transaldolase and PEP synthase expression levels on SA production were studied. Synthesis of SA was also examined in an *E. coli* strain lacking a native PTS glucose transport system. Transaldolase amplification gave no increment in terms of SA yield or titer. The effect of transketolase overexpression was encouraging by itself but was quite dramatic when coupled with that of PEP synthase. Use of a non-PEP utilizing glucose facilitator uptake system also gave significant improvements in SA production. Titers and yields for SA production by all the biocatalysts are reported and compared.

Synthesis of SA was also examined in a biocatalyst derived from *E. coli* B as opposed to RB791. *E. coli* B lacks a number of proteases, which could result in higher DAHP synthase and transketolase activity levels, especially in the stationary phase.[93] Examination of these strains under fed-batch fermentor conditions indicated enhanced DAHP synthase and transketolase activity levels as compared to the corresponding RB791 version. However, no improvement in SA production was observed.

Biocatalysts and Fed-Batch Fermentation Conditions

A) Shared Genomic Traits and Plasmid Elements

Three constructs, SP1.1, SP1.1*pts* and EB1.1, were used as the hosts for SA synthesis. The SP1.1 host strain was derived from RB791 and lacks catalytically active shikimate kinase resulting in SA accumulation. Construction of SP1.1 began with the homologous recombination of the *aroB* gene into the *serA* locus of *E. coli* RB791

resulting in RB791 *serA::aroB*.[48,76] RB791 *serA::aroB* was then subjected to two successive P1 phage-mediated transductions to transfer the *aroL478*::Tn*10* and *aroK*::Cm[R] loci of ALO807 onto the genome and eliminating shikimate kinase activity.[11] SP1.1*pts* was derived from SP1.1 and lacks a native PTS system for glucose uptake. This was achieved by P1 phage-mediated transduction of Δ(*ptsHptsIcrr*)::Kan[R] thereby disrupting the *ptsH*, *ptsI* and *crr* loci involved with *E. coli* glucose uptake (Figure 21). P1 phage was propagated from TP2811, which was generously provided by Professor Sophie Lévy.[94] EB1.1 was constructed from *E. coli* B and incorporates the same deletions as in SP1.1. All strains lack the capability for de novo aromatic amino acid and aromatic vitamin biosynthesis, necessitating their growth in medium supplemented with L-phenylalanine, L-tryptophan, L-tyrosine, *p*-hydroxybenzoic acid, *p*-aminobenzoic acid, and 2, 3-dihydroxybenzoic.

DAHP synthase is known to be regulated by feedback inhibition by aromatic amino acids. DAHP synthase catalyzes the condensation of E4P to PEP resulting in DAHP, the first committed intermediate in the aromatic amino biosynthetic pathway. Elevated expression levels of DAHP synthase are therefore critical for high SA yields. All SA producing strains hence utilize a plasmid localized mutant isozyme of DAHP synthase, designated as *aroF*[FBR], which is feedback insensitive to the aromatic amino acids.[65,76] However, increased activity levels of DAHP synthase meant that *aroB* encoded native DHQ synthase levels were now inadequate to convert the higher levels of DAHP to DHQ at a rate fast enough to avoid DAHP accumulation.[95] This problem was circumvented by site-specific insertion of an additional copy of *aroB* into the genomic *serA* locus of the *E. coli* strain via homologous recombination. Temperature sensitive

plasmid pKL3.82A was used for the homologous recombination.[48] The procedure used

for the recombination is described in Chapter 5 of this thesis. The *serA* locus encodes for

3-phosphoglycerate dehydrogenase, a key enzyme required for L-serine biosynthesis.[96]

This strategy hence required localization of the *serA* gene on all plasmids, which also

provided a convenient method for plasmid maintenance during fed-batch fermentor

cultivation. Shikimate dehydrogenase encoded by the *aroE* gene is known to be feedback

inhibited by SA resulting in incomplete conversion of DHS to SA.[95a] Overexpression of

aroE is therefore necessary for improved SA yields and low DHS accumulation. This

was achieved by plasmid localization of the *aroE* gene under the control of the *tac*

promoter. The sequence of events for the construction of SP1.1 and the structure of the

basic plasmid pKD12.112A are as shown in Figure 34.

Host Strain:

RB791

   │ *serA::aroB*
   │ (homologous recombination)
   ▼

RB791 *serA::aroB*

   │ *aroL::*Tn*10*
   │ (P1 transduction)
   ▼

┌─────────────────────────────────┐
│ RB791 *serA::aroB aroL::*Tn*10* │
│ ‖   │
│ **SP1.3**   │
└─────────────────────────────────┘

   │ *aroK::*Cm^R
   │ (P1 transduction)
   ▼

┌───┐
│ RB791 *serA::aroB aroL::*Tn*10 aroK::*Cm^R │
│ ‖   │
│ **SP1.1**   │
└───┘

Plasmid:

pKD12.112
aroF^{FBR}

P$_{tac}$P$_{aroE}$ *aroE*
serA
β-lac
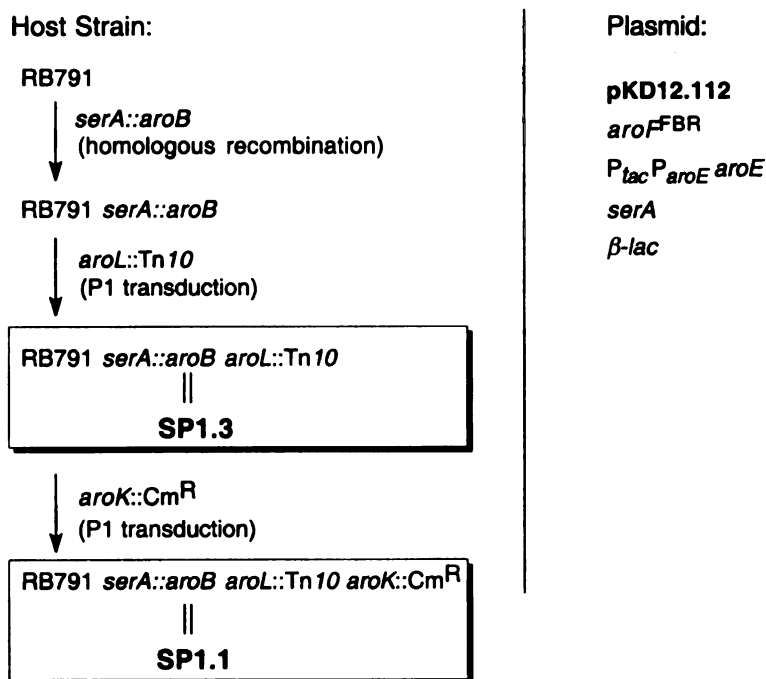
Figure 34. Strain SP1.1 and Plasmid pKD12.112A

B) Fed-Batch Fermentor Conditions

Fed-batch fermentations were performed in a 2.0 L capacity Biostat MD B-Braun fermentor equipped with a DCU system and a Dell Optiplex Gs⁺ 5166M personal computer utilizing B-Braun MFCS/win software for data acquisition and automatic process monitoring. The fermentation vessel was modified by introduction of a stainless steel baffle cage containing four 1/4" x 4" baffles for all fermentations. Fermentations were run at 33 °C, pH 7.0 and the dissolved oxygen (D.O.) level was maintained at 10%. All three parameters were controlled by PID control loops. A Metler-Toledo 12 mm sterilizable O_2 sensor fitted with an Ingold A-type permeable membrane was used for monitoring D.O. levels.

Inoculants were initially grown in 5 mL of complete M9 medium for 24 h at 37 °C and 250 rpm. This culture was then transferred to 100 mL of the same medium and grown under identical conditions for 10 h before being transferred to the fermentor. The initial glucose concentration was kept at 30 g/L. The entire fermentation can be divided into three stages, each of which corresponds to a different procedure for controlling the D.O. level at 10%. In the first stage, the air flow was kept constant at 0.06 L/L/min and the stirrer was ramped up from 50 rpm to 750 rpm at a rate sufficient enough to maintain the D.O. at 10%. Once the stirrer reached its preset maximum of 750 rpm, the mass flow controller increased the air flow from 0.06 L/L/min to 1.0 L/L/min. These two stages take anywhere from 9 h to 18 h for completion depending on the strain under investigation. Until this stage, except for the initial 30 g/L, no additional glucose was added. As soon as the air flow reached 1.0 L/L/min at a constant impeller speed of 750 rpm, the glucose pump was switched on and hereafter the D.O. level was maintained

st
g
to
g
u
ir
si
ar

in
de
66
w
a
o
c
f

steady at 10% by varying the stirrer from 750 rpm to 1600 rpm. Concentration of the glucose solution added was 60% (w/v). The rate of glucose addition was controlled so as to maintain a glucose concentration of approximately 25 g/L in the fermentation at any given time. Determination of glucose concentrations during the fermentation was done using the Glucose (HK) 20 assay kit purchased from Sigma. After the third stage was initiated, glucose concentration in the fermentation culture was measured every hour for six hours. For the next six hours, glucose concentration was monitored every two hours and thereafter measurements were done every six hours until the end of the run.

Fermentation runs typically entered logarithmic phase of growth 6 h after inoculation and usually achieved stationary growth phase after 24 h. Microbial cell density normally reached 25 g/L to 30 g/L dry cell weight. Fermentations were run for 60 h. The cultures took on a dark color as the fermentation progressed and after 60 h were deep black in color. Rate of production of SA generally picked up after 18 h and attained a plateau in 54 h to 60 h. DHS and quinic acid (QA) accumulation was also observed in all the fermentations. The formation of these by-products is discussed in detail in Chapter 4 of this thesis. In fact, the dark color associated with all SA fermentations is due to the air oxidation of DHS to gallic acid.

Overexpression of Transketolase and Transaldolase Under Fed-

Batch Fermentor Conditions

The first biocatalyst which was tested as a shikimate producer was SP1.1/pKD12.112A. Plasmid pKD12.112A carries a copy of $aroF^{FBR}$ under the control of its native promoter, a copy of the $aroE$ locus under the control of the tac promoter, a copy of the $serA$ gene and the β-lac gene conferring Ap resistance. This strain lacks any capability to alleviate E4P limitations. The construction of pKD12.112A was initiated by ligation of the 1.2-kb $P_{tac}aroE$ fragment into pKL4.20B (Figure 35). Plasmid pKL4.20B had been previously created in the laboratory and carries the $aroF^{FBR}$ locus on a pSU18 vector. Vector pSU18 is a 2.3-kb plasmid carrying a $p15A$ origin of replication and has a high copy number of approximately 12 per cell.[97] It also contains a lac promoter and a genetic marker encoding for Cm resistance. The $P_{tac}aroE$ fragment was obtained by PCR amplification from pIA321,[98] digested with KpnI and ligated with pKL4.20B (3.6-kb) which had been linearized by KpnI treatment. This resulted in the 4.8-kb plasmid, pKD12.036A (Figure 35). The orientation of the $P_{tac}aroE$ locus in pKD12.036A is in the opposite direction as that of $aroF^{FBR}$. The $serA$ locus was obtained by digestion of pD2625[95b] with EcoRV and DraI. Blunt end ligation of this 1.9-kb fragment into pKD12.036, which had been linearized by SmaI digestion, afforded the 6.7-kb plasmid pKD12.047A (Figure 36). The orientation of the $serA$ gene was in the same direction as that of $P_{tac}aroE$. The β-lac gene was amplified by PCR from pUC18, treated with NcoI and ligated into the NcoI site of pKD12.047A resulting in the 7.7-kb plasmid pKD12.112A (Figure 37).
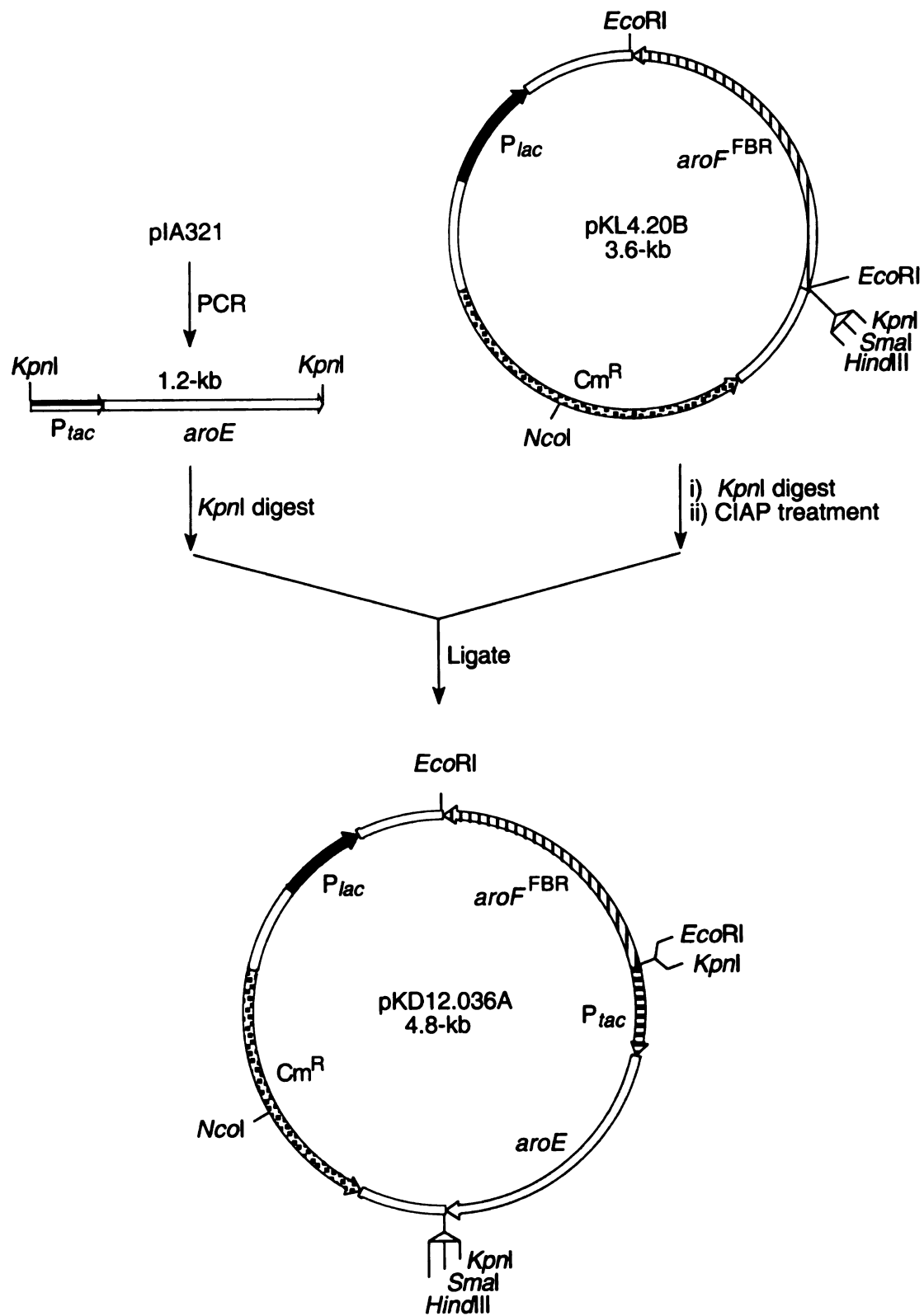
Figure 35. Preparation of Plasmid pKD12.036A.
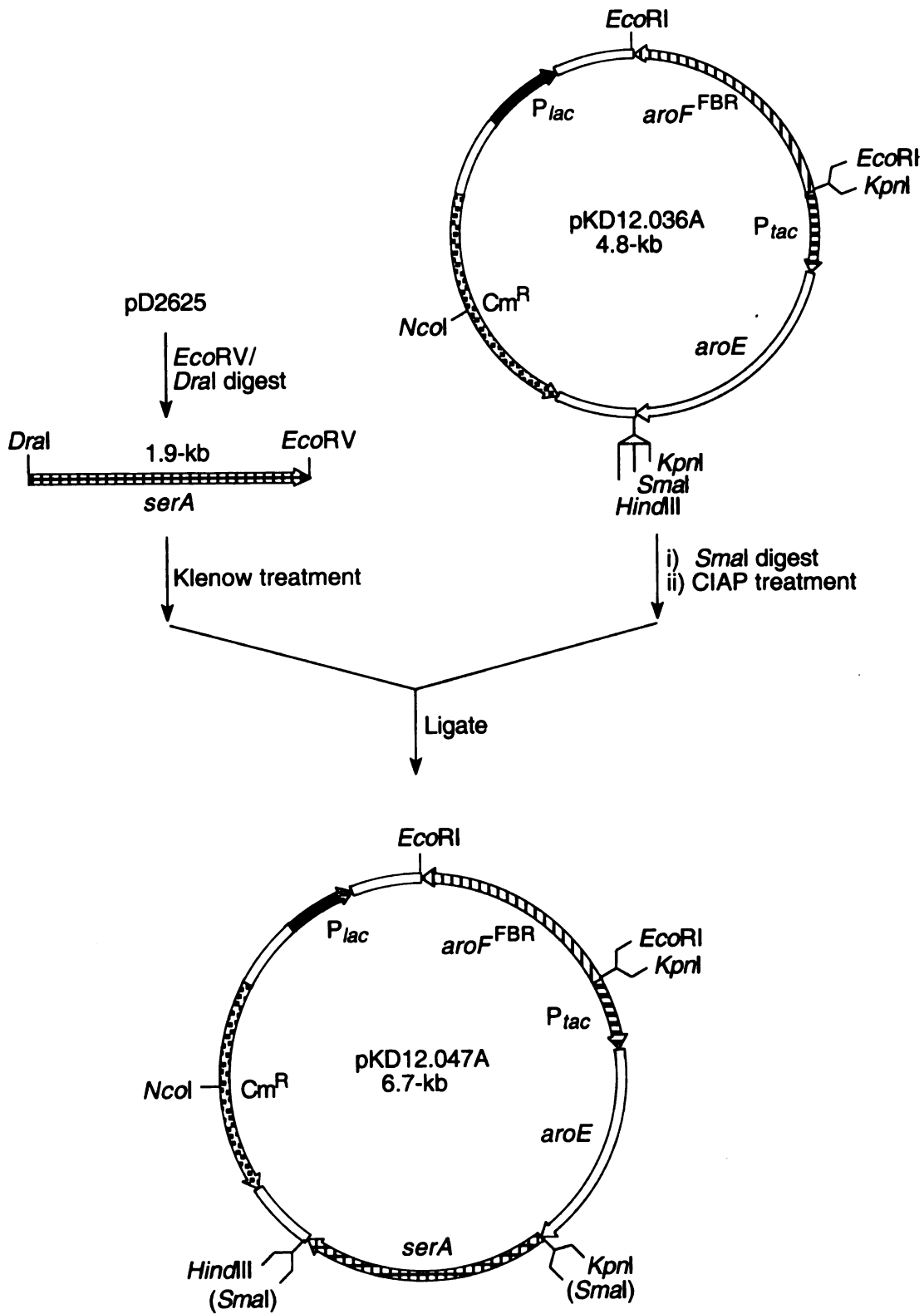
Figure 36. Preparation of Plasmid pKD12.047A.

pUC18

PCR

NcoI   1.0-kb   NcoI

Ap^R

NcoI digest

pKD12.047A
6.7-kb

P$_{lac}$
aroF^{FBR}
EcoRI
Kpnl
P$_{tac}$
aroE
serA
NcoI — Cm^R
EcoRI
HindIII
(SmaI)
KpnI
(SmaI)

i) NcoI digest
ii) CIAP treatment

Ligate

pKD12.112A
7.7-kb

EcoRI
P$_{lac}$
aroF^{FBR}
EcoRI
Kpnl
NcoI
P$_{tac}$
Ap^R
aroE
NcoI
serA
HindIII
(SmaI)
KpnI
(SmaI)
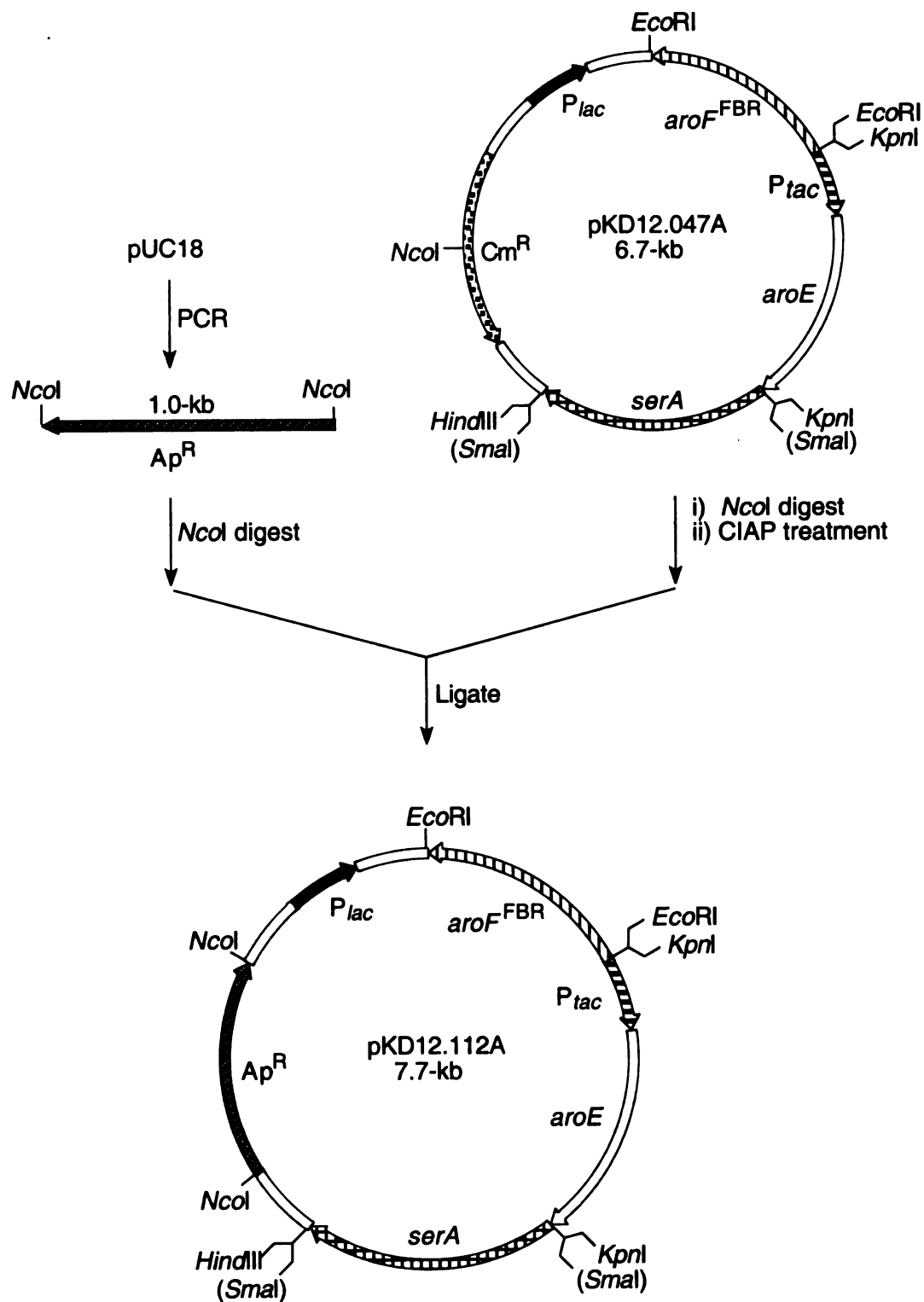
Figure 37. Preparation of Plasmid pKD12.112A.

SP1.1/pKD12.112A was examined under fed-batch fermentor conditions. After

60 h this biocatalyst had produced 38 g/L SA in 12% yield (mol of SA produced/ mol of

glucose consumed) (Figure 38) (entry 1, Table 4). The maximum productivity of SA was

between 18 h and 36 h, approximately 1 g/L/h, after which it slowed down to 0.5 g/L/h,

but production never leveled off. Accumulation of DHS and QA as by-products was also

observed. The total yield of the fermentation, taking in account SA, DHS and QA, was

15%. DAHP synthase specific activity was measured every six hours, starting at 12 h

into the run, up to 48 h. DAHP synthase specific activity remained moderately high and

stable throughout the run and showed only a slight decline from 42 h to 48 h (entry 1,

Table 2).
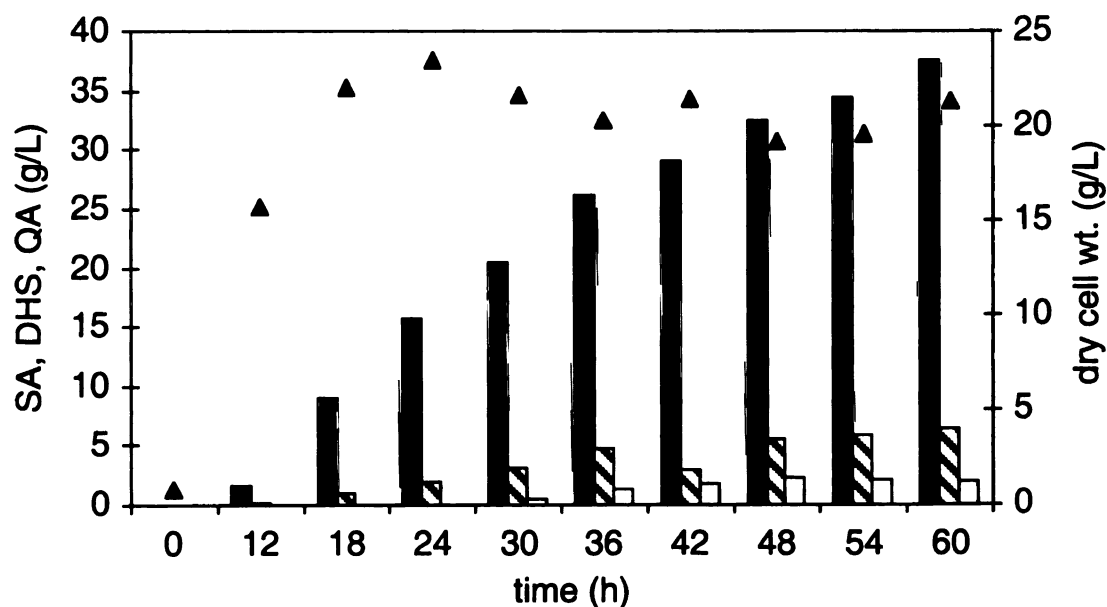
Figure 38. SP1.1/pKD12.112A fed-batch fermentation time course.
▲ Dry cell wt. (g/L); ■ SA (g/L); ▨ DHS(g/L); ☐ QA(g/L).

pMF51A

*Bam*HI digest

*Bam*HI   2.2-kb   *Bam*HI

tktA

Klenow treatment

*Eco*RI

*Nco*I   P*lac*

aroF^FBR   *Eco*RI / *Kpn*I

Ap^R   pKD12.112A 7.7-kb   P*tac*

aroE

*Nco*I

*Hind*III (*Sma*I)   serA   *Kpn*I (*Sma*I)

i) *Hind*III digest
ii) Klenow treatment
iii) CIAP treatment

Ligate

*Eco*RI

*Nco*I   P*lac*

aroF^FBR   *Eco*RI / *Kpn*I

P*tac*

Ap^R   pKD12.138A 9.9-kb   aroE

*Nco*I

(*Hind*III)   *tktA*   serA   *Kpn*I (*Sma*I)

(*Hind*III) (*Sma*I)
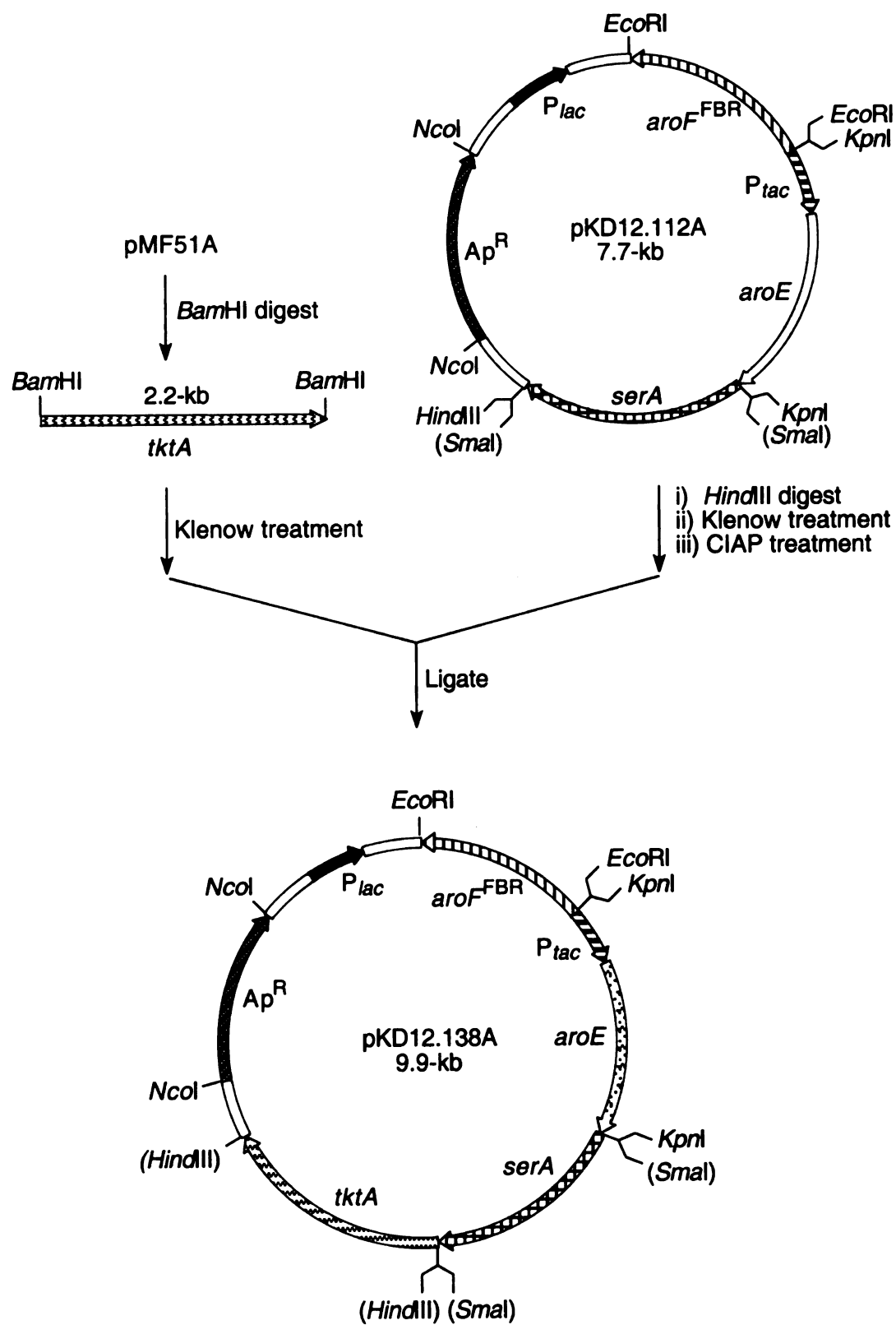
Figure 39 . Preparation of Plasmid pKD12.138A.

As stated before, DAHP synthase activity is known to be limited by E4P availability, which is in turn controlled by transketolase and transaldolase expression.[68] These enzymes are operative in the non-oxidative pentose phosphate pathway and are responsible for the interconversion of C-4, C-5, C-6 and C-7 aldoses and ketoses (Figure 20). Therefore, the next logical avenue to pursue was to amplify either transketolase or transaldolase expression. Plasmid pKD12.138A was created by cloning of the *tktA* locus, encoding for transketolase, into pKD12.112A (Figure 39). Plasmid pKD12.112A was digested with *Hind*III and treated with Klenow fragment. Following digestion of pMF51A[72a] with *Bam*HI, the 2.2-kb *tktA* fragment was blunt ended using Klenow fragment and ligated into linearized pKD12.112A using T4 ligase resulting in the 9.9-kb plasmid, pKD12.138A. The *tktA* gene is transcribed in the same direction as the *serA* gene.

Figure 40. SP1.1/pKD12.138A fed-batch fermentation time course.
▲ Dry cell wt. (g/L); ■ SA (g/L); ▨ DHS(g/L); ☐ QA(g/L).

Plasmid pKD12.138A was transformed into SP1.1 and this biocatalyst was examined under fed-batch fermentation conditions. At the end of 60 h, SP1.1/pKD12.138A had produced 52 g/L of SA in 18 % (mol/mol) yield (Figure 40) (entry 2, Table 4). A corresponding increase in accumulation of DHS and QA was also observed and the total yield (mol/mol) was determined to be 24% from glucose. The DAHP synthase activity levels were however measured to be much lower than those for SP1.1/pKD12.112A (entry 2, Table 2). A plausible reasoning for this decline is the metabolic burden imposed on the system due to expression of the additional *tktA* gene.

Table 2. DAHP synthase activities (μmol/min/mg) for PEP limited biocatalysts.

Entry no.	Strain	[SA] (g/L)	DAHP synthase specific activities			
			12 h	24 h	36 h	48 h
1	SP1.1/pKD12.112A	38	0.37	0.35	0.37	0.31
2	SP1.1/pKD12.138A	52	0.068	0.19	0.13	0.096
3	SP1.1/pSC4.295A	32*	1.36	0.47	0.46	0.61

* Amount accumulated after 48 h as opposed to 60 h.

Alleviation of E4P limitation was also attempted by localization of the *talB* locus, encoding for transaldolase, in plasmid pSC4.295A (Figure 41). The 1.3-kb *talB* fragment was isolated by digestion of pMF52A[72a] with *Nco*I. Plasmid pKD12.047A was linearized by treatment with *Nco*I and ligated with the *talB* gene using T4 ligase resulting in the 8.0-kb plasmid, pSC4.295.
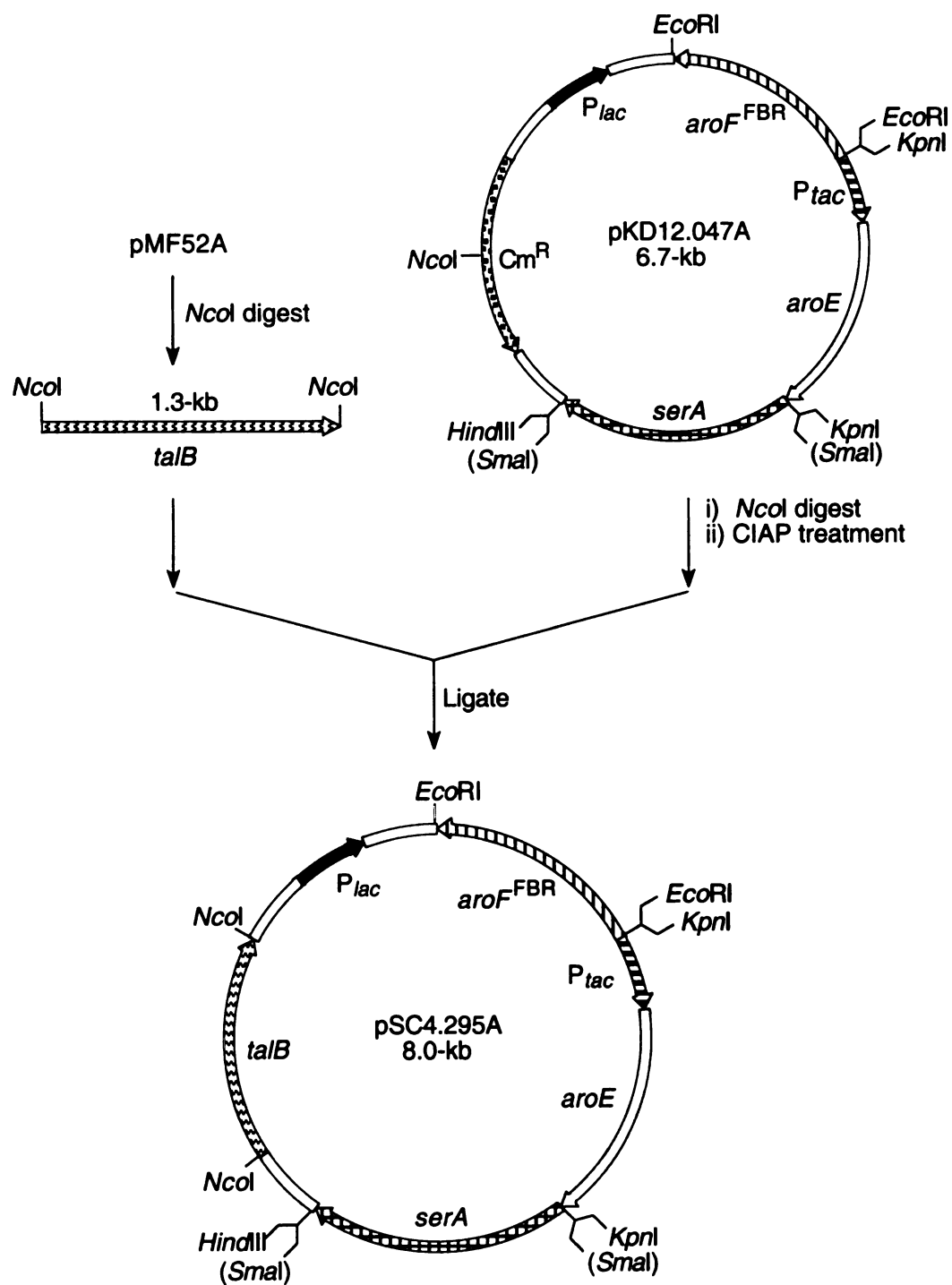
Figure 41. Preparation of Plasmid pSC4.295A.

The SA producing capability of SP1.1/pSC4.295 was determined under fermentation conditions and the results were not encouraging. Accumulation of only 32 g/L SA was observed after 48 h (Figure 42) (entry 3, Table 4), which was identical to that obtained with SP1.1/pKD12.112A, and hence the fermentation was terminated at that stage. This result indicated that *talB* overexpression had negligible effect in increasing carbon flow into the common pathway. Activity of DAHP synthase remained high throughout the run and was not considered as a factor in the low SA production (entry 3, Table 2).
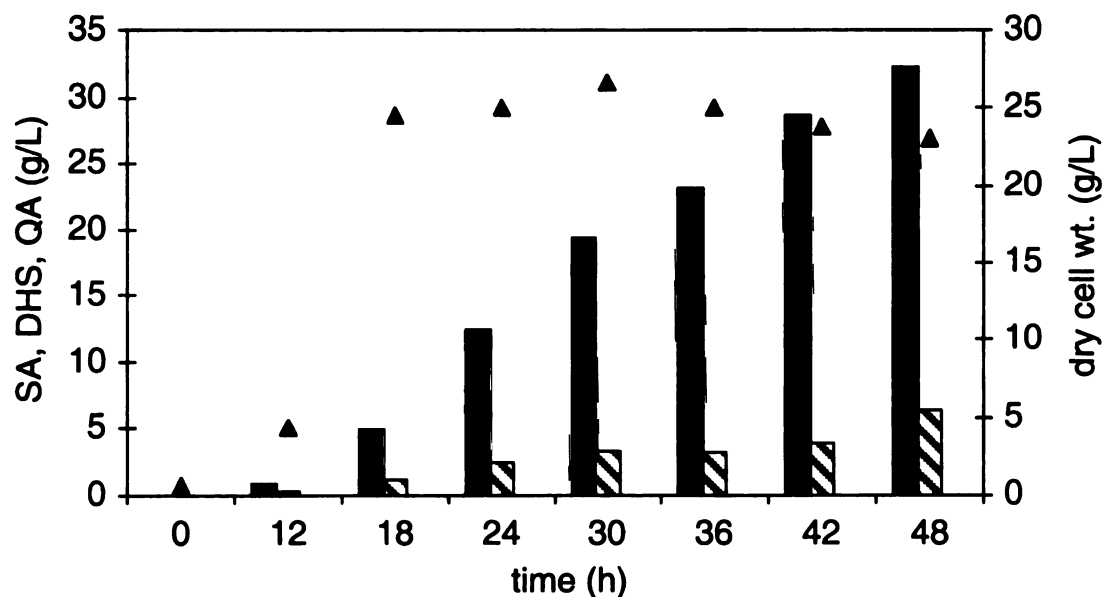
Figure 42. SP1.1/pSC4.295A fed-batch fermentation time course.
▲ Dry cell wt. (g/L);   ■ SA (g/L);   ☒ DHS(g/L);   ☐ QA(g/L).

Production of SA as a Function of Increased PEP availability

With E4P levels no longer being a limiting factor in SA synthesis, the next aspect examined was availability of PEP. Intracellular concentrations of PEP can be improved by increasing in vivo PEP synthase activity levels.[61d,e] This was realized by plasmid localization of the *pps* gene (Figure 43). Digestion of pKL1.87B[99] with *Eco*RI and *Hind*III afforded the 3.0-kb *pps* gene, which was subsequently treated with Klenow fragment. Plasmid pKD12.138A was digested with *Nco*I and the 8.9-kb fragment treated with Klenow fragment. Ligation of the *pps* gene into linearized pKD12.138A afforded pKD15.071B. Transcription of the *pps* gene is in the orientation opposite to that of the *tktA* gene.

Coupling *pps* amplification with that of *tktA* had a dramatic effect on SA production. Strain SP1.1/pKD15.071B synthesized 66 g/L of SA in 23% (mol/mol) yield (Figure 44) (entry 4, Table 4). The overall yield taking into account DHS and QA accumulation was calculated to be 29% indicating an increase in carbon being shuttled into the common pathway. Surprisingly, DAHP synthase activity levels were measured to be higher than those observed for SP1.1/pKD12.138A (entry 1, Table 3). This was not expected considering that transcription of *pps* in addition to the *tktA* gene should subject the system to further metabolic stress and hence lower DAHP synthase activity.
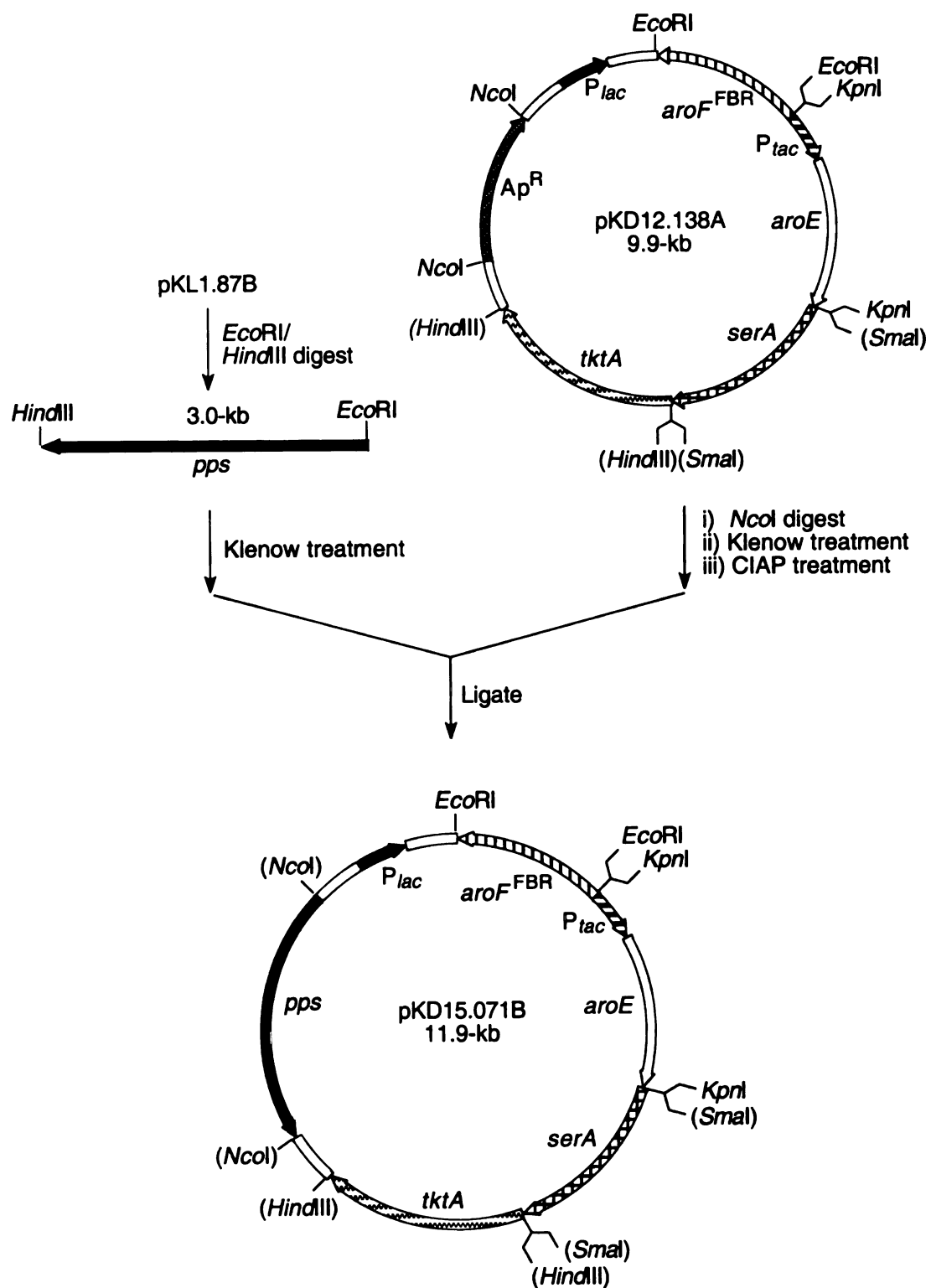
Figure 43. Preparation of Plasmid pKD15.071B.
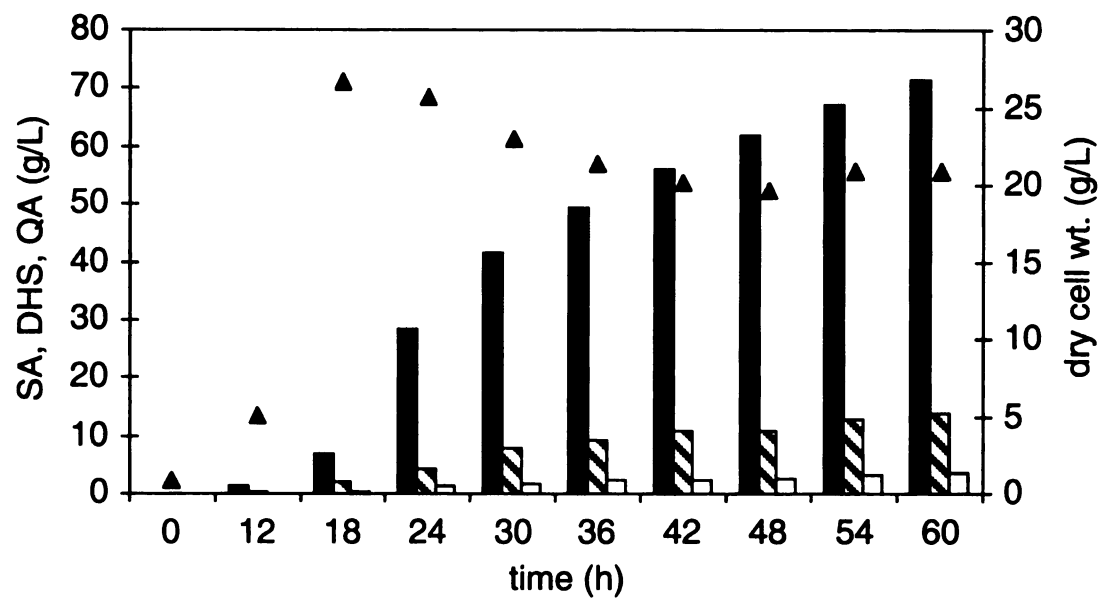
Figure 44. SP1.1/pKD15.071B fed-batch fermentation time course.
▲ Dry cell wt. (g/L); ■ SA (g/L); ▨ DHS(g/L); ☐ QA(g/L).

The primary effect of *pps* overexpression is to nullify PEP limitation caused by PTS-mediated glucose uptake. The same effect can be realized by utilization of a non-PEP dependent mode of glucose transport. *Zymomonas mobilis* is known to utilize a facilitated diffusion system (Figure 24). Ingram and co-workers have successfully utilized the *Z. mobilis* glucose facilitator gene designated *glf*, to complement glucose transport in *E. coli* strains lacking a functional native glucose uptake system.[73c,d] In order to study the effect that facilitated diffusion would have on SA production, the *glf* gene was localized on plasmid pSC5.112 under the control of the *tac* promoter (Figure 45).
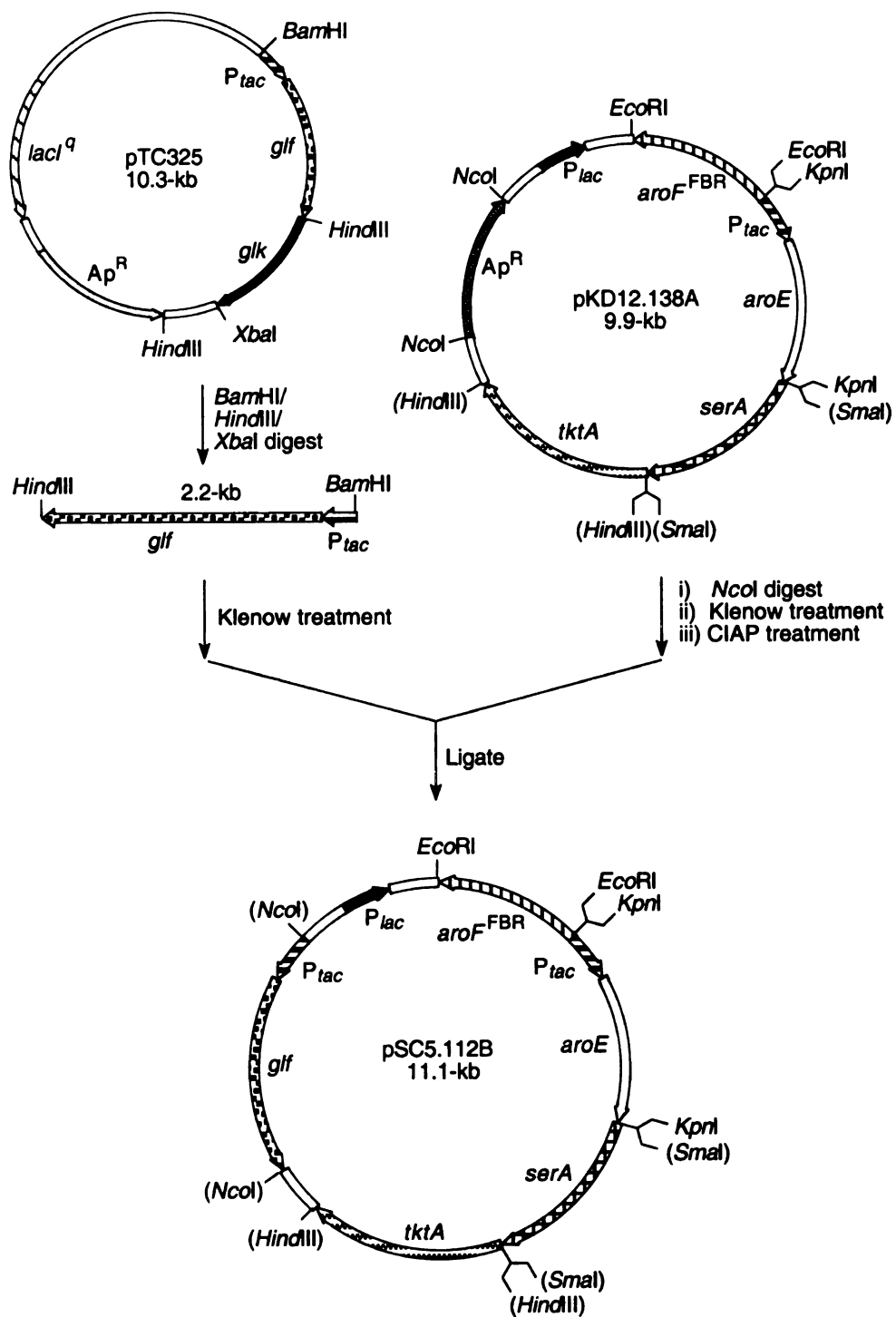
Figure 45. Preparation of Plasmid pSC5.112B.

The 2.2-kb $P_{lac}glf$ fragment was obtained by digestion of pTC325[73d] with BamHI,

HindIII and XbaI followed by treatment with Klenow fragment. Digestion of

pKD12.138A with NcoI excised the 1.0-kb β-lac gene and the remaining 8.9-kb fragment

was treated with Klenow fragment. Ligation of the $P_{lac}glf$ fragment into linearized

pKD12.138A afforded pSC5.112B.

Use of the glucose facilitator system to increase PEP levels had a positive impact

on SA production. After 60 h, SP1.1/pSC5.112B had synthesized 70 g/L of SA in

addition to 19.4 g/L DHS and 6 g/L QA (Figure 46) (entry 5, Table 4). The result was

nearly the same as that observed when overexpression of PEP synthase was utilized to

improve PEP influx into the common pathway. However, since PEP synthase is a

heavily regulated enzyme, its applicability as a long term solution is questionable and use

of the facilitated diffusion system might provide an attractive alternative.
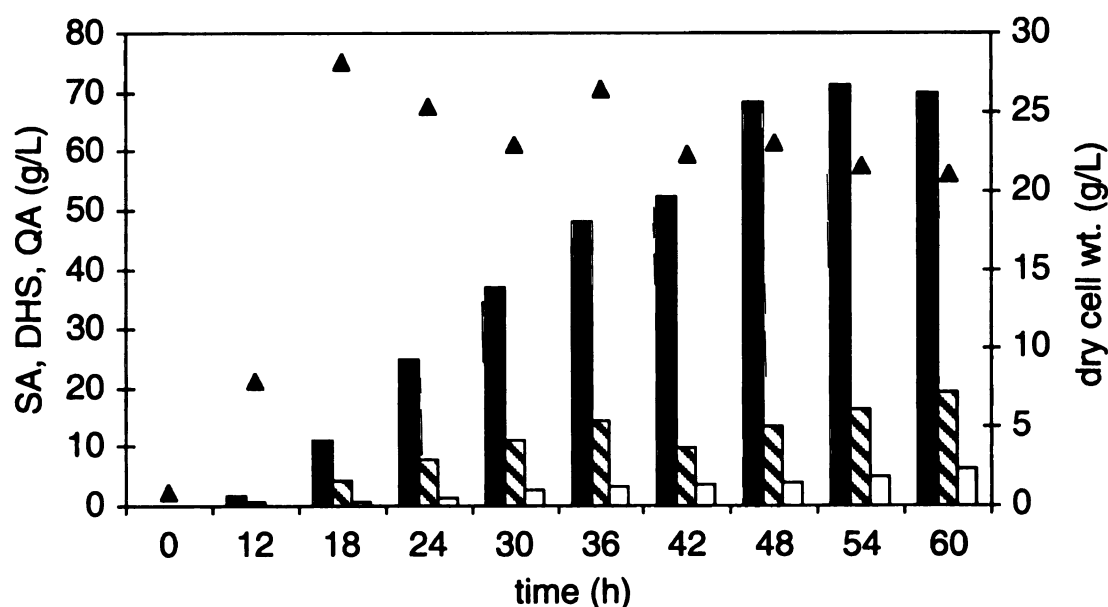
Figure 46. SP1.1/pSC5.112B fed-batch fermentation time course.
▲ Dry cell wt. (g/L);   ■ SA (g/L);   ⧅ DHS(g/L);   ▯ QA(g/L).

Table 3. DAHP synthase activities (μmol/min/mg) for non-PEP limited biocatalysts.

Entry no.	Strain	[SA] (g/L)	DAHP synthase specific activities			
			12 h	24 h	36 h	48 h
1	SP1.1/pKD15.071B	66	0.16	0.32	0.26	0.20
2	SP1.1/pSC5.112B	70	0.076	0.21	0.19	0.18

The results discussed earlier with SP1.1/pSC5.112B involved the use of the glucose facilitator protein in the presence of a functional PTS system. Examination of the overall impact that facilitated diffusion by itself has on SA production entailed the use of an *E. coli* host in which the native PTS system has been compromised. This was accomplished by disruption of three genes involved in PTS-mediated glucose uptake namely, *ptsH*, *ptsI*, and *crr* (Figure 21) to furnish the strain SP1.1*pts*. Deletion of these genes renders the strain defective not only in glucose transport, but also in glucose phosphorylation. Hence, effectiveness of utilizing the glucose facilitator protein is contingent upon providing the requisite glucose kinase activity. Plasmid pTC325, which was used as the source of the *glf* locus, also carries the *glk* gene encoding for the *Z. mobilis* glucose kinase enzyme (Figure 45). Digestion of pTC325 with *Bam*HI and *Xba*I excises the 3.9-kb P_{tac} *glf glk* fragment, which was reacted with Klenow fragment. Plasmid pKD12.138A was digested with *Nco*I and the 8.9-kb fragment treated with Klenow fragment. Ligation of the two DNA segments afforded the 12.8-kb plasmid, pSC6.090B (Figure 47).
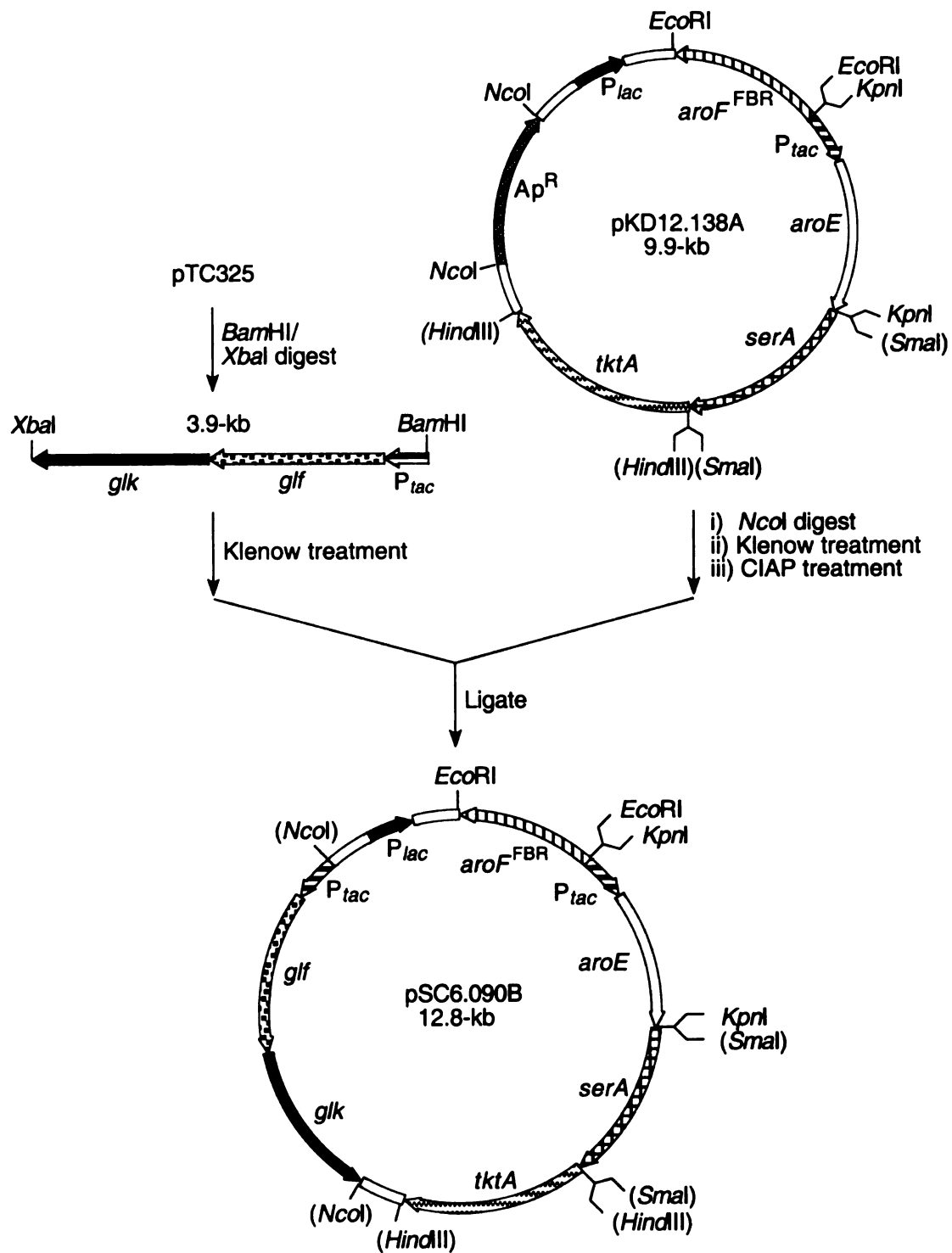
Figure 47. Preparation of Plasmid pSC6.090B.

Plasmid pSC6.090B was transformed into SP1.1*pts* and this strain was evaluated under fermentation conditions. SP1.1*pts*/pSC6.090B produced 71 g/L of SA after 60 h in 27% (mol/ mol) yield (Figure 48) (entry 6, Table 4), and appeared to be only slightly better than SP1.1/pKD15.071B or SP1.1/pSC5.112B. But a closer examination of the production profile indicated that this biocatalyst had synthesized 54 g/L of SA after only 30 h as opposed to 32 g/L for SP1.1/pKD15.071B and 37 g/L for SP1.1/pSC5.112B. Unfortunately, this rapid accumulation rate was not sustained and the end result was similar to those obtained with the aforementioned biocatalysts. Possible reasons for the decline in production will be discussed later in this Chapter. The effectiveness of pSC6.090B in a system with a functional PTS system was also investigated by transforming the plasmid into SP1.1. Fermentation with this strain however provided only 46 g/L SA after 60 h in 21% (mol/mol) yield (Figure 49) (entry 7, Table 4). A distinguishing feature of this fermentation was the accumulation of 19 g/L of acetate. The low level of SA accumulation may be a direct result of the acetate being toxic to the cells.

Acetic acid is a by-product of glucose metabolism, and its level can affect the production of the fermentation process by slowing the bacterial growth and/or inhibiting recombinant protein biosynthesis.[100] Acetate accumulation presumably occurs due to overloading of the tricarboxylic acid (TCA) pathway by fast oxidation through glycolysis. Under high glucose concentrations, excess acetyl CoA flows into the TCA cycle which ultimately translates into higher acetate formation. Strain SP1.1/pSC6.090B possesses an intact PTS system as well as an amplified facilitated glucose uptake mechanism. Intake of glucose by the cell would therefore be at an unprecedented level.

As opposed to SP1.1/pSC5.112B, which also utilizes facilitated diffusion coupled with the PTS system, strain SP1.1/pSC6.090B carries the *glk* gene which appears to make some difference.
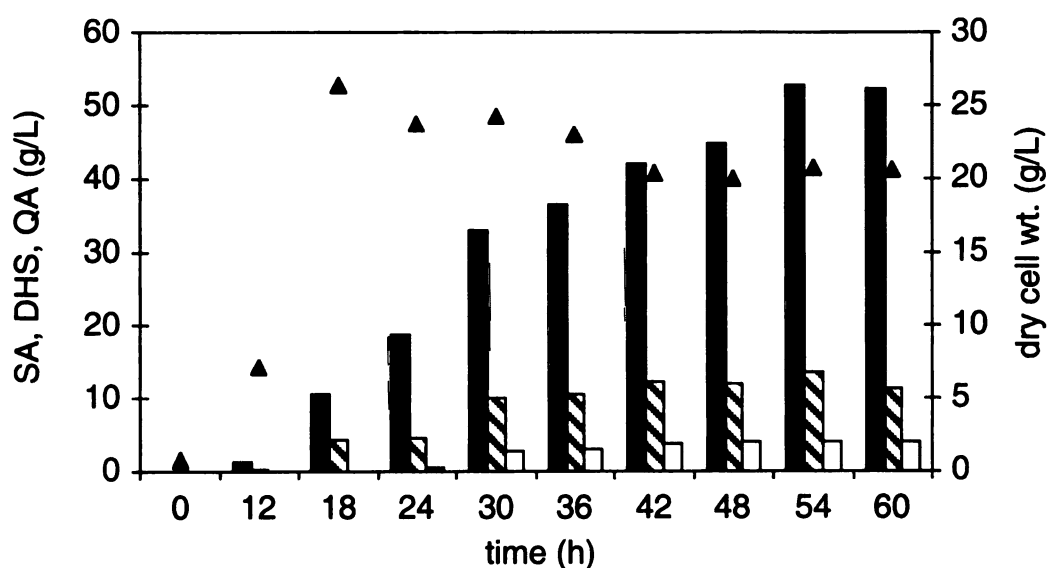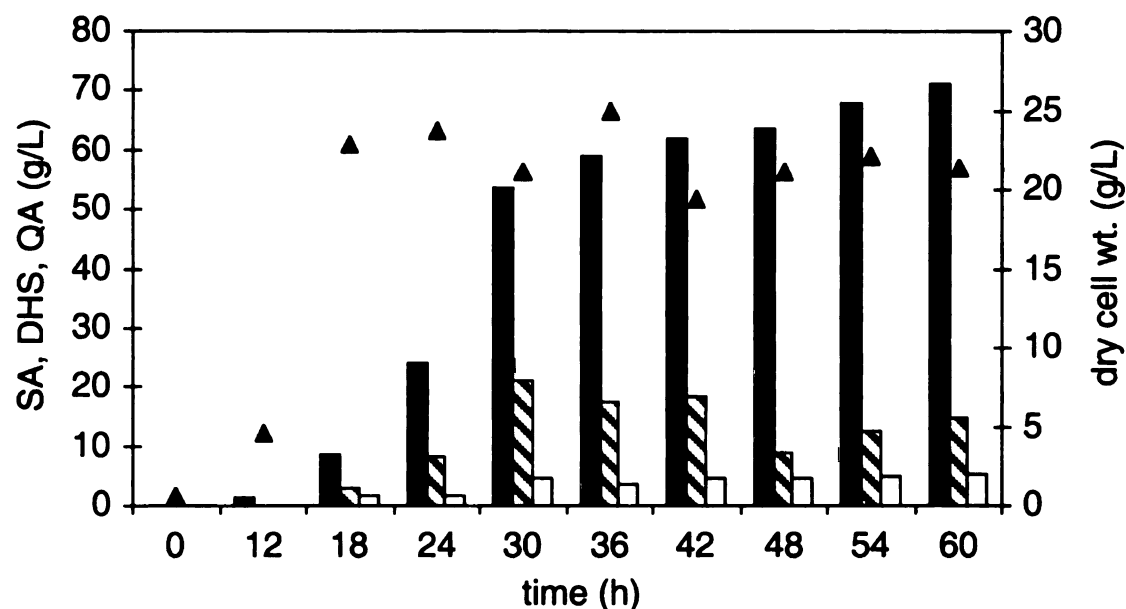

Figure 48. SP1.1*pts*/pSC6.090B fed-batch fermentation time course.

▲ Dry cell wt. (g/L);   ■ SA (g/L);   ▨ DHS(g/L);   ▯ QA(g/L).
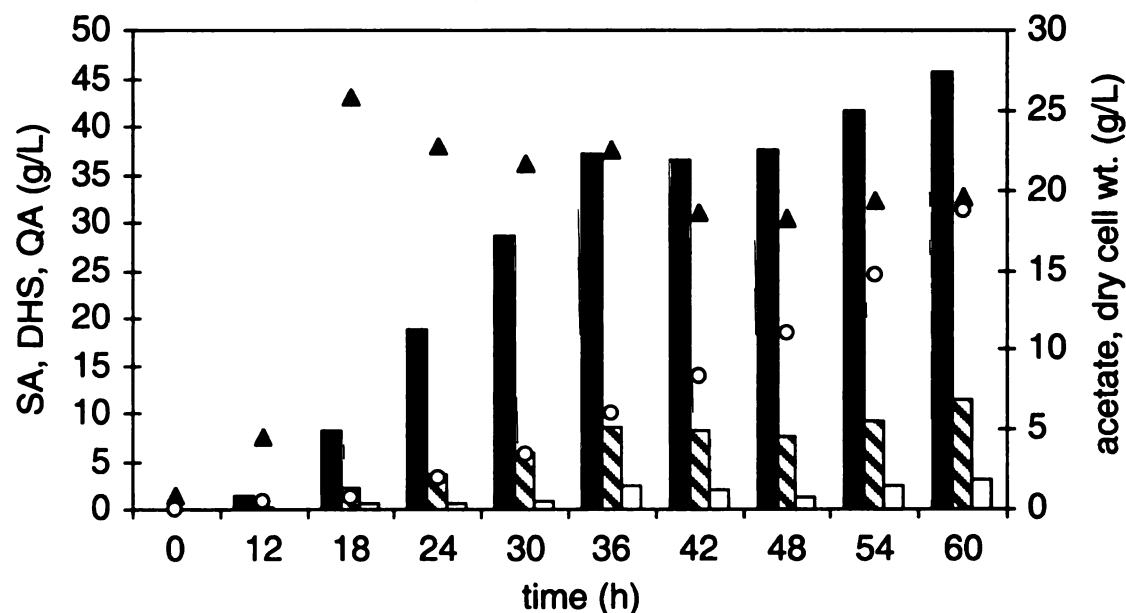
Figure 49. SP1.1/pSC6.090B fed-batch fermentation time course.

▲ Dry cell wt. (g/L);   ■ SA (g/L);   ▨ DHS(g/L);   ▯ QA(g/L)

○ acetate (g/L).

Plasmid pSC6.162A was constructed to study the effect of stacking the *pps* and

glf genes in the same system. Localization of the 2.2-kb $P_{tac}glf$ fragment from pTC325

into pKL1.87A resulted in pSC6.142B, in which the $P_{tac}glf$ fragment was transcribed

opposite to the *pps* gene (Figure 50). The 5.2-kb $P_{tac}glf$ *pps* portion was subsequently

excised out of pSC6.142B by *Bam*HI/*Hind*III digestion, treated with Klenow fragment

and inserted into the *Nco*I site of pKD12.138A to generate pSC6.162A(Figure 51).

Plasmid pSC6.162A was transformed into SP1.1 and the resulting strain was

cultured under fermentation conditions. Coupling overexpression of the glucose

facilitator enzyme with that of PEP synthase did not give any increment in SA production

over the strains overexpressing either one of the two enzymes. After 60 h, 67 g/L of SA

in 26% (mol/ mol) yield was obtained along with a total yield of 34% (mol/mol) (Figure

52) (entry 8, Table 4). No benefit with respect to rate of production was accrued either.
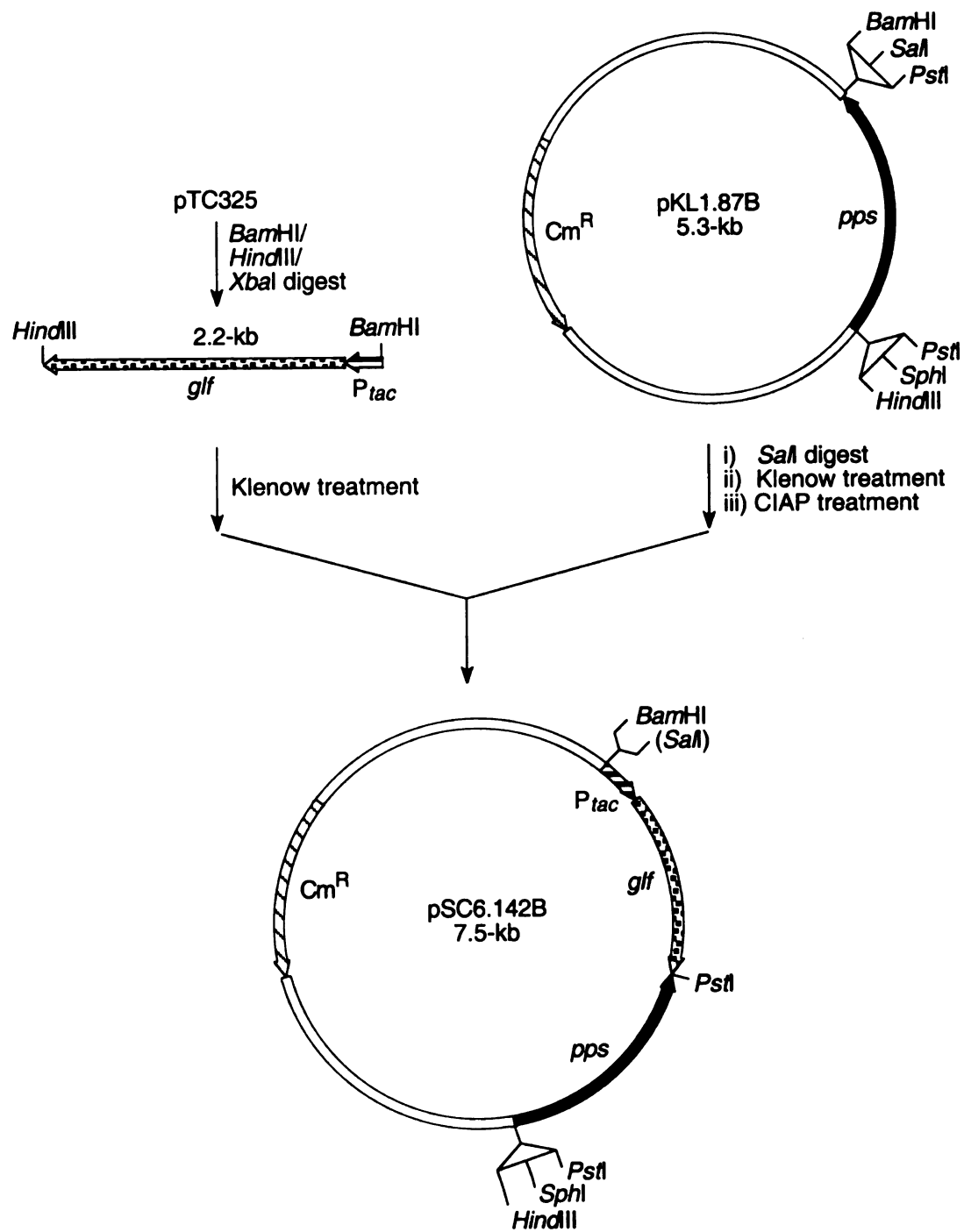
Figure 50. Preparation of Plasmid pSC6.142B.
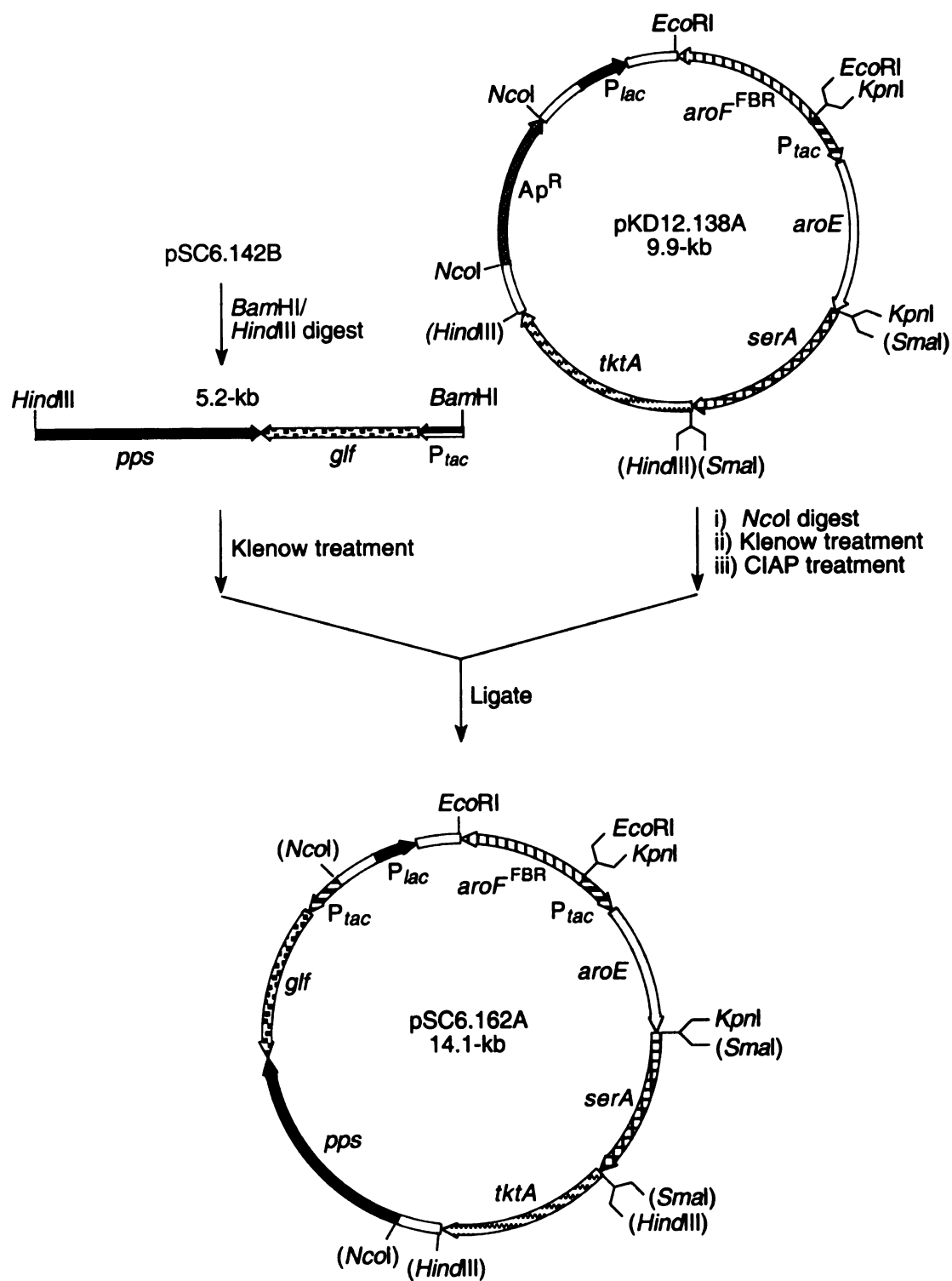
Figure 51. Preparation of Plasmid pSC6.162A.
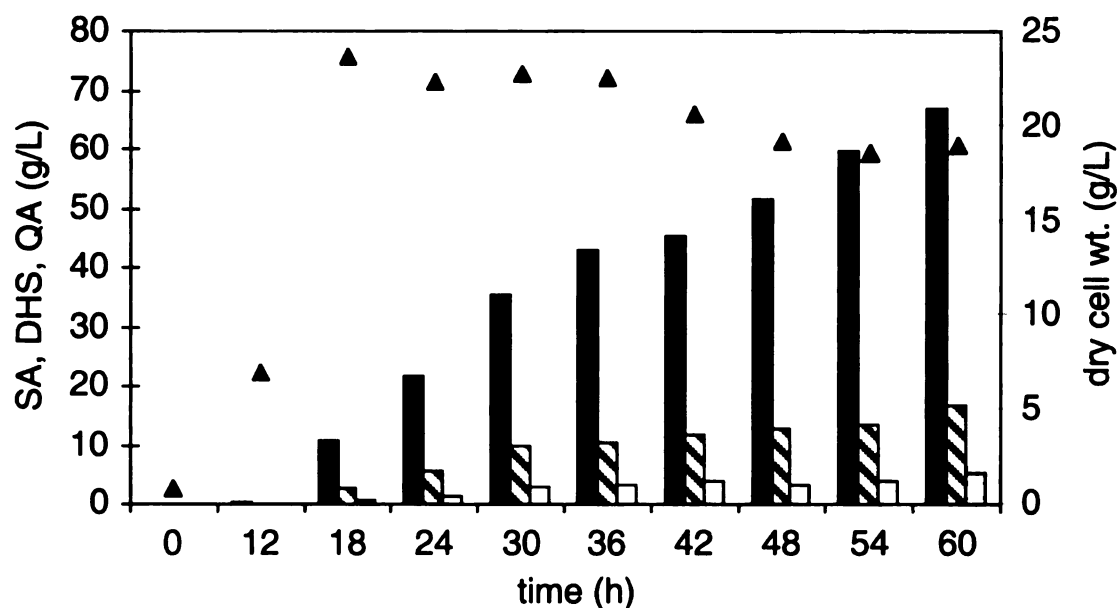
Figure 52. SP1.1/pSC6.162A fed-batch fermentation time course.

▲ Dry cell wt. (g/L);   ■ SA (g/L);   ◣ DHS(g/L); | | QA(g/L).

Plasmid pSC6.301A was constructed to evaluate the impact of PEP synthase

overexpression coupled to that of the glucose facilitator and glucose kinase proteins.

Excision of the *pps* gene from pKL1.87B by digestion with *Bam*HI and *Hind*III was

followed by treatment with Klenow fragment. Plasmid pSC6.090B was linearized by

reaction with *Xba*I and the 12.1-kb fragment was treated with Klenow fragment.

Ligation of the two fragments resulted in the 15.1-kb plasmid pSC6.301A (Figure 53).

Transcription of the *pps* was in the same orientation as that of *tktA*.
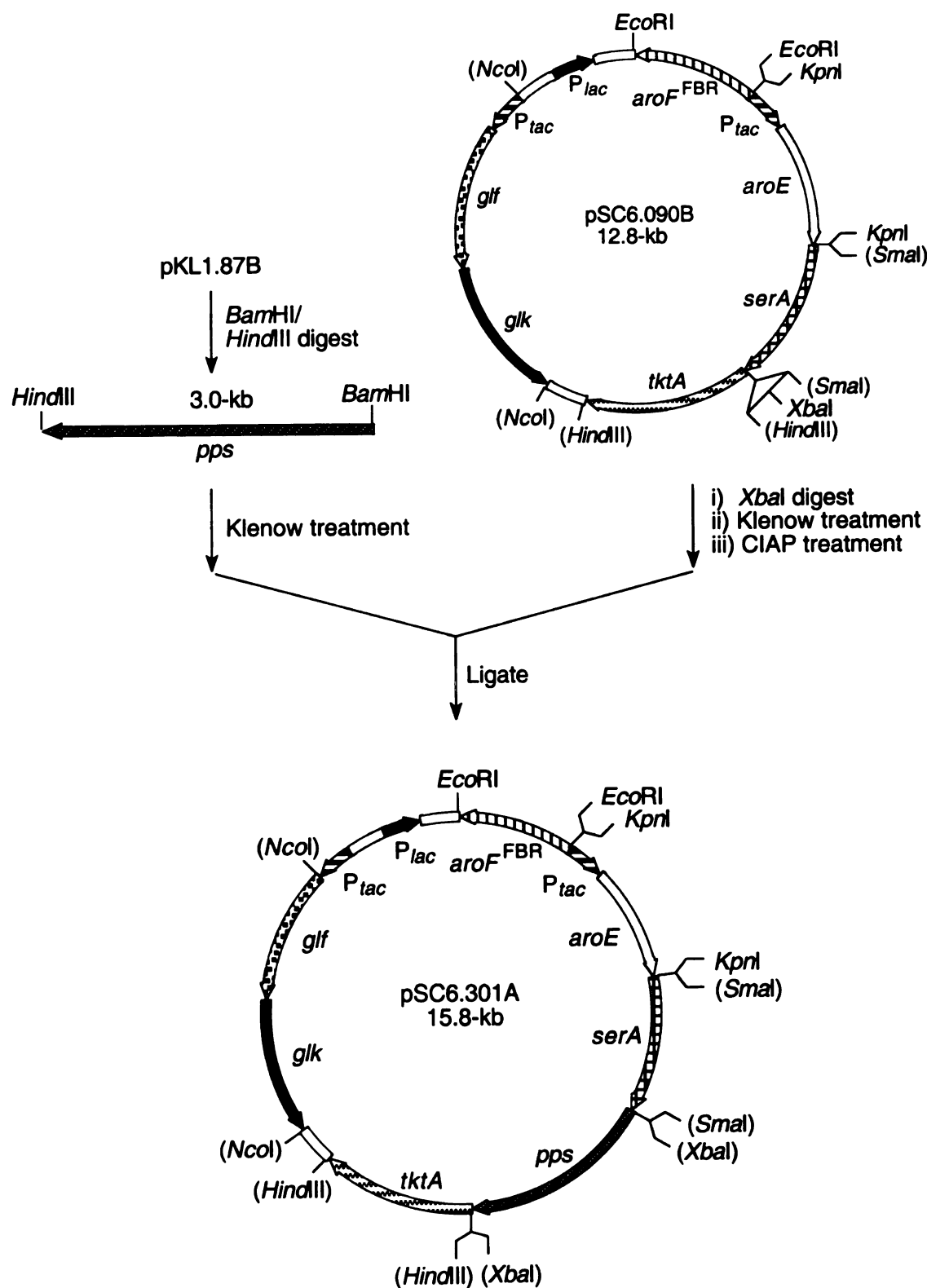
Figure 53. Preparation of Plasmid pSC6.301A.

This plasmid was transformed into SP1.1 as well as SP1.1*pts* and both strains were run on the fermentor. Neither biocatalyst proved to be a good SA producer as illustrated by in Figures 54 and 55. In fact, accumulation of large amounts of acetate was observed in both fermentations, with SP1.1*pts*/pSC6.301A producing the highest amount of acetate (30 g/L) recorded so far among strains designed to synthesize SA. It is very likely that the high acetate concentrations compromised the health of the cells resulting in poor production of SA.
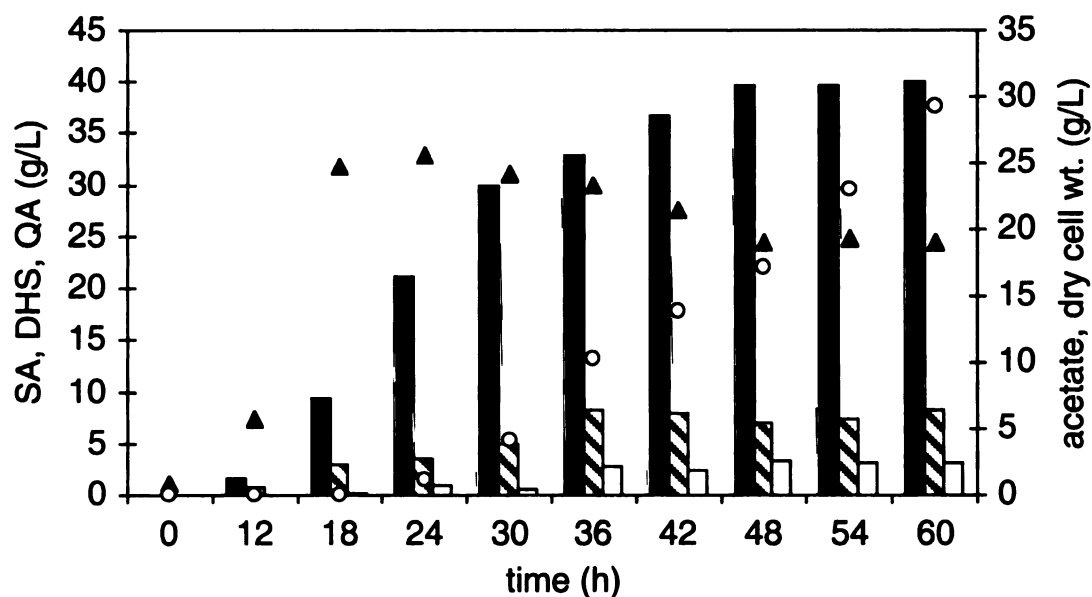
Figure 54. SP1.1*pts*/pSC6.301A fed-batch fermentation time course.
▲ Dry cell wt. (g/L);   ■ SA (g/L);   ░ DHS(g/L);   ▢ QA(g/L)
░ acetate (g/L).
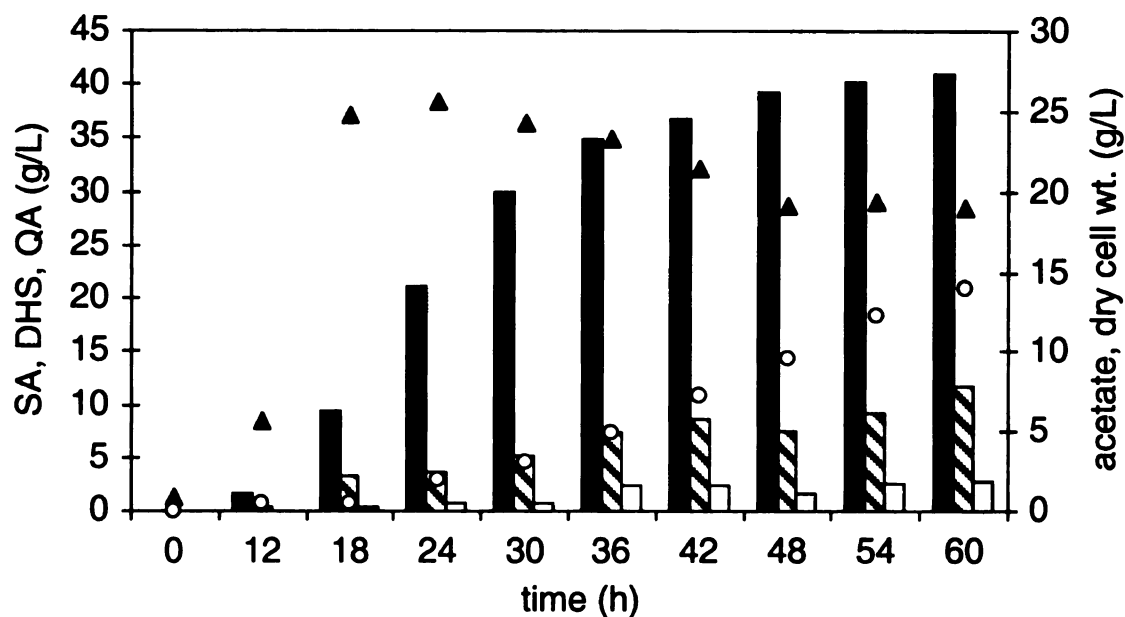
Figure 55. SP1.1/pSC6.301A fed-batch fermentation time course.

▲ Dry cell wt. (g/L); ■ SA (g/L); ◪ DHS(g/L); ▯ QA(g/L)
○ acetate (g/L).

**Table 4. Titers and yields for SA production by SP1.1 based biocatalysts.**

Entry no.	Strain	[SA] (g/L)	SA yield (mol/mol)	[DHS] (g/L)	[QA] (g/L)	Total yield (mol/mol)
1	SP1.1/pKD12.112A	38	12%	6	2	15%
2	SP1.1/pKD12.138A	52	18%	11	4	24%
3	SP1.1/pSC4.295A	32	16%	6	0	19%
4	SP1.1/pKD15.071B	66	23%	16	4	29%
5	SP1.1/pSC5.112B	70	24%	19	6	32%
6	SP1.1pts/pSC6.090B	71	27%	15	5	34%
7	SP1.1/pSC6.090B	46	21%	16	3	28%
8	SP1.1/pSC6.162A	67	26%	17	5	34%
9	SP1.1pts/pSC6.301A	40	15%	9	3	19%
10	SP1.1/pSC6.301A	41	16%	12	2	21%

Examination of Lowered Osmotic Stress on SA Production

By this stage, it was fairly surprising that the production levels of most of the strains peaked out at close to 70 g/L SA after 60 h. For example, stacking the *glf* and *pps* genes was expected to give at least a slight increment over the strains overexpressing the individual genes. But as indicated in Table 4, that was not the case. It was also surprising how the productivity of SP1.1*pts*/pSC6.090B suddenly leveled off after a sudden burst in SA synthesis. If this construct had sustained the high level of SA production for a slightly longer period, it could have accumulated greater than 71 g/L SA. It was entirely possible that the barrier of approximately 70 g/L was the maximum production capability of the biocatalysts designed so far. Obtaining higher SA titers and yields would then involve optimizing the activity of enzymes like DAHP synthase, transketolase, shikimate dehydrogenase, etc. Additional copies of the genes encoding for these enzymes could be localized on a new plasmid or on the genome. Utilization of stronger promoters could also be investigated. But the possibility also existed that some of the strains could indeed synthesize more SA but were restricted in their ability to do so by the prevailing conditions in the fermentor. One factor could be that the high concentrations of SA itself might be impeding further production. It was considered prudent to discount the latter possibility before constructing new plasmids or strains.

Strain SP1.1/pKD15.071B was selected to establish whether high external SA concentration was responsible for the limitation on product synthesis. As was discussed earlier, this biocatalyst had the capability to produce 66 g/L of SA after 60 h (entry 4, Table 4). For the purpose of this investigation SP1.1/pKD15.071B was run under normal fermentation conditions and at 18 h and 24 h into the experiment, 10 g each of SA was

added into the fermentor. If external SA concentrations had no influence whatsoever on the efficiency of the biocatalyst, then SP1.1/pKD15.071B would accumulate at least 86 g/L SA after 60 h. On the other hand, if SA concentration did indeed have a deleterious effect on SA production, then the fermentation would result in accumulation of only 70 g/L SA after 60 h. As illustrated in Figure 56, this experiment yielded 71 g/L of SA after 60 h. This experiment provided evidence that high SA accumulation was indeed limiting its own biocatalytic synthesis. Hence, construction of a new plasmid or strain to afford higher SA titers would not be useful unless the mechanism for this limitation is understood and solved.
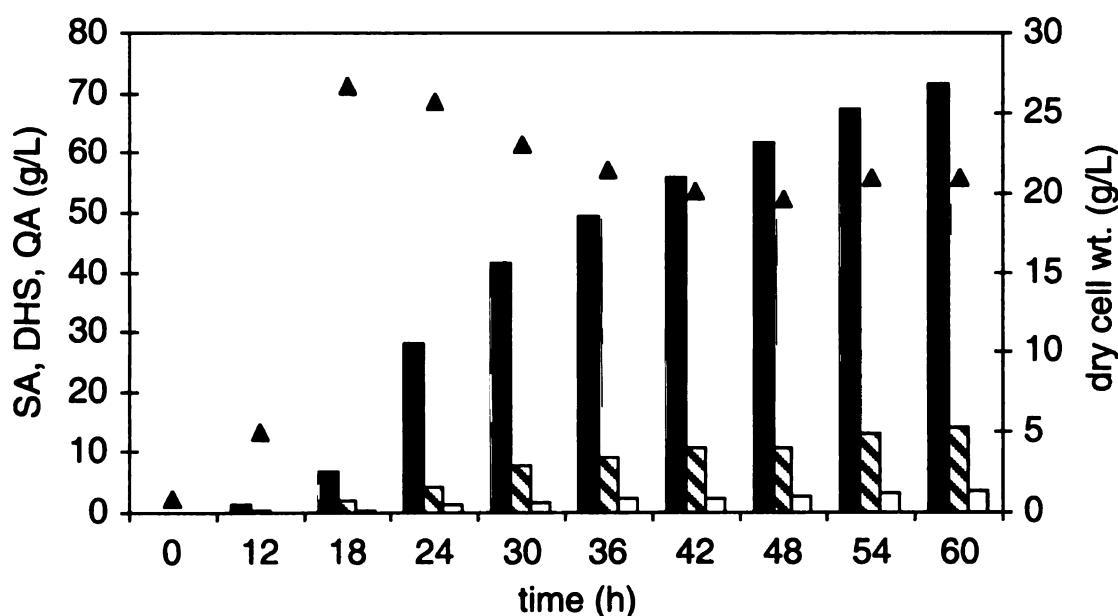
Figure 56. Time course for fed-batch fermentation experiment involving addition of 20 g SA to SP1.1/pKD15.071B culture.
▲ Dry cell wt. (g/L);   ■ SA (g/L);   ⊠ DHS(g/L);   ☐ QA(g/L)

Several plausible explanations can be offered to account for the restrictive effect of high SA concentrations on the biocatalyst. The simplest explanation is that beyond a certain concentration, SA acts as an inhibitor to one of the common pathway enzymes or

to an enzyme essential to the cell metabolism. Another possibility is that the cell machinery is still functional and is still capable of SA synthesis. But the high levels of product accumulation could have shut down the necessary export systems required by the cell, which in turn would shut down SA production. The option which was finally investigated as the most likely cause, was that of osmotic stress.[101] In fermentation processes with high product yields, it is known that cells are exposed to high osmotic stress from the medium components and the product. This stress can inactivate the cells and limit product accumulation. The use of osmoprotectants in such fermentations is fairly widespread. Compounds like betaine, proline, choline and ectoine are zwetterionic solutes, which can stimulate the growth rate of bacteria in media of high osmolality (Figure 57).[102] Betaine has been reported to be the osmoregulant of choice for *E. coli*. Therefore, for the purpose of this study betaine was used to study the effect of lowered osmotic stress on a SA producing system.
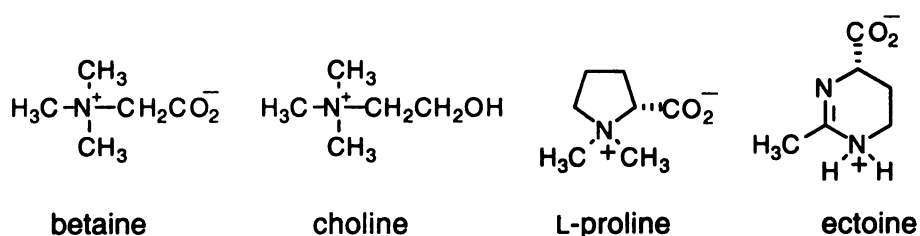
Figure 57. Common osmoprotectants used in microbial fermentations.

Strain SP1.1/pKD15.071B was cultured under normal fermentation conditions with 10 mM betaine added as an osmoprotectant. No improvement was seen in the titer or yield of SA after 60 h (Figure 58) (entry 2, Table 5). The concentration of betaine was hence increased to 100 mM and the fermentation repeated. In this instance, the titer of

SA declined compared to normal runs indicating that high concentrations of betaine might be detrimental (Figure 59) (entry 3, Table 5). A couple of aspects of this fermentation are worth nothing though. The amount of DHS produced was the highest ever measured and hence the total yield was quite high at 38% (mol/mol). Also, at the end of the run, it became clear that the cells had taken up approximately 30 mM betaine, which gave an indication of what the optimum betaine concentration might be for use in the fermentation. Therefore, a third fermentation was set up containing 30 mM betaine and performed in an identical fashion as before. After 60 h, SP1.1/pKD15.071B had accumulated 71 g/L SA in 26 (mol/mol) yield, which is the best result observed so far for this strain (Figure 60) (entry 4, Table 5). The conclusion can therefore be drawn that even though osmotic stress does play some role in suppressing SA production, other factors exist that need to be investigated.
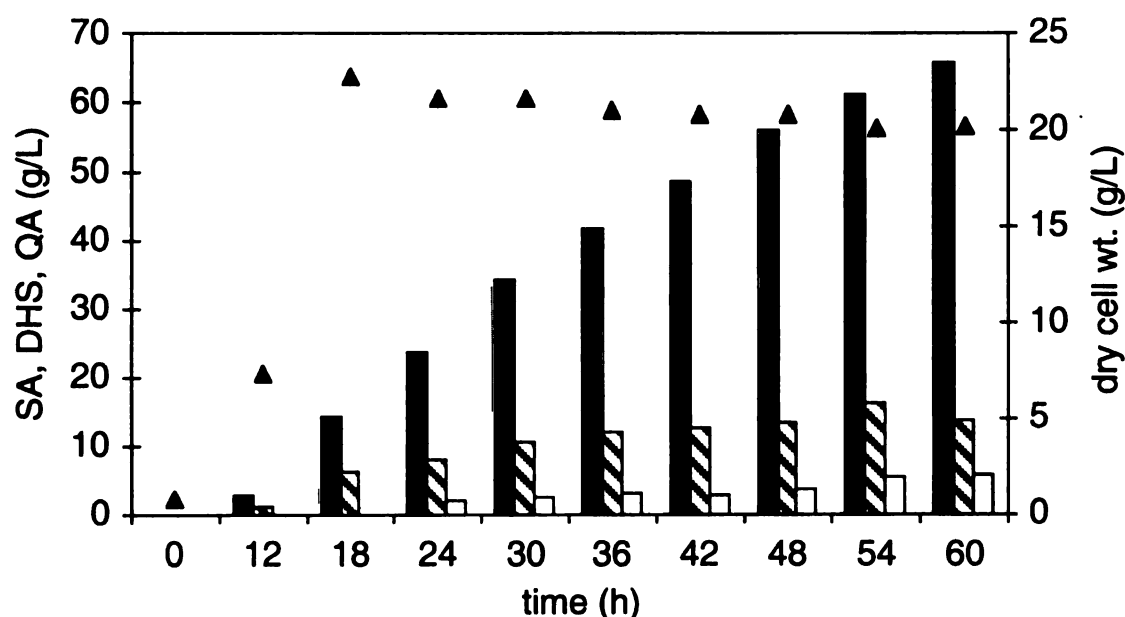
Figure 58. SP1.1/pKD15.071B fed-batch fermentation time course with 10 mM betaine.

▲ Dry cell wt. (g/L); ■ SA (g/L); ▨ DHS(g/L); ☐ QA(g/L)
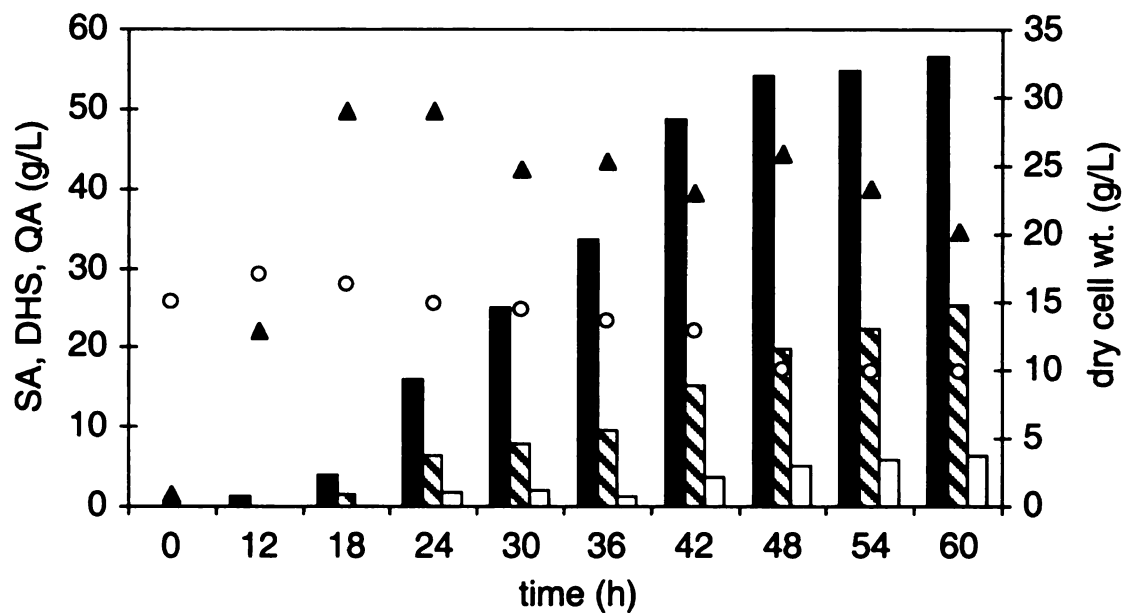
Figure 59. SP1.1/pKD15.071B fed-batch fermentation time course with 100 mM betaine.

▲ Dry cell wt. (g/L); ■ SA (g/L); ◥◥◥ DHS(g/L); | QA(g/L)
betaine (g/L).
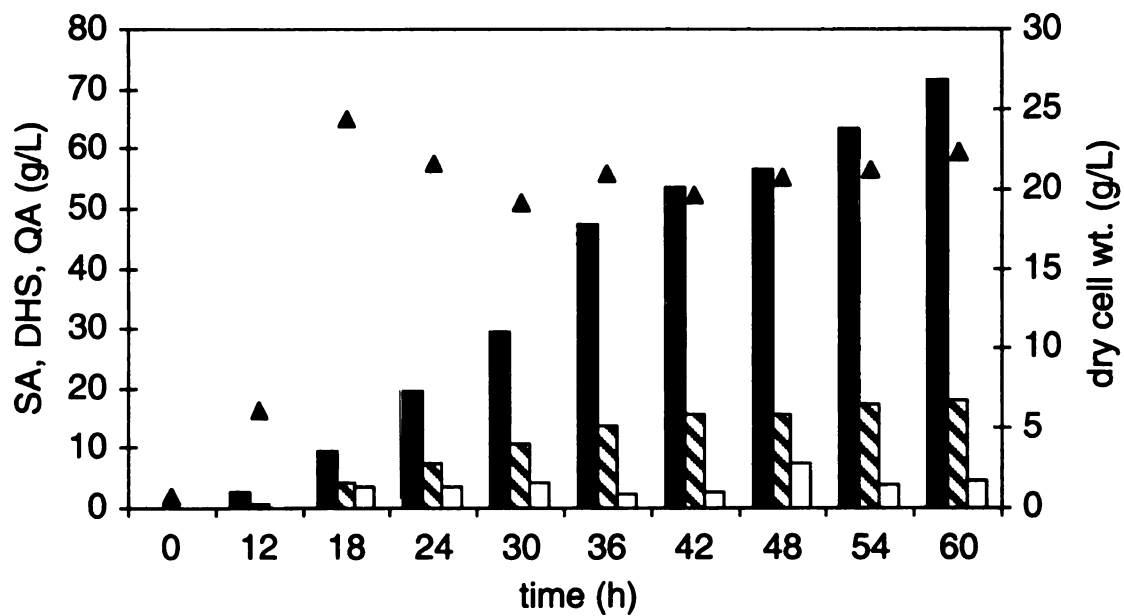
Figure 60. SP1.1/pKD15.071B fed-batch fermentation time course with 30 mM betaine.

▲ Dry cell wt. (g/L); ■ SA (g/L); ◥◥◥ DHS(g/L); | QA(g/L)

Table 5. Effect of varying betaine concentrations on production of SA by SP1.1/pKD15.071B.

Entry no.	Strain	[SA] (g/L)	SA yield (mol/mol)	[DHS] (g/L)	[QA] (g/L)	Total yield (mol/mol)
1	SP1.1/pKD15.071B 0 mM betaine	66	23%	16	4	29%
2	SP1.1/pKD15.071B 10 mM betaine	66	22%	14	6	28%
3	SP1.1/pKD15.071B 100 mM betaine	57	25%	25	6	38%
4	SP1.1/pKD15.071B 30 mM betaine	71	26%	18	5	34%

Comparison of SA Production Capabilities Between

E. coli B and *E. coli* K12

The growth rate of *E. coli* B has been reported to be much more rapid as compared to *E. coli* K12 (RB791).[103] A faster and more rigorous growth pattern may result in faster accumulation of SA and the higher cell mass generated could also result in more SA production. Also, in *E. coli* K12, DAHP synthase is precedented to be labile to proteolytic activity during the stationary phase of growth. *E. coli* B on the other hand is known to be naturally deficient in the Lon proteases.[93] It is believed that the Lon proteases are the major proteases catalyzing the endoproteolytic cleavage of proteins in the cell. Strains disrupted in the *lon* gene produce several phenotypic changes including increased sensitivity to UV and ionizing radiation, overproduction of mucopolysaccharide, reduced lysogenization of bacteriophages lambda and P1, and most importantly, reduced protein degradation.[93d] Examination of the enzyme activity levels for the biocatalysts derived from RB791 illustrates how DAHP synthase activity levels tend to fade away after 24 h into the fermentation run (Tables 2 and 3). Given the lack of proteolytic activity during stationary phase in *E. coli* B, use of a biocatalyst derived from this strain could help avoid this problem, making it quite an attractive alternative to *E. coli* K12.

An *E. coli* B derivative EB1.1, capable of synthesizing SA, was constructed carrying the identical deletions as in SP1.1. Plasmid pKD12.112A was transformed into EB1.1 and the strain was tested under fermentation conditions. Production levels of SA (39 g/L) were disappointingly the same as that observed with SP1.1/pKD12.112A albeit with a higher yield of 17% (mol/mol) (Figure 61) (entry 1, Table 6).
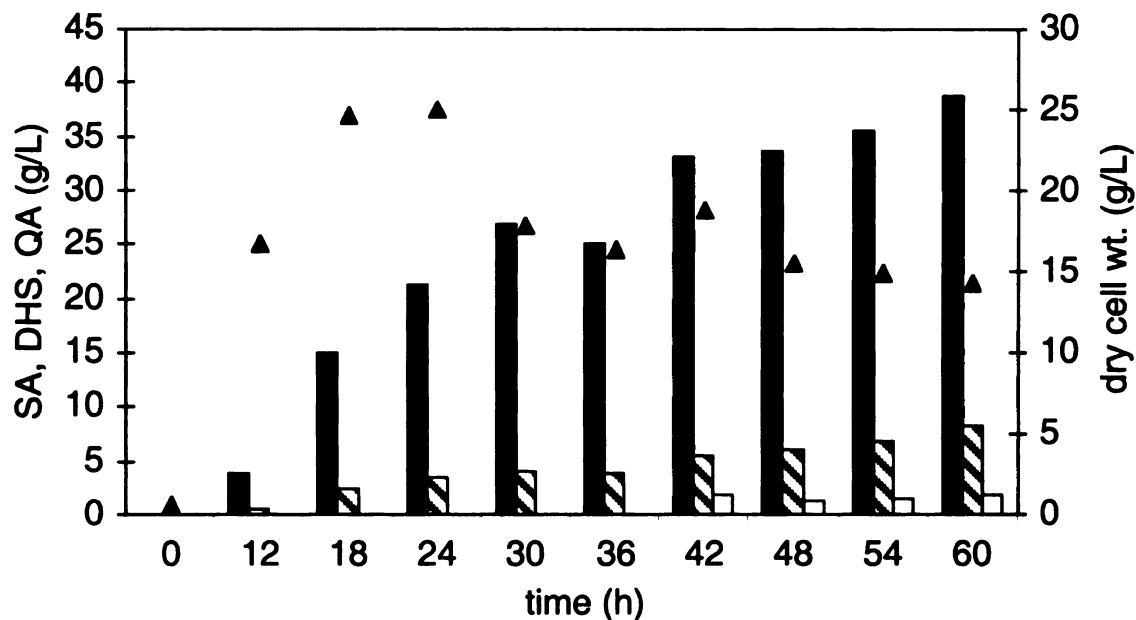
Figure 61. EB1.1/pKD12.112A fed-batch fermentation time course.
▲ Dry cell wt. (g/L); ■ SA (g/L); ▨ DHS(g/L); ▯ QA(g/L)

The OD_{600} values recorded for the EB1.1/pKD12.112A cell density during the course of the fermentation were abnormally higher than those observed for any of the SP1.1 or SP1.1*pts* runs. However, for EB1.1 a conversion factor of 0.29 g/L/OD_{600} had to be applied in order to arrive at an accurate estimate of the dry cell weight (g/L). This value was an average value obtained by centrifugation (16000 x *g*, 10 min) of 20 mL aliquots of fermentation culture taken every 6 h and drying the washed, harvested cells to a constant weight at 100 °C. The corresponding value for RB791 derived strains was 0.43 g/L/OD_{600}. The net result was that even though the OD_{600} values measured for *E. coli* B fermentations were very high, the final dry cell weight values were the same as those for the corresponding *E. coli* K-12 runs.

The fermentation with EB1.1/pKD12.138A did not show any improvement over EB1.1/pKD12.112A, which was unexpected (Figure 62) (entry 2, Table 6). Experiments

with SP1.1 had shown that amplification of transketolase activity improved the SA yield (entries 1 and 2, Table 4) and titer significantly, but no such effect was seen with EB1.1 (entries 1 and 2, Table 6) and in some cases SP1.1 proved to be a better biocatalyst.
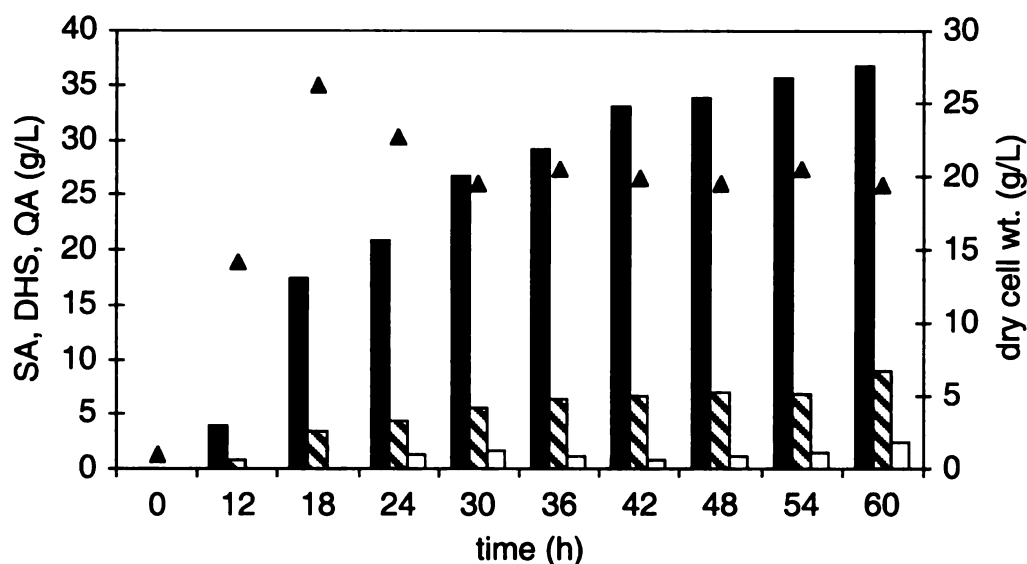
Figure 62. EB1.1/pKD12.138A fed-batch fermentation time course.
▲ Dry cell wt. (g/L);   ▇ SA (g/L);   ◩ DHS(g/L);   ☐ QA(g/L)

In order to verify that that the biocatalyst was not limited in PEP, EB1.1 was transformed with the *pps* encoding plasmid pKD15.071B. Fed-batch fermentation with this strain also proved to be disappointing and produced only 44 g/L SA in 18% yield after 60 h (Figure 63) (entry 3, Table 6). This result seemed to hint that an SP1.1 derived host was superior to one based on EB1.1.
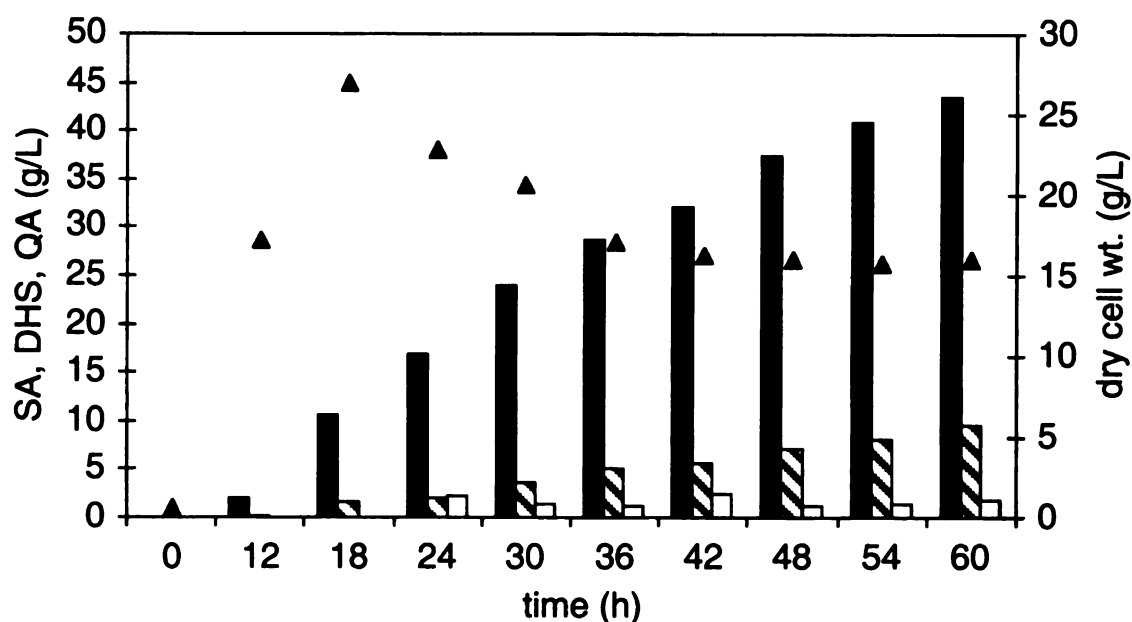
Figure 63. EB1.1/pKD15.071B fed-batch fermentation time course.

▲ Dry cell wt. (g/L); ■ SA (g/L); ▨ DHS(g/L); ☐ QA(g/L)

**Table 6. Titers and yields for SA production by EB1.1 based biocatalysts.**

Entry no.	Strain	[SA] (g/L)	SA yield (mol/mol)	[DHS] (g/L)	[QA] (g/L)	Total yield (mol/mol)
1	EB1.1/pKD12.112A	39	17%	8	2	21%
2	EB1.1/pKD12.138A	37	22%	9	2	28%
3	EB1.1/pKD15.071B	44	18%	10	2	22%

Comparison of the values in Table 7 indicate that DAHP synthase specific activity levels for the *E. coli* B strain (entries 1 and 2, Table 7) are indeed much higher than the corresponding values for the *E. coli* K12 phenotype (entries 3 and 4, Table 7). More significant are the transketolase activity values reported in Table 8. Native *E. coli* B transketolase specific activity (entry 1, Table 8)) was measured to be higher than

overexpressed transketolase activity in *E. coli* K12 (entry 4, Table 8). These higher specific activities however did not translate into enhanced SA levels.

Table 7. Comparison of DAHP synthase activities (μmol/min/mg) between EB1.1 and SP1.1 biocatalysts.

Entry no.	Strain	[SA] (g/L)	DAHP synthase specific activities			
			12 h	24 h	36 h	48 h
1	EB1.1/pKD12.112A	39	1.51	1.13	0.99	0.84
2	EB1.1/pKD12.138A	37	0.82	0.80	0.49	0.41
3	SP1.1/pKD12.112A	38	0.37	0.35	0.37	0.31
4	SP1.1/pKD12.138A	52	0.068	0.19	0.13	0.096

Table 8. Comparison of transketolase activities (μmol/min/mg) between EB1.1 and SP1.1 biocatalysts.

Entry no.	Strain	[SA] (g/L)	Transketolase specific activities			
			12 h	24 h	36 h	48 h
1	EB1.1/pKD12.112A	39	0.073	0.17	0.34	0.39
2	EB1.1/pKD12.138A	37	0.11	0.50	0.73	0.53
3	SP1.1/pKD12.112A	38	0.024	0.10	0.14	0.18
4	SP1.1/pKD12.138A	52	0.11	0.17	0.21	0.35

Discussion

A) Comparison of Titers and Yields

Efficiency of a biocatalyst can be evaluated by comparing the yield of SA produced to the theoretical maximum yield (mol of SA produced/ mol of glucose consumed). Determining the theoretical maximum yield for biocatalytic synthesis of SA begins with balancing the E4P and PEP inputs with the products and by-products formed (Eq. (1)). The input of E4P and PEP required for SA synthesis is then equated with the amount of glucose required to form these substrates (Eq. (2a)). In order to account for the operation of the PTS-mediated glucose uptake system, a pyruvic acid term is added (Eq. (2a)). A coefficient of 2.33 is required to balance the number of carbon atoms in the glucose input to the number of carbon atoms formed in PEP, E4P and pyruvic acid (Eq. (2b)). Hence, synthesis of 1 mole of SA requires the consumption of 2.33 moles of glucose resulting in a theoretical maximum yield of 43% (mol of SA produced/ mol of glucose consumed).

$$(1) \; PEP + E4P \longrightarrow 2H_3PO_4 + H_2O + SA$$

$$(2a) \; x \; glucose \longrightarrow PEP + E4P + x \; pyruvic \; acid$$

$$(2b) \; x \; 6 \, (C) \longrightarrow 3 \, (C) + 4(C) + x \; 3(C)$$

Use of the non-native, facilitated diffusion system for glucose transport eliminates the conversion of 1 mol of PEP to 1 mol of pyruvate. Exclusion of the term for pyruvic acid from equation (2b) leads to a coefficient of 1.17 and hence a maximum theoretical

yield for SA of 86% (mol of SA produced/ mol of glucose consumed) in the absence of PTS-mediated glucose uptake.

Fermentations producing SA also accumulate moderate amounts of DHS and QA. Therefore, in order to arrive at an accurate estimate of carbon flow into the pathway leading to SA, accumulation of DHS and QA must also be considered when calculating the yield of the fermentation. No biocatalytic strain investigated so far has come close to the maximum theoretical yield of 43% (mol/ mol) for SA. This is true irrespective of whether or not the strain was dependent on the native PTS system for glucose uptake. Draths and co-workers have reported[104] the use of SP1.1/pKD12.112A under slightly different fed-batch fermentation conditions, details of which are described in chapter 4. The fermentation produced 18.6 g/L SA along with 7.8 g/L quinic acid QA and 4.4 g/L of DHS after 42 h. This fermentation suffered from a serious drawback involving the concomitant formation of QA in large amounts. Efforts have since been made to rectify this problem and have been discussed in detail in Chapter 4.

Under the fermentation conditions described in this chapter, SP1.1/pKD12.112A, produced 38 g/L SA in 12% (mol/ mol) yield. As expected, E4P was indeed a limiting factor in SA synthesis and as observed with SP1.1/pKD12.138A, amplified expression of *tktA* gave an increment in SA yield (18%) and titer (52 g/L). The total yield taking into account DHS and QA was 24%. Alleviation of PEP limitation however gave the biggest boost to SA production. The highest titer and yield obtained in a PTS-dependent strain was with SP1.1/pSC5.112B. This strain overexpressed the *glf* locus from *Z. mobilis* and produced 70 g/L in 24% yield. The total yield for this system was 34%. Strain SP1.1/pKD15.071B, overexpressing for *pps*, also gave comparable values within

experimental error. The strain affording the best results was SP1.1*pts*/pSC6.090B, which

produced 71 g/L SA in 27% (mol/ mol) yield. Accumulation of 15 g/L DHS and 5 g/L

QA was also observed resulting in a total yield of 34%.

B) Effects of Increased PEP Availability

The intracellular concentrations of E4P and PEP have been established to be

limiting factors for directing more carbon into the common pathway after DAHP

synthase has been overexpressed. Li and co-workers have recently reported the

biocatalytic synthesis of DHS and demonstrated the pronounced effect of *tktA*

overexpression even in absence of *pps* overexpression.[76] Liao and co-workers have

established that overexpression of *pps* improves carbon flow into the common pathway

only in presence of amplified *tktA* expression, but the reverse does not hold true.[61d,e]

Hence, in a biocatalytic environment possessing ample PEP concentrations and

overexpressed, feedback insensitive DAHP synthase, E4P availability is a critical factor

limiting aromatic amino acid biosynthesis. As expected, overexpression of transketolase

did benefit SA synthesis even in the absence of PEP synthase overexpression. All studies

done thereafter involved investigating the effect of increased intracellular PEP

concentration in the presence of overexpressed transketolase.

Although many enzymes including PEP carboxylase, PEP kinase, and PEP

carboxykinase utilize PEP as a substrate, one of the biggest drains on PEP availability for

aromatic amino acid biosynthesis, is the PTS system for glucose uptake.[71] Under the

fermentation conditions employed, the cells remain under a very glucose-rich

environment throughout the course of the fermentation. It is therefore quite reasonable to

expect the availability of PEP flowing into the common pathway to be quite minimal. Out of all the various strategies employed for increasing in vivo PEP availability, amplified expression of PEP synthase is particularly effective. Overexpression of PEP synthase allows for PTS-generated pyruvate to be recycled back to PEP. The other option of course is to utilize a non-PTS dependent mode for glucose transport, which would hence allow most of the PEP to be channeled into the common pathway. Both alternatives were examined to improve shikimate production and both strategies gave results complimentary to each other. Overexpression of *E. coli* PEP synthase or *Z. mobilis* glucose facilitator protein in SP1.1 gave an increment of approximately 20 g/L SA over the corresponding PEP limited strain SP1.1/pKD12.138A. The result obtained with facilitated diffusion was quite heartening, given that PEP synthase is a heavily regulated enzyme. In fact, its overexpression has been reported to inhibit growth of *E. coli*. Glucose uptake by facilitated diffusion on the other hand is a low affinity, high velocity transport and does not utilize the PTS system nor does it alter PEP synthase expression levels. The optimum utilization of facilitated diffusion was however realized when the native PTS glucose uptake system was no longer functional and glucose uptake was totally dependent on facilitated diffusion. Biocatalyst SP1.1*pts*/pSC6.090B gave the best results in terms of SA yield, titer, and rate of production among all SA producing strains. Between 24 h and 30 h, this biocatalyst accumulated SA at the rate of 5 g/L/h as opposed to approximately 2 g/L/h for SP1.1/pKD15.071B and SP1.1/pSC5.112B. However, the effects of *pps* and *glf* overexpression were not additive and no improvement was observed when these genes were used simultaneously in the same biocatalyst as observed with SP1.1/pSC6.162A, SP1.1/pSC6.301A and

SP1.1*pts*/pSC6.301A. This result may indicate that in vivo PEP concentration was now sufficiently high, but some other enzyme may now be rate limiting. The likelihood of high SA concentration inhibiting its own synthesis cannot be discounted either and in fact results have been obtained consistent with this possibility. Research is currently underway to investigate how to navigate this problem.

C) *E. coli* B v/s *E. coli* K12

DAHP synthase and transketolase activities have been proven to dictate the efficiency of any biocatalyst designed to produce a common pathway intermediate/metabolite. Under fed-batch fermentor conditions, biocatalysts derived from *E. coli* K12 (RB791) typically suffer from a steady reduction in enzyme activity once the cell growth reaches stationary phase. Loss in enzyme activity has also been shown to correspond to decline in the rate of production. This phenomenon has been observed with fermentations producing SA. Examination of the values reported in tables 3, 4 and 5, indicates that except for SP1.1/pKD12.112A and SP1.1/pSC4.295A, DAHP synthase activity levels were quite low for the other fermentations. The metabolic burden associated with overexpressing the additional genes took an obvious toll on the strain. It is quite possible that higher SA yields might be obtained if a biocatalyst was designed which was capable of maintaining high and steady enzyme activity levels even in stationary phase. A host strain that could be designed to serve this purpose is *E. coli* B. This microbe is known to be naturally deficient in a number of proteases, which could very well be the solution to achieving higher DAHP synthase activity.

The biocatalyst EB1.1 is identical to SP1.1 in all respects except that it is derived from *E. coli* B instead of RB791. Examination of fermentation results obtained with EB1.1 indicates that DAHP synthase and transketolase activities were indeed much higher than the SP1.1 counterpart. In fact native transketolase activity levels in EB1.1 were higher than overexpressed levels in SP1.1. However, the stable and high enzyme activities did not translate into improved SA titers or yields and EB1.1 proved to be an inferior biocatalyst to SP1.1. It is quite possible that the export system of *E. coli* B is inferior to that of RB791. A maximum barrier of approximately 70 g/L SA has been observed with RB791 derived catalysts. This barrier maybe closer to 40 g/L for strains constructed from *E. coli* B. These results illustrate that although in vivo enzyme activities play an important role in determining the yield and titer of SA, they are not the sole governing factor. There might be other controlling aspects involved with SA production, which might not be in sync with the high enzyme activities in order to derive any benefit from them. Biosynthesis is a process that involves a delicate balancing of a range of cellular processes. Optimum results are obtained when all these processes function in a synchronous fashion with matching efficiencies. We seem to have struck the right chord in RB791, but we still need to probe for the right tune in *E. coli* B.

Synthesis of Phenol from Shikimic Acid

The credentials of SA as an industrially relevant chemical have already been well established.[90,92] Providing further credence to its potential as a valuable starting material comes with the establishment of a synthetic route to phenol from SA. Annual worldwide production of phenol is estimated to be about 5.2×10^8 kg and is entirely based on synthetic processes.[105] The reactivity of the aromatic ring in phenol as well as the presence of a functionalizable hydroxy group makes phenol one of the most widely used chemicals in industry. Commercial uses of phenol include application in phenolic resins, synthesis of bisphenol A, caprolactam, aniline, and alkylphenols.[105]

The leading commercial route to phenol is via the oxidation of cumene, which accounts for 95% of the global phenol production.[105] Alkylation of benzene with propylene under Friedel-Crafts conditions affords cumene. Oxidation of cumene yields cumene hydroperoxide which upon subsequent cleavage results in phenol and acetone. The process utilizes carcinogenic, toxic materials and most importantly involves peroxide intermediates adding the risk of violent explosions to the already hazardous operation.

SA produced by fed-batch fermentations in high titers and yields from glucose can be transformed into phenol by acid catalyzed dehydration.[40] In a high pressure, stainless steel reaction vessel, SA was dissolved in degassed, carbonated water. The vessel was sealed and submerged in a sand bath and the temperature of the sand was slowly raised to 350 °C at a rate of 1.5 °C/min. The reaction vessel was heated at 350 °C for 30 min, allowed to cool to RT and the aqueous reaction mixture extracted with ether. Concentration of the organic layer gave a residue which when subjected to Kugelrohr distillation under reduced pressure afforded pure phenol as white crystals.

The residue remaining behind after the phenol distilled over mainly consisted of

m-hydroxybenzoic acid. This residue was dissolved in boiling water and returned to the

reaction vessel. A small amount of copper powder was added, the vessel sealed and the

temperature raised to 350 °C at the rate of 1.5 °C/min. After 3 h at 350 °C, the vessel

was cooled to RT and subjected to the identical work-up and purification protocols as

described earlier. The overall yield of phenol from both reactions was 51% based on the

starting SA used.
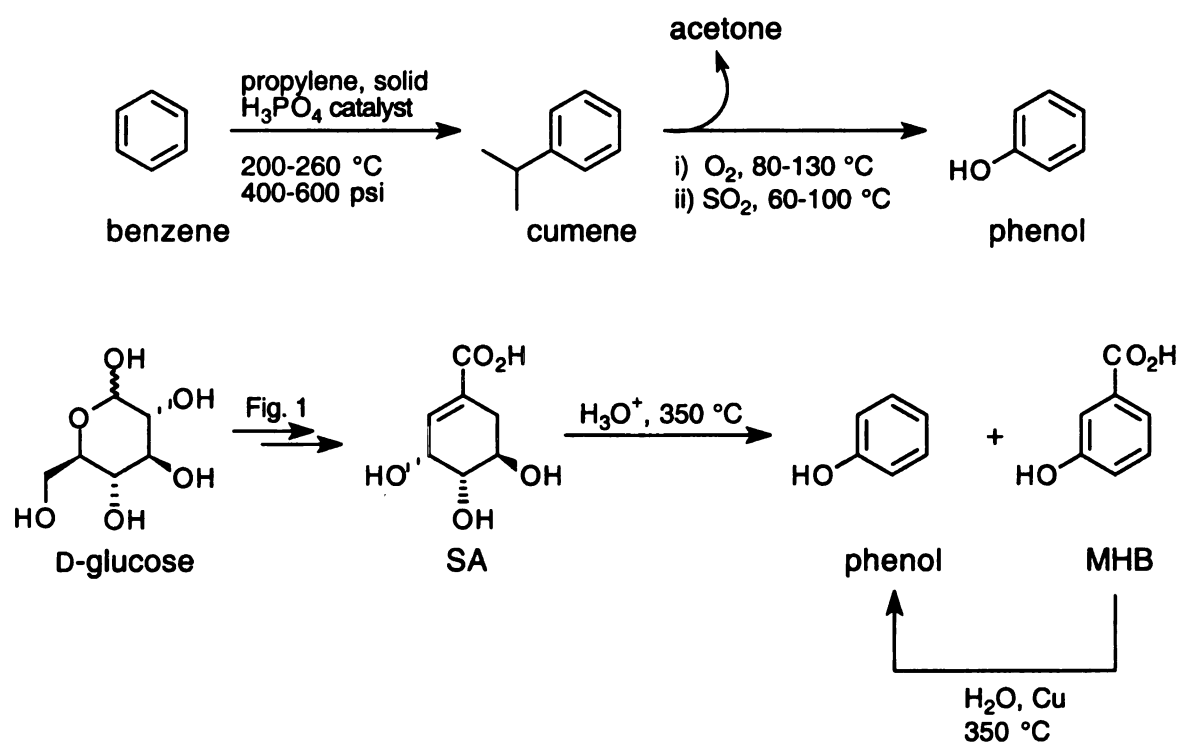
Figure 64. Comparison of phenol synthesis from benzene and D-glucose.

This conversion represents a novel scheme to convert glucose to phenol via the

intermediacy of SA. Its overall impact in providing for a safer and environmentally

benign process for producing phenol is quite significant. Development of this route

exemplifies how biocatalysis can be utilized as a very valuable tool for the safe, efficient,

and cheap production of a wide range of chemicals.

CHAPTER 4

INVESTIGATIONS INTO SHIKIMIC ACID-QUINIC ACID EQUILIBRATION

Introduction

During the early stages of development of a SA producing biocatalyst, a mixture of SA, QA and DHS was routinely seen when the strains were cultured under fed-batch fermentation conditions. For example, Draths and co-workers have reported results discussing the synthesis of SA from D-glucose in SP1.1/pKD12.112.[104] This strain produced 25.8 g/L SA along with 8.1 g/L quinic acid (QA) and 6.5 g/L of 3-dehydroshikimic acid (DHS) after 48 hours (Figure 64) (entry 1, Table 9).
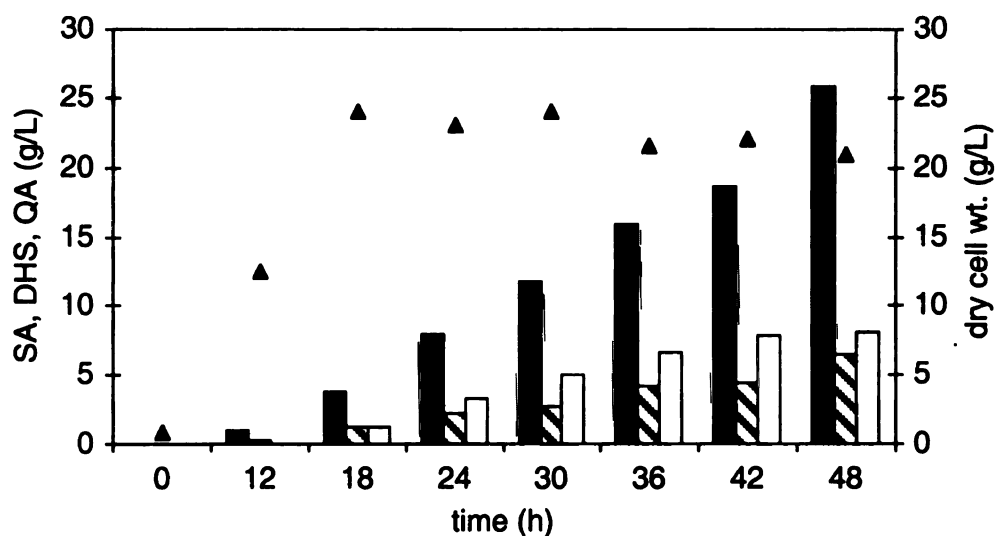
Figure 65. SP1.1/pKD12.112A fed-batch fermentation time course. Glucose limited conditions, K_c = 0.1.

▲ Dry cell wt. (g/L); ■ SA (g/L); ▨ DHS(g/L); ☐ QA(g/L).

It is important to mention that these results were obtained under glucose-limited fed-batch fermentation conditions, which are vastly different from the glucose-rich conditions described in Chapter 3 of this thesis. QA is a secondary metabolite of the common pathway for aromatic amino acid biosynthesis, produced by the reduction of DHQ by shikimate dehydrogenase.[104] The accumulation of QA is a serious drawback because it represents a drain on realizable SA yields and titers. More importantly QA co-purifies along with SA and unless the SA is well in excess of the QA, it is not trivial to obtain pure SA.[106]

DHS on the other hand most likely arises due to the feedback inhibition of shikimate dehydrogenase by SA.[95a] As highlighted in Chapter 3 of this thesis, accumulation of as much as 20 g/L DHS has been observed in SA producing fermentations. Although, it does not pose any hindrance in terms of SA purification, its production co-relates directly to a loss in SA titer and yield. Development of an efficient process for the industrial production of SA would therefore entail understanding and eliminating the source of the QA and DHS contamination.

Before the advent of the excess glucose conditions described in Chapter 3 of this thesis, fermentations typically employed limited glucose concentrations. It was under these glucose-limited conditions that QA contamination was routinely observed. Karen Draths and Dave Knop were successful in eliminating QA formation via catabolite repression by increasing glucose concentrations.[104,107] This indicated that formation of QA is dependent on uptake of a compound from the external medium, which under the increased glucose levels is no longer possible. Since SA was in abundance in the

fermentation broth and since a metabolic pathway exists for the conversion of SA to QA, it was quite possible that uptake of SA was the source of QA contamination.

In this study, several experiments were performed to validate the theory of QA arising due to uptake and in vivo processing of SA. Results were obtained that were consistent with this line of thought. Increased glucose concentrations and use of a glucose analogue dramatically shifted the SA/QA ratios in favor of SA. A variation of SP1.1 was also constructed in which the gene proposed to be responsible for shikimate uptake was knocked out. However, use of this strain did not eliminate SA/QA equilibration. Hence, although fed-batch fermentation conditions have been developed which eliminate SA/QA equilibration, the problem still remains to be solved at the genetic level.

Fed-Batch Fermentor Conditions

The fed-batch fermentor equipment was the same as that described in Chapter 3 except that the baffle cage was not used. Fermentations were run at 33 °C, pH 7.0 and the dissolved oxygen (D.O.) level was maintained at 10%. Initial glucose concentration was kept at 20 g/L. The major differences in the fermentation conditions used in Chapter 3 and the studies described in this Chapter lie in the operating parameters used for controlling the oxygen level.

In the first stage, the stirrer was ramped up to 940 rpm instead of 750 rpm. Once the stirrer reached this preset limit, it was maintained at this speed and the airflow was ramped up from 0.06 L/L/min to 1.0 L/L/min in order to keep the D.O. level at 10%. In the third stage, at an impeller rate of 940 rpm and airflow of 1.0 L/L/min, the D.O. levels

were maintained steady at 10% by oxygen sensor controlled glucose feeding for the remainder of the fermentation. Glucose levels were therefore maintained at the bare minimal level required to maintain healthy cell growth and at no stage in the fermentation was there any excess glucose present. At the beginning of the third stage, D.O. levels did fall below 10% due to residual initial glucose still present. This lasted for approximately 30 min until all the glucose was consumed and the controlled glucose feeding was started. The fermentations were typically run for 48 h after which oxygen sensor control of glucose became difficult to control and indiscriminate addition of glucose would take place.

SA/QA Equilibration: Is Uptake of SA the Source of QA Contamination?

The observation of SA/QA equilibration was first reported by Draths and co-workers in 1999.[104] The strain SP1.1/pKD12.112A produced SA and QA in a molar ratio of 3.5:1 after 48 h (entry 1, Table 9). The synthesis of QA by SP1.1/pKD12.112A was extremely surprising, given the absence in *E. coli* of quinate dehydrogenase, an oxidoreductase which interconverts DHQ and QA. Given the similarity in structure between DHQ and DHS, the possibility arose that *aroE* encoded shikimate dehydrogenase could catalyze the reduction of DHS to SA as well as that of DHQ to QA. Incubation of DHQ with shikimate dehydrogenase resulted in oxidation of NADPH and concomitant formation of QA.[104] The observed rate was approximately one tenth of the rate for shikimate dehydrogenase catalyzed conversion of DHS to SA. Considering these facts, a reasonable strategy to eliminate QA contamination would be to minimize

cytosolic concentrations of DHQ. This could be accomplished by overexpressing *aroD* encoded DHQ dehydrogenase. However, even amplified expression of DHQ dehydratase did not reduce the level of SA/QA equilibration under fed-batch fermentor conditions.[104] This result indicated that QA formation may not result via de novo biosynthesis but rather from equilibration of initially synthesized SA (Figure 65).
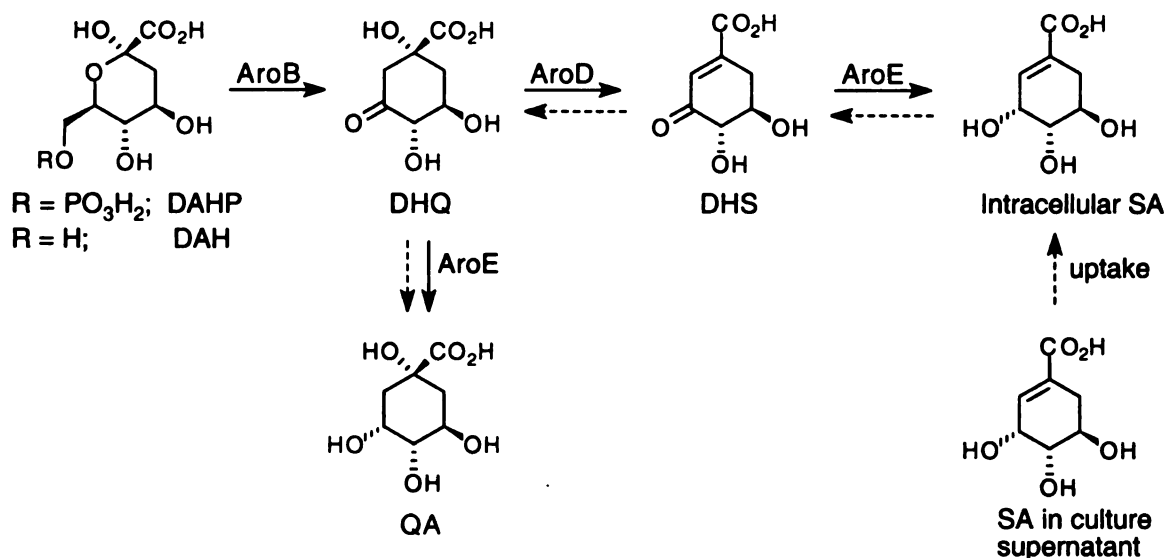
Figure 66. The two possible pathways leading to QA production.

Although *E. coli* does not have the capability to catabolize SA, it has been reported to possess a transport system specific for SA uptake.[108] It is quite possible that SA transport in *E. coli* may be an evolutionary vestige of a previous ability to catabolize SA as a sole source of carbon for growth and metabolism. When *E. coli* cells are offered multiple carbon sources, the carbohydrate-metabolizing enzymes are expressed in a hierarchical fashion. Glucose is the preferred substrate and its presence blocks the transport of other sugars as well as other less favored carbon sources. Glucose catabolism is also known to reduce the rate of expression of genes encoding the catabolic enzymes for other sources of carbon. This phenomenon is termed catabolite

repression.[71,109] Uptake of SA could therefore be hindered by high glucose concentrations in the fermentor.

The rate of glucose addition to the fermentor is controlled by the proportional-integral-derivative (PID) setting gain (K_c). The fermentation with SP1.1/pKD12.112A, which resulted in a 3.5:1 ratio of SA/QA employed a normal PID setting of $K_c = 0.1$. Adjusting the PID setting to $K_c = 0.8$ increased glucose availability, but subjected the cells to a much more aggressive feeding regimen. When a PID setting of $K_c = 0.1$ was employed, the glucose feeding rate and dissolved oxygen level usually stabilized a couple of hours after the third phase was initiated and did not fluctuate much for the remainder of the experiment. With a PID setting of $K_c = 0.8$ however, the glucose feed response was so rapid that a pulsed addition regimen set in, inducing a pulsed dissolved oxygen profile. Dissolved oxygen stayed at 0% until a glucose pulse was consumed and then started increasing rapidly. As soon as the oxygen level reached 10%, the glucose pump, which so far was inactive, switched on and its output ramped up swiftly. Glucose addition continued at a rapid rate until the dissolved oxygen peaked between 20 - 30%. A dramatic decline in the dissolved oxygen level was then observed due to the excess glucose now present in the medium. The glucose addition also decreased at a commensurate rate and turned off completely at 10% dissolved oxygen level. The dissolved oxygen kept dropping until it was close to 0%. It remained steady at this level until all the glucose was consumed and then the cycle was repeated.

The effect of this pattern of glucose addition and dissolved oxygen level was a drastic reduction in the formation of QA by SP1.1/pKD12.112A throughout the fermentation period (Figure 66).[104] Since the only difference between this experiment

and the one run with $K_c = 0.1$ was the level of glucose, the observed decrease in QA formation could be attributed to glucose induced catabolite repression of SA uptake. The overall SA titer was much lower due to the metabolic burden imposed on the cells by the oscillatory, critically damped control scheme (entry 2, Table 9).
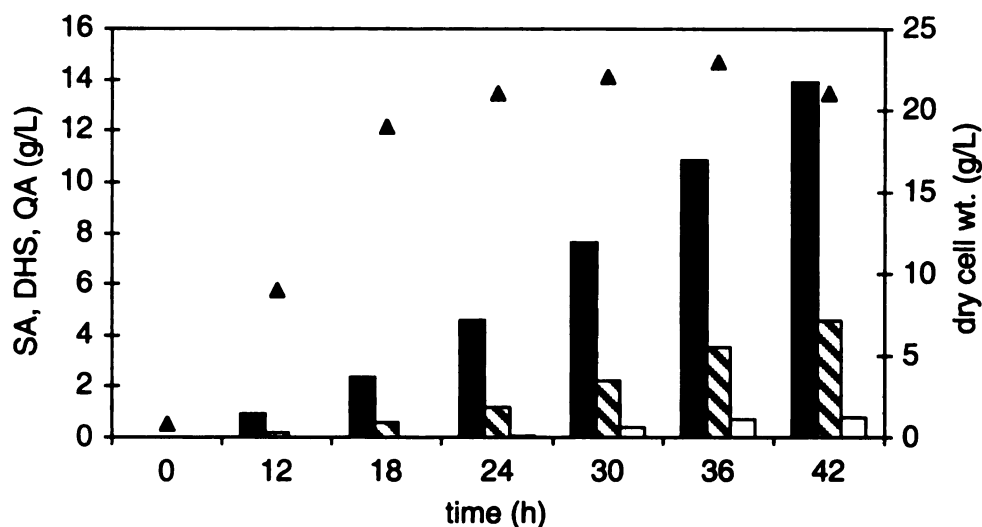
Figure 67. SP1.1/pKD12.112A fed-batch fermentation time course. Glucose limited conditions, $K_c = 0.8$.

▲ Dry cell wt. (g/L);   ■ SA (g/L);   ⧅ DHS(g/L);   ⃞ QA(g/L).

This result reinforces the theory that QA contamination occurs due to uptake of SA from the fermentation broth and its in vivo processing to QA. However, use of this pulsed glucose addition scheme cannot be used for an industrial scale process. Lowering of the metabolic capacity of the cells resulted in loss of dissolved oxygen control and unregulated glucose addition, necessitating shutting down of the fermentation after 42 h. Furthermore, increase in the PID setting could suppress QA formation only in SP1.1/pKD12.112A and had no effect on fermentations involving SP1.1/pKD12.138A (entry 5, Table 9). This strain takes advantage of transketolase overexpression and is

capable of producing high titers and yields of SA as described in Chapter 3. However,

QA contamination negates any potential application of SP1.1/pKD12.138A on an

industrial scale. A universally applicable method was therefore sought after for the

suppression of QA synthesis.

$$HO-CH_2$$

methyl-α-D-glucopyranoside
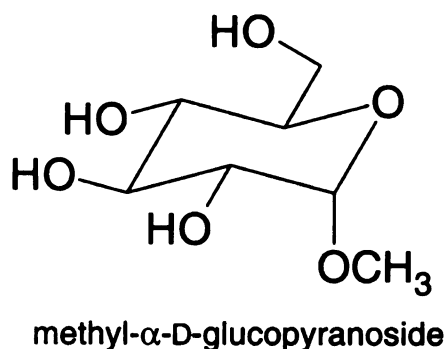
Figure 68. Structure of methyl-α-D-glucopyranoside (MGP).

The compound methyl-α-D-glucopyranoside (MGP) is a non-hydrolyzable

glucose analogue which is known to be a substrate for the PTS system of glucose

transport (Figure 67).[109a,110] It has also been shown to exhibit the same catabolite

repressive tendencies as glucose. MGP undergoes phosphorylation while being

transported across the cell membrane, akin to glucose. However, unlike phosphorylated

glucose, the phosphorylated MGP cannot be catabolized by the cell. It is therefore

dephosphorylated by the cytosolic phosphatases and channeled out of the cell. Export of

free MGP has been postulated to occur as an exchange for phosphorylated MGP.

Extracellular concentrations of MGP would therefore be expected to remain constant and

hence a continuous addition of MGP is not needed.[110b] A concentration of 1 mM MGP

was found to be saturating in terms of MGP transport and phosphorylation. The most

important ramification of this process was that high glucose levels were no longer needed

to maintain a catabolic repressive effect on shikimic acid uptake. Hence, a normal PID setting of $K_c = 0.1$ could be employed, ensuring that the cells remained viable for longer durations of time.

Strain SP1.1/pKD12.112A was cultured under normal fermentation conditions in the presence of 1 mM MGP. No quinic acid formation was observed even after 48 h using a PID setting of $K_c = 0.1$ (Figure 68). This result is in stark contrast to that observed when the same strain was cultivated under identical fermentation conditions in the absence of MGP, when a 3.5:1 ratio of SA/QA was observed. This method of suppressing QA synthesis was also more appealing than employing a $K_c = 0.8$ as evidenced by the higher SA yield and titer (entry 3, Table 9), as also the improved dissolved oxygen control up to 48 h.[107]
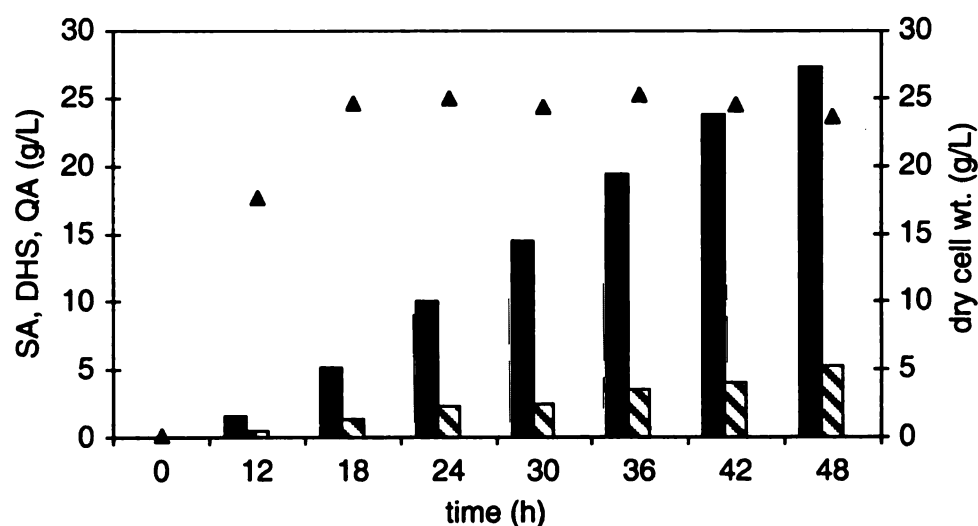
Figure 69. SP1.1/pKD12.112A fed-batch fermentation time course. Glucose limited conditions, $K_c = 0.1$, 1mM MGP.

▲ Dry cell wt. (g/L);   ■ SA (g/L);   ▨ DHS(g/L);   ☐ QA(g/L).

Strain SP1.1/pKD12.138A gave a SA/QA ratio of 1.6:1 after 48 h under normal

fed-batch fermentation conditions at a PID setting of K_c = 0.1 (Figure 69) (entry 4, Table

9). Increasing the gain to K_c = 0.8 worsened the situation giving a SA/QA ratio of 1.4:1

with much lower yields and titers after 42 h (entry 5, Table 9). By contrast, conducting a

fed-batch fermentation with SP1.1/pKD12.138A with a PID setting of K_c = 0.1 in the

presence of 1 mM MGP reduced the QA contamination to trace amounts (Figure 70).

After 48 h, this fermentation afforded 34.5 g/L SA in 19% yield with a 14.1:1 ratio of

SA/QA (entry 6, Table 9), thereby allowing the impact of transketolase overexpression

on yield and titer to be realized.[107]
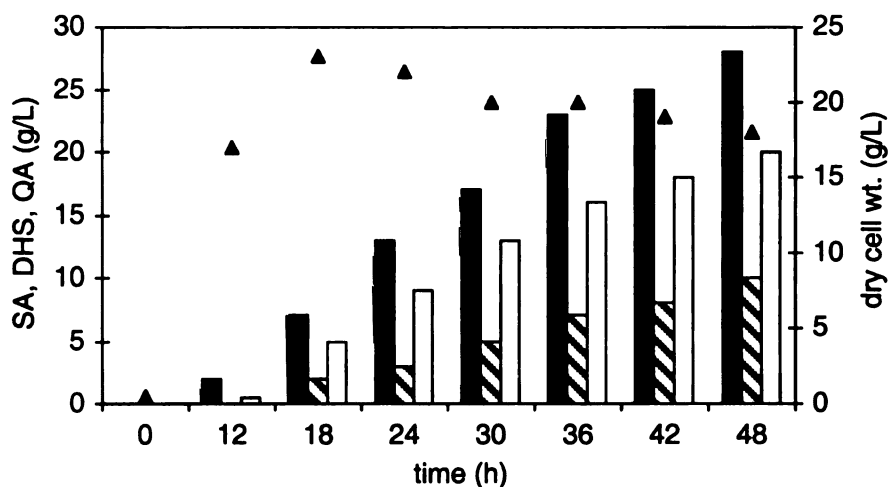
Figure 70. SP1.1/pKD12.138A fed-batch fermentation time course. Glucose limited
conditions, K_c = 0.1, 0 mM MGP.
▲ Dry cell wt. (g/L);　■ SA (g/L);　▧ DHS(g/L);　☐ QA(g/L).
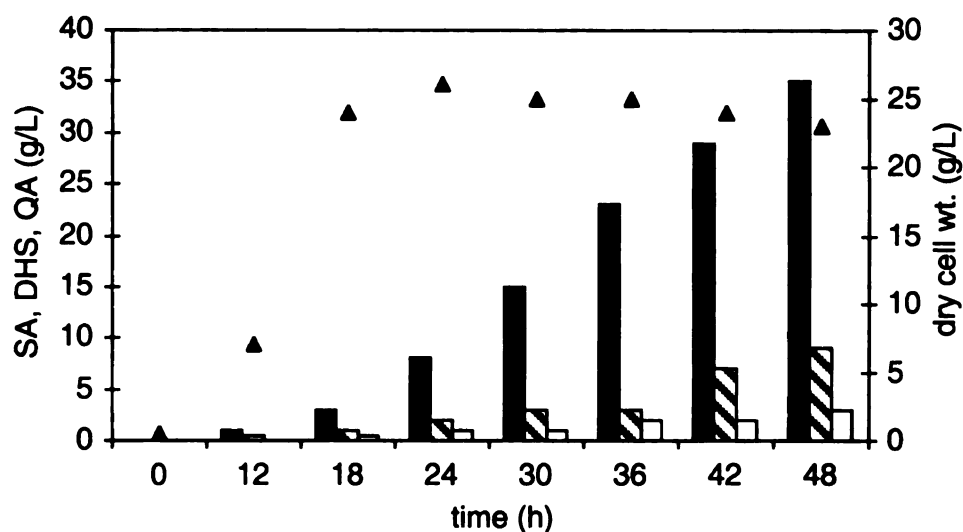
Figure 71. SP1.1/pKD12.138A fed-batch fermentation time course. Glucose limited conditions, K_c = 0.1, 1 mM MGP.

▲ Dry cell wt. (g/L); ■ SA (g/L); ◼ DHS(g/L); ⎸ ⎸ QA(g/L).

Table 9. Titers and yields of SA produced under various glucose-limited conditions.

Entry no.	Strain	K_c	[MGP] (mM)	[SA] (g/L)	[QA] (g/L)	[DHS] (g/L)	SA/ QA ratio	SA yield (mol/mol)	Total yield (mol/mol)
1	SP1.1/pKD12.112A	0.1	0	25.8	8.1	6.5	3.5:1	13%	20%
2	SP1.1/pKD12.112A	0.8	0	13.7	1.2	4.6	12:1	10%	14%
3	SP1.1/pKD12.112A	0.1	1	27.3	0.0	5.3	–	15%	18%
4	SP1.1/pKD12.138A	0.1	0	28.0	19.3	10.8	1.6:1	14%	29%
5	SP1.1/pKD12.138A	0.8	0	11.7	9.4	5.7	1.4:1	8%	18%
6	SP1.1/pKD12.138A	0.1	1	34.5	2.8	8.8	14.1:1	19%	25%

Experimental Evidence Supporting QA Formation Via SA Uptake

As illustrated in Figure 65, there are two possible avenues to consider as sources of the QA contamination. It could be arising via de novo biosynthesis or it could occur by uptake of SA from the culture supernatant and its in vivo processing to QA. Both mechanisms utilize the ability of *aroE* encoded shikimate dehydrogenase to reduce DHQ as well as DHS to QA and SA respectively. The fact that lowering the intracellular concentrations of DHQ by overexpression of *aroD* encoded DHQ dehydratase had no effect on QA accumulation weakens the argument in favor of de novo synthesis. Information gleaned from results discussed earlier in this Chapter, implicate uptake of SA as the culprit leading to QA formation. Moreover, if QA formation were occurring via de novo synthesis, then accumulation of some DHQ would be expected. Biocatalysts designed to biosynthesize QA, namely QP1.1/pKD12.138A, routinely produce DHQ as a contaminant in fed-batch fermentations. This phenomenon is not observed during SA producing fermentations.

In order to establish the mode of formation of QA with some degree of confidence strain SC1.0 was constructed (Figure 71). This biocatalyst was derived from *E. coli* RB791*serA* also known as JWF1. The *aroL* and *aroK* encoded isozymes of shikimate kinase were rendered inactive by successive P1 phage-mediated transductions of *aroL*::Tn*10* and *aroK*::Cm^R resulting in strain SC1.1. A final P1 phage-mediated transduction of *aroB*::Tn*5* resulted in loss of *aroB* encoded DHQ synthase activity. P1 phage was propagated from JB5.[95b]

Strain construction   Selections used for identifying correct phenotype

	M9/glu	M9/glu/ser
RB791 serA⁻	− − −	+ + +

aroL::Tn10		

	LB/Tc	M9/glu/ser
RB791 serA⁻ aroL::Tn10	+ + +	+ + +

aroK::CmR		

	LB/Tc/Cm	M9/glu/ser
RB791 serA⁻ aroL::Tn10 aroK::CmR	+ + +	− − −

aroB::Tn5		

	LB/Tc/Cm/Kn	
RB791 serA⁻ aroL::Tn10 aroK::CmR aroB::Tn5	+ + +	
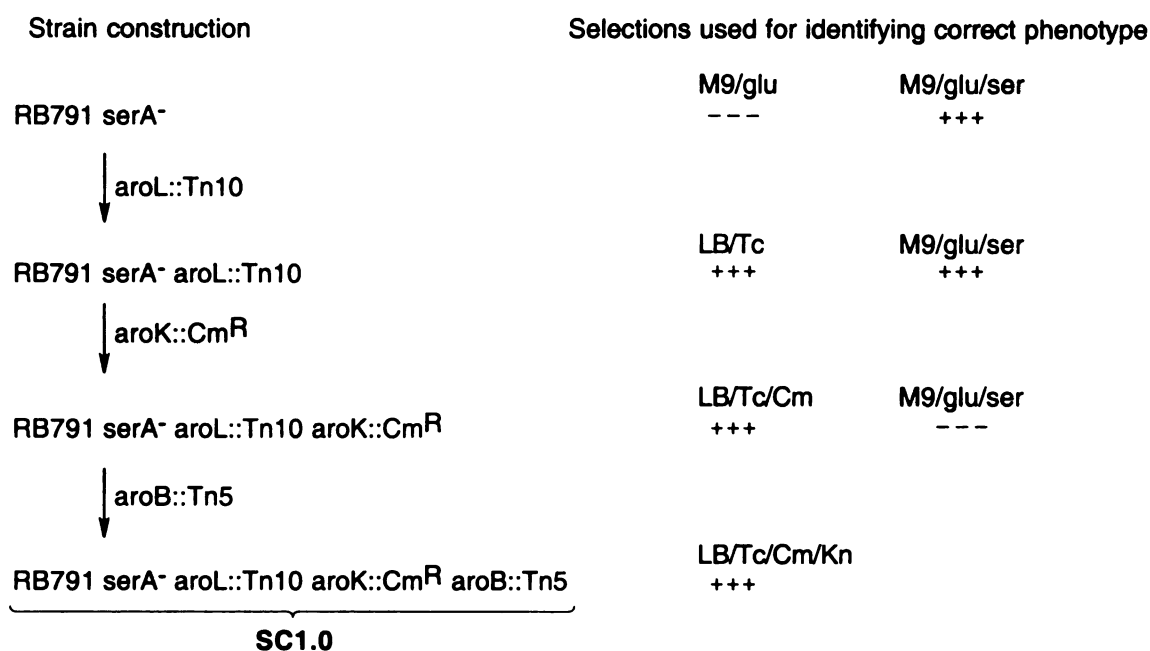
SC1.0

Figure 72. Construction and selection of SC1.0.

The overall effect of this operation was that the entire common pathway in SC1.0 was confined between SA and DHQ (Figure 72). Most importantly, this strain lacked the capability for SA and QA synthesis, which was critical for the success of the investigation. SA could be manually added to a fermentation culture of SC1.0 transformed with an appropriate plasmid. If any QA formation were to be observed during the fermentation, it would have to occur via import of SA into the cell and its in vivo conversion to QA.
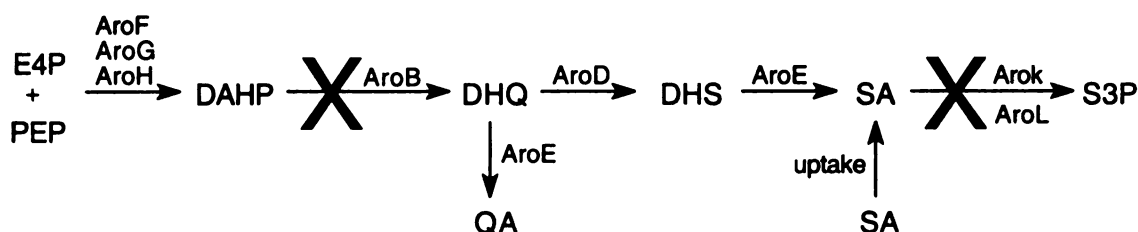
Figure 73. The modified shikimate pathway in SC1.0.

Plasmid pKD12.138 was transformed into SC1.0 and fed-batch fermentations were conducted with this strain. The first fed-batch fermentation performed with SC1.0/pKD12.138A was under normal conditions with no addition of SA. This run was used as the control experiment and confirmed that the biocatalyst indeed was not able to synthesize SA and QA. It did however succeed in accumulating 68 g/L of DAH in the culture supernatant after 48 h. Observation of DAH is an artifact of the loss of DHQ synthase activity resulting in formation of DAHP, which gets dephosphorylated and exported out the cell as DAH.

Once it had been established that SC1.0/pKD12.138A was incapable of in vivo synthesis of SA or QA, the main experiment was proceeded with. SC1.0/pKD12.138A was cultured under normal fermentation conditions and at 18 h into the run, 10 g of SA was added to the fermentation. The fermentation was continued for 48 h and aliquots were removed every 6 h. Analysis of the fermentation samples indicated that 62 g/L of DAH had been produced. However, no QA was observed and the original amount of SA added into the fermentation (10 g) was measured to be unchanged. It was quite possible that the elevated levels of DAH/DAHP being synthesized by the strain interfered with SA uptake. Production of DAH/DAHP could be minimized by shutting the glucose feed once the cells attained maximum growth and entered stationary phase of growth. Depriving the cells from glucose might also serve a dual purpose. In the absence of glucose the cells would be starved for a carbon source and since SA would most likely be the only one present in substantial amounts, chances of its uptake would be enhanced.

The fermentation with SC1.0/pKD12.138A was repeated under normal cultivation conditions. In this experiment, 10 g of SA was added at 12 h instead of 18 h to provide

the cells sufficient time to uptake the SA. At 18 h, the glucose pump was turned off and the fermentation was continued for 48 h. Analysis of fermentation samples confirmed that shutting down the glucose feed did indeed lower DAH/DAHP synthesis dramatically. Only 7 g/L of DAH was measured after 48 h as opposed to 62 g/L observed in previous fermentations. However, the negative aspect of the experiment was the complete absence of any QA formation whatsoever. Attention was also given to the fact that deprivation of glucose drastically affected the growth of the cells. A maximum dry cell weight of 14 g/L at 24 h was measured for this strain when the glucose pump was shut down at 18 h. The maximum dry cell weight recorded for SC1.0/pKD12.138A was 24 g/L at 30 h when the glucose feed was continued with for 48 h. Two likely scenarios therefore emerged to account for absence of SA/QA equilibration. It was quite likely that the sickness of the cells caused by lack of glucose prevented uptake of SA. This was indeed a strong possibility because SA/QA equilibration was normally observed to set in when cell growth was at peak efficiency. The other possibility was to accept that QA formation was not a result of SA uptake but due to the presence of a de novo biosynthetic route. A conclusive interpretation could therefore not be drawn from this body of work.

A close examination of the problems associated with the study discussed earlier, highlighted the importance of sustaining good biocatalyst growth but without accumulation of any product which might interfere in the uptake mechanism. An alternative approach was therefore designed. Since inactivation of DHQ synthase coupled with overexpression of $aroF^{FBR}$ encoded DAHP synthase was responsible for accumulation of DAH/DAHP, it was decided to instead inactivate DAHP synthase. The common pathway would then be corralled between DAHP and SA instead of DHQ and

SA (Figure 73). An added advantage of this approach was that SP1.1 could be used as the host strain, since the native *E. coli* DAHP synthase isozymes are feedback inhibited by the aromatic amino acids. Regular addition of aromatic amino acids during the fermentation would therefore ensure suppression of genomic DAHP synthase. Glucose addition could therefore be continued throughout the fermentation period thereby maintaining healthy cell growth without accumulation of any product. The plasmid required for the investigation would have to incorporate all the genes present in pKD12.138A except for $aroF^{FBR}$, which encodes for feedback insensitive DAHP synthase.
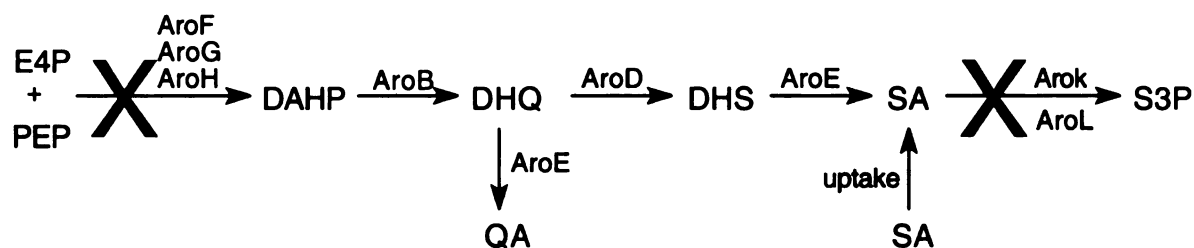
Figure 74. Effect of inactivating DAHP synthase in SP1.1.

The $aroF^{FBR}$ locus in pKD12.138A possesses a *Bgl*II restriction site which is a unique site in the plasmid. Digestion of pKD12.138A with *Bgl*II resulted in a linear plasmid which was treated with Klenow fragment. Ligation of the linear plasmid afforded pSC5.214A, which was identical to pKD12.138A in all respects except for the presence of the inactive $aroF^{FBR}$ gene (Figure 74). Plasmid pSC5.214A was transformed into SP1.1 and this strain was used in the fermentation experiments designed to decipher the mode of formation of QA.
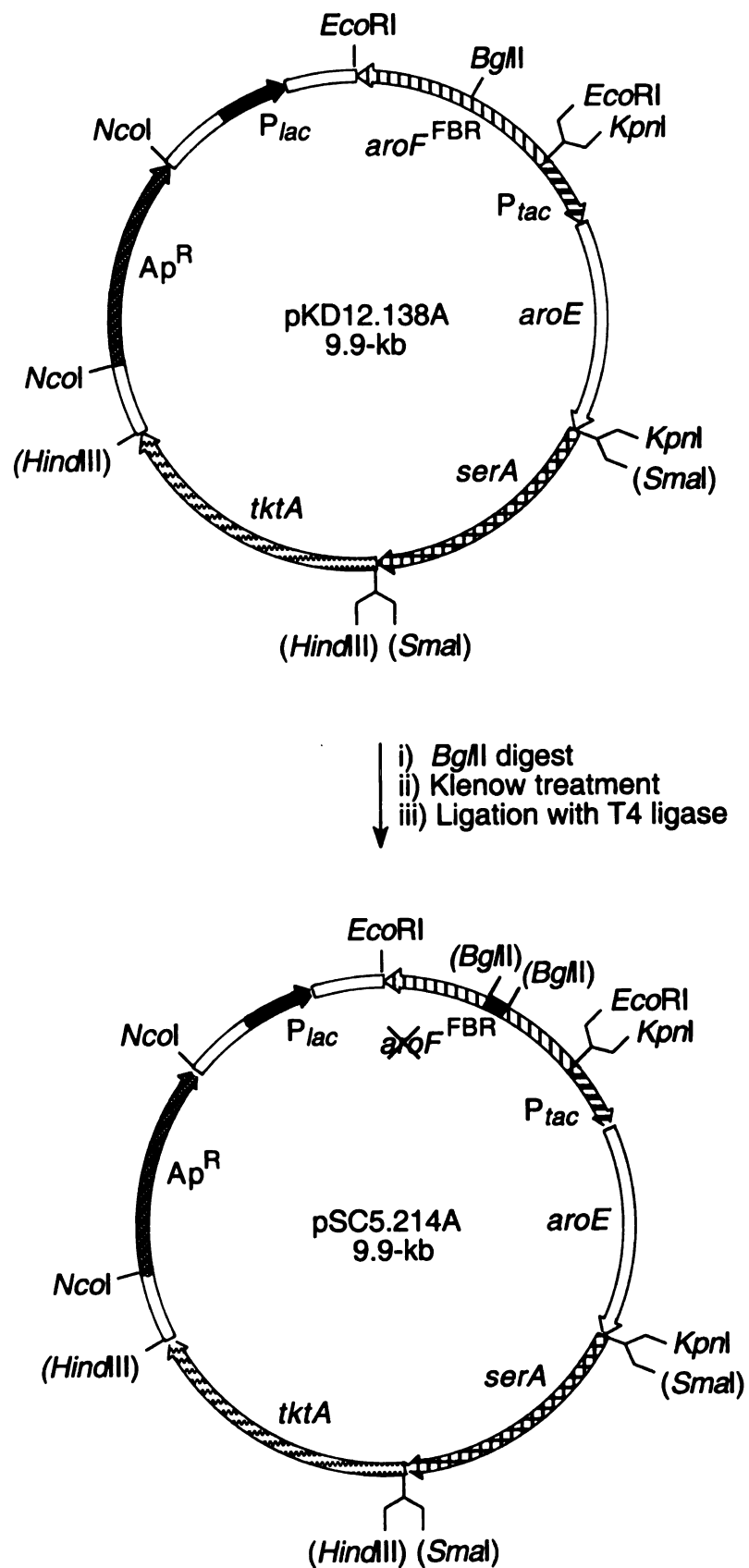
Figure 75. Preparation of Plasmid pSC5.214A.

The first fed-batch fermentation performed with SP1.1/pSC5.214A was under normal conditions and provided information as to its production capabilities. After 48 h, accumulation of 24 g/L SA and 3.5 g/L DHS was recorded (Figure 75). No QA production was observed. No additional aromatic amino acids were added apart from the initial dosage required to sustain cell growth and hence native DAHP synthase remained active during the fermentation.
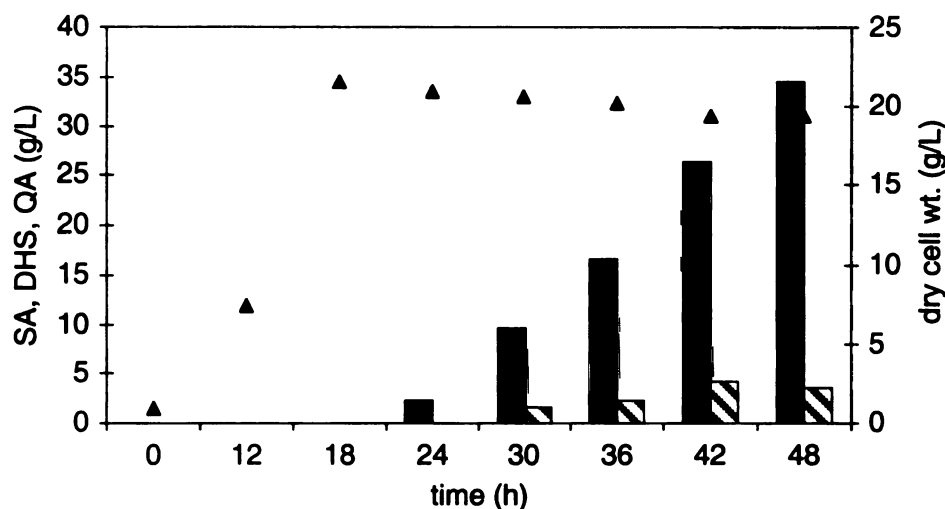
Figure 76. SP1.1/pSC5.214A fed-batch fermentation time course. Glucose limited conditions, no extra aromatic amino acids added.
▲ Dry cell wt. (g/L); ■ SA (g/L); ▧ DHS(g/L); QA(g/L).

The next experiment conducted with SP1.1/pSC5.214A was to observe the effects of maintaining a finite concentration of aromatic amino acids in the fermentation at all times. Apart from the aromatic amino acids added at 0 h for normal cell growth, 0.7 g phenylalanine, 0.7 g tyrosine, and 0.35 g tryptophan were added at 18 h and 30 h into the fermentation. After 48 h, analysis of the fermentation samples indicated that no SA, DHS or QA were produced implying the complete suppression of native DAHP synthase.

It was also worth noting that the cells exhibited robust growth and hence the problems associated with SC1.0/pKD12.138A could be avoided.

SP1.1/pSC5.214A was cultured under fed-batch fermentation conditions identical to those described above with the periodic addition of aromatic amino acids. The main difference was the addition of 10 g SA at 12 h into the fermentation. No QA acid formation was observed until 24 h into the experiment. Traces of QA were then measured to have been formed between 24 h and 30 h followed by a sudden burst in QA production with a concomitant depletion in SA amounts between 30 h and 36 h. After 48 h, a final SA/QA ratio of 0.76:1 was measured providing irrefutable evidence that involvement of SA uptake and its in vivo processing was responsible for the formation of QA. In addition, 2.5 g/L of DHS was also recorded to have been formed after 48 h.
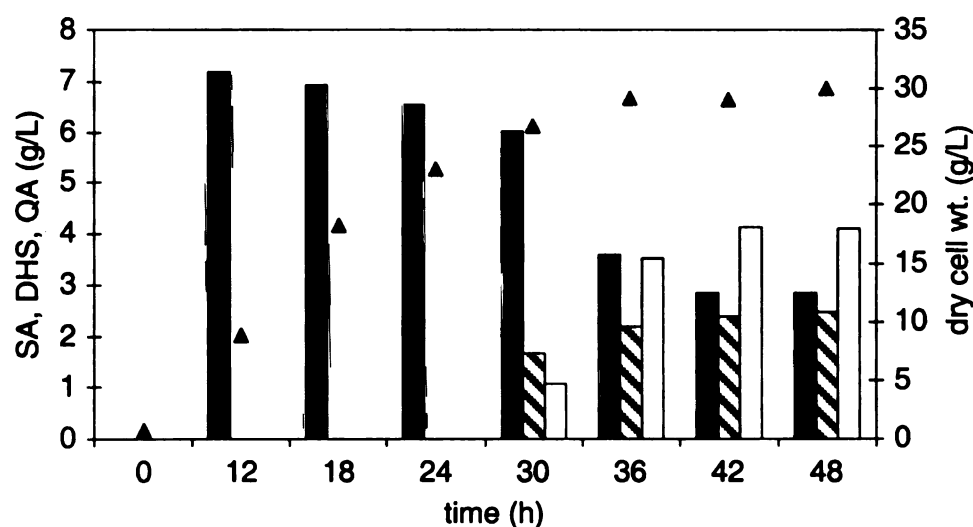
Figure 77. SP1.1/pSC5.214A fed-batch fermentation time course. Glucose limited conditions; aromatic amino acids added at 0 h, 18 h and 30 h; 10 g SA added at 12 h.
▲ Dry cell wt. (g/L);   ■ SA (g/L);   ▨ DHS(g/L);   ▢ QA(g/L).

Establishment of the role of SA uptake in the formation of QA provided an avenue to explore which could lead to elimination of SA/QA equilibration. Extensive research has been conducted on identifying the genetic basis for SA uptake. In 1998, Pittard and co-workers cloned and sequenced a 1.3-kb DNA fragment labeled *shiA*, which was shown to be responsible for the ability of *E. coli* to import SA.[111] Introduction of a mutation into the *shiA* locus rendered the cell unable to transport SA.

The strain JP11123 carrying the *shiA*::Kan[R] locus had been previously constructed by Pittard and co-workers.[111] P1 phage-mediated transduction of *shiA*::Kan[R] from JP11123 into SP1.1 resulted in SP1.1*shiA* which should now be unable to transport SA and hence be incapable of producing QA. Plasmid pKD12.138A was transformed into SP1.1*shiA* and the resulting biocatalyst SP1.1*shiA*/pSC5.214A was tested under normal fed-batch fermentation conditions. As described earlier, at 0 h, 18 h, and 30 h into the fermentation, 0.7 g phenylalanine, 0.7 g tyrosine, and 0.35 g tryptophan were added to inhibit native DAHP synthase. 10 g SA was added to the culture at 12 h into the fermentation. The fermentation was allowed to complete 48 h and the samples analyzed. Knocking out the *shiA* locus in SP1.1 had no effect on SA/QA equilibration (Figure 78) and the result obtained was essentially the same as that observed with SP1.1/pSC5.214A. Since this strain lacks the capability to synthesize QA but production of this compound is still observed, the most likely explanation is that there may be multiple proteins responsible for SA uptake.
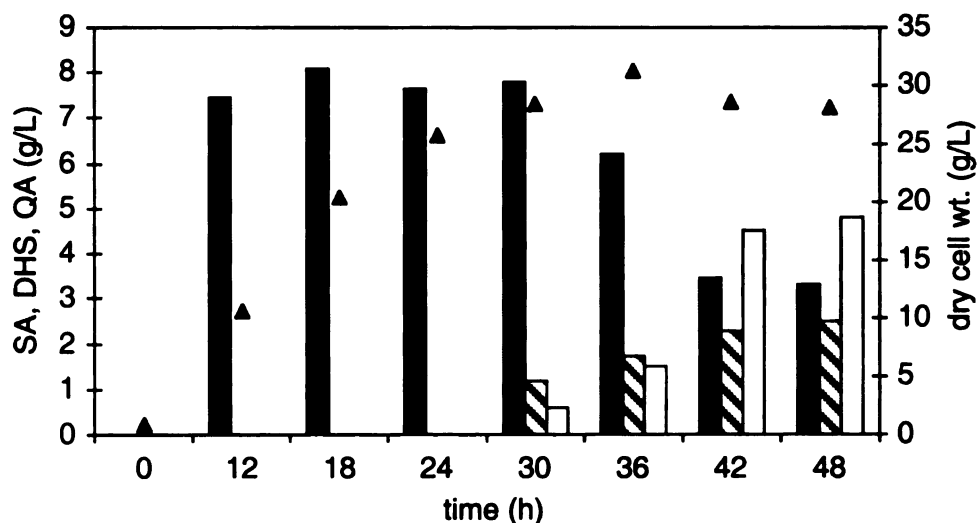
Figure 78. SP1.1shiA/pSC5.214A fed-batch fermentation time course. Glucose limited conditions; aromatic amino acids added at 0 h, 18 h and 30 h; 10 g SA added at 12 h.

▲ Dry cell wt. (g/L); ■ SA (g/L); ▨ DHS(g/L); ☐ QA(g/L).

Comparison was also made between SP1.1/pKD12.138A and SP1.1shiA/pKD12.138A under fed-batch fermentation conditions with a $K_c = 0.1$ setting, in the absence of MGP. These conditions produced 28 g/L SA and 19.3 g/L QA in a molar ratio of 1.6:1 with SP1.1/pKD12.138A (Figure 69). Introduction of the shiA phenotype gave no discernable advantage and in fact, SP1.1shiA/pKD12.138A gave a worse SA/QA ratio of 1.1:1 (Figure 79).
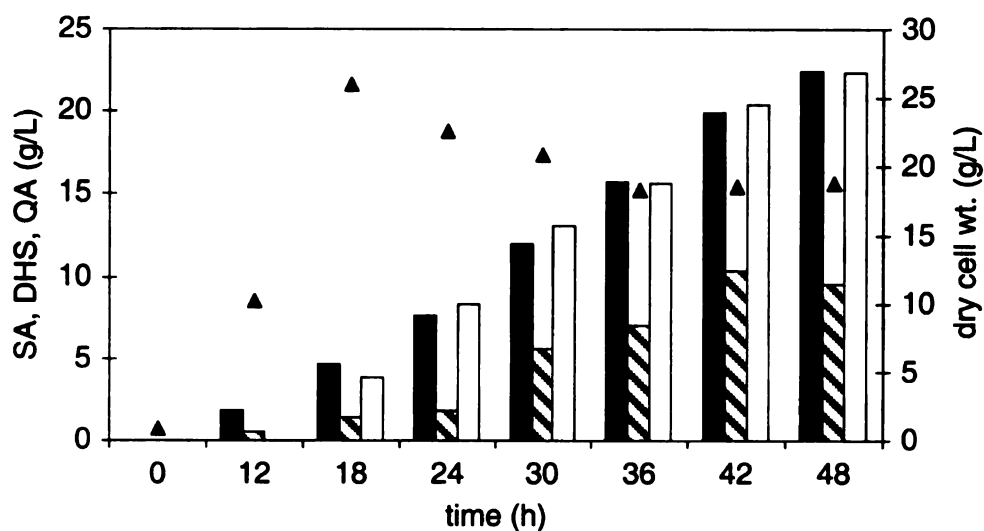
Figure 79. SP1.1*shiA*/pKD12.138A fed-batch fermentation time course. Glucose limited conditions, $K_c = 0.1$, 0 mM MGP.

▲ Dry cell wt. (g/L); ■ SA (g/L); ⧄ DHS(g/L); QA(g/L).

Discussion

Before the emergence of glucose-rich fed-batch fermentor conditions described in

Chapter 3 of this thesis, biocatalysts were routinely cultured under conditions limited in

glucose. A resulting manifestation of these conditions was the observation of QA being

co-synthesized along with SA. Normal fed-batch fermentations were run by maintaining

the glucose feed pump proportional-integral-derivative (PID) gain setting of $K_c = 0.1$.

The ramification of this value on the fermentation conditions was that the glucose

concentration throughout the fermentation period, was just sufficient to sustain healthy

growth of the cells and ensure a 10% dissolved oxygen value. The input of glucose into

the fermentation was exactly matched by its consumption by the cells and at no given

time could excess glucose be measured to be present in the culture supernatant. When a

PID gain setting of $K_c = 0.8$ was adopted, the only experimental parameter being changed was the rate of glucose feeding. Instead of a steady feeding pattern, a pulsed glucose addition was assumed resulting in a pulsed dissolved oxygen profile. The overall effect was to maintain a higher effective concentration of glucose in the fermentation, which translated into disappearance of QA formation. The disappearance of QA formation hinted at the involvement of an uptake phenomenon, which was now catabolically repressed by the increased glucose levels.

Suppression of QA production via the utilization of a PID setting of $K_c = 0.8$ came with its share of penalties. The pulsed feeding regimen caused early loss of dissolved oxygen control resulting in unregulated addition of glucose, forcing shutdown of the fermentation at 42 h. The approach was found to succeed only for SP1.1/pKD12.112A and not be viable for strains capable of producing higher amounts of SA namely, SP1.1/pKD12.138A. In addition, the feeding regimen was detrimental to the health of the cells affecting yields and titers of SA. Hence this method was not considered as the ideal route to pursue and alternative options were considered.

The use of MGP was based on the notion that at $K_c = 0.8$, glucose induced catabolite repression prevented uptake of SA, thereby accounting for the disappearance of QA. Various reports have acknowledged the ability of MGP to mimic glucose in various situations including its ability to effect catabolite repression on non-carbohydrate substrates. Use of MGP would permit use of normal fermentation conditions with a PID setting of $K_c = 0.1$, thereby ensuring normal cell growth and higher SA titers. An addition of 1 mM MGP at the beginning of the fermentation was found to be sufficient to last the entire duration of the fermentation. Strains SP1.1/pKD12.112A and

SP1.1/pKD12.138A were tested under these conditions and both gave positive results. Good dissolved oxygen control was maintained throughout the fermentation and at the end of 48 h no QA was detected in the culture supernatant. Apart from the fact that both strains produced SA free from QA contamination, it was important to acknowledge that they did so in reasonable titers and yields. The observation that maintaining a finite carbohydrate concentration was key to suppressing QA formation lent credence to the theory of SA uptake being the source of the problem. These results also represented the first instance of fermentation conditions being available for industrial production of SA.

Research conducted to this point provided results consistent with QA synthesis occurring due to import of SA by the cell followed by in vivo processing via the common pathway. They by no means discounted the possibility that QA could also arise by de novo biosynthesis. It was therefore important to test for accumulation of QA within a system in which the capability for de novo synthesis of QA was not functional. The biocatalyst SP1.1/pSC5.214A perfectly suited these requirements and provided a means to lock the common pathway between DAHP and SA with no possibility for de novo synthesis. Under normal fermentation conditions, SP1.1/pSC5.214 was able to exhibit SA/QA equilibration when the only possibility for QA formation was via uptake of added SA from the culture medium.

SA transport has for long been hypothesized to be mediated by multiple loci in the E. coli genome.[108,111] Recently the major locus purported to be responsible for SA uptake named shiA has been cloned and sequenced.[111] The Kan[R] gene was inserted within the shiA locus and the resulting shiA::Kan[R] fragment was introduced into the E. coli genome by homologous recombination. The resultant strain JP11123 exhibited a marked inability

to import SA from the external medium as compared to the parent strain AB2826. Restoration of SA uptake capability in JP11123 was observed upon introduction of a plasmid carrying wild-type *shiA*.

Transduction of the *shiA*::Kan^R locus into SP1.1 was intended to provide a strain devoid of any SA/QA equilibration tendencies. However, the ability of SP1.1*shiA*/pSC5.214 to produce both QA and DHS from exogenously supplied SA contradicts the notion that mutants deficient in *shiA* activity are unable to transport SA. However, as stated before, multiple loci have been held responsible for SA transport in the past. Evidence for the *shiA⁻* phenotype of JP11123 was obtained by monitoring for uptake of [^{14}C]-SA. These experiments were performed for 90 seconds at cell densities of approximately 0.11 g/L.[111] On the other hand, fermentations performed with SP1.1*shiA*/pSC5.214A were run for 48 h and SA/QA equilibration was observed only after 36 h at cell densities of approximately 25 g/L. The longer fermentation times and greater then 200-fold cell density could very well allow for sufficient amplification of residual uptake activity resulting in SA/QA equilibration. It is therefore entirely possible that residual SA uptake activity associated with the remaining loci might be responsible for the results observed with SP1.1*shiA*/pSC5.214A.

Even though use of fermentation conditions described in Chapter 2 and 3 have now been successfully implemented to circumvent the problem of SA/QA equilibration, the fact remains that the problem still persists at a genetic level. Another problem that hasnt received sufficient attention is that of DHS accumulation. Even under glucose-rich conditions, amounts of DHS accumulating in SA fermentations are quite substantial (15-20 g/L, Table 4, Chapter 3). Part of the problem lies in the feedback inhibition of

shikimate dehydrogenase by SA. But at least some fault rests on the import of SA by the cell and its conversion to DHS by the reverse reaction of shikimate dehydrogenase. Attenuation of this problem could result in the ideal situation of a biocatalyst synthesizing pure SA devoid of major contaminants in high titers and yields.

CHAPTER 5

EXPERIMENTAL

General Methods

General Chemistry

All reactions sensitive to air and moisture were carried out in oven and/or flame dried glassware under positive argon pressure. Air or moisture sensitive reagents and solvents were transferred to reaction flasks fitted with rubber septa via syringes or cannula. Unless otherwise specified, all reactions were carried out at room temperature. Solvents were removed using either a Büchi rotary evaporator at water aspirator pressure or under high vacuum (0.5 mm Hg). Hydrogenation was performed on a Parr hydrogenation apparatus under 50 psi of hydrogen.

Reagents and Solvents

HMPA was dried and stored over activated Linde 4 Å molecular sieves under nitrogen. CH_2Cl_2 and Et_3N were distilled from calcium hydride under nitrogen. THF was distilled under nitrogen from sodium benzophenone ketyl. Water used in purifications was glass distilled deionized. All other reagents and solvents were used as available from commercial sources or purified according to published procedure. Organic solutions of products were dried over anhydrous $MgSO_4$.

Chromatography

Radial chromatography was carried out with a Harrison Associates Chromatotron using 1, 2 or 4 mm layers of silica gel 60 PF_{254} containing gypsum (E. Merck). Silica gel 60 (40-63 μm, E. Merck) was used for flash chromatography. Analytical thin-layer chromatography (TLC) utilized precoated plates of silica gel 60 F-254 (0.25 mm, Whatman). TLC plates were visualized by immersion in anisaldehyde stain (by volume: 95% ethanol, 3.5% sulfuric acid, 1% acetic acid and 2.5 % anisaldehyde) followed by heating.

Diethylaminoethyl cellulose (DEAE) was purchased from Whatman, Dowex 50 (H^+) from Sigma, hydroxylapatite (HA) from Bio-Rad, and Dymatrex Red A from Amicon. Depending on its use, DEAE was recycled and cleaned with either 1M $Et_3NH^+HCO_3^-$ (TEAB) or 0.5 M KCl followed by exhaustive washing with water. TEAB buffer was prepared by bubbling CO_2 gas through an aqueous solution of Et_3N until the pH reached 7.5 at 0 °C. Dowex 50 (H^+) was cleaned before use by treatment with bromine at pH 14, extensive rinsing with water followed by washing with 6N aqueous hydrochloric acid, and finally washing with water until the pH of the eluent tested neutral. All aqueous chromatographic purifications were carried out at 4 °C

Spectroscopic and Analytical Measurements

^{1}H NMR and ^{13}C NMR spectra were recorded on a Varian VX-300 FT-NMR spectrometer. Chemical shifts for ^{1}H NMR spectra are reported in parts per million (ppm) relative to internal tetramethyl silane (Me_4Si, δ = 0.0 ppm) with $CDCl_3$ as the solvent, and to sodium 3-(trimethylsilyl) propionate-2,2,3,3-d_4 (TSP, δ = 0.0 ppm) when

D₂O was the solvent. The following abbreviations are used to describe spin multiplicity: s (singlet), d (doublet), t (triplet), m (unresolved multiplet) and dd (doublet of doublets). Chemical shifts for ^{13}C NMR spectra are reported in ppm relative to $CDCl_3$ (δ = 77.0 ppm) or internal standard acetonitrile (CH_3CN, δ = 3.69 ppm) in D_2O. Fast atom bombardment (FAB) mass spectra were obtained on a double-focusing Kratos MS50 mass spectrometer employing glycerol as the matrix. Elemental analysis were performed by Atlantic Microlab Inc. (Norcross, GA). UV and visible spectra were recorded on a Perkin-Elmer Lambda 3B spectrometer or a Hewlett Packard 8452A diode array spectrometer.

Enzyme Assays

General Information

3-deoxy-D-*arabino*-heptulosonic acid (DAH) was biosynthesized using the *E. coli* strain AB2848/pKL1.87A/pMF52A. The supernatant from 1 L of culture was passed through 500 mL Dowex 50 (H⁺) and the clear eluent adjusted to pH 8.0 using freshly prepared 1 M lithium hydroxide. After the solution was concentrated down to dryness, the oily residue was stirred with 1 L methanol at 4 °C for 1 h. The white precipitate was filtered off and the filtrate concentrated under reduced pressure. The residue was dissolved in water, passed down Dowex 50 (H⁺) and the eluent concentrated to dryness to give DAH. The conversion of DAH to 3-deoxy-D-*arabino*-heptulosonic acid 7-phosphate (DAHP) followed the same protocol as reported by Frost and Knowles.[112]

DHQ synthase was purified in the Co⁺² form using *E. coli* RB791/pJB14 according the procedure of Frost and co-workers.[113] Purification of DHQ synthase in the

Zn^{+2} form followed the same procedure but with replacement of $CoCl_2$ in all the buffers with 75 μM $ZnSO_4.7H_2O$. DHQ dehydratase was purified from *E. coli* AB2848/pKD201 according to the protocol established by Chaudhuri and co-workers.[86] Concentrations of phosphorous containing compounds were determined by the method developed by Avila and Ames.[114] Protein solutions were concentrated by ultrafiltration using either PM-10 Diaflo membranes or Centricon concentrators from Amicon.

Cell lysis was achieved by two passes through a French pressure cell (SLM Aminco) at 16000 psi and the cellular debris was separated from the lysate by centrifugation (48000 x *g*, 20 min, 4 °C). Protein concentration was quantified using the Bradford dye-binding procedure with assay solution from Bio-Rad.

DAHP synthase assay

DAHP synthase activities were measured using the procedure reported by Schoner.[115] Harvested cells were resuspended in 50mM potassium phosphate (pH 6.5) containing 10mM PEP and 0.05mM $CoCl_2$. After the cells were disrupted by passage through a French press, the lysate was diluted in a solution of 50 mM potassium phosphate (pH 7.0), 0.5 mM PEP and 250 mM 1,3-propanediol. A dilute solution of E4P was concentrated to 12 mM and the pH was adjusted to 7.0 with KOH. Two solutions were prepared and incubated separately at 37 °C for 5 min. The first solution (1 mL, pH 7.0) contained 6 mM E4P, 12 mM PEP, 1 mg ovalbumin and 25 mM potassium phosphate. The second solution was 0.5 mL of diluted lysate. The two solutions were mixed (time = 0) and incubated at 37 °C. At regular time intervals, 0.15 mL samples were removed from the reaction mixture and quenched with 0.1 mL of 10%

trichloroacetic acid (w/v). Precipitated protein was removed by centrifugation and the DAHP level in each sample was determined using the thiobarbiturate assay.

To a 0.1 mL aliquot of DAHP containing sample was added 0.1 mL of 0.2 M $NaIO_4$ in 8.2 M H_3PO_4 and the mixture incubated at 37 °C for 5 min. The reaction was quenched by addition of 0.8 M $NaAsO_2$ in 0.5 M Na_2SO_4 and 0.1 M H_2SO_4 (0.5 mL) and vortexed until a dark brown color appeared. This solution was finally treated with 3 mL of 0.04 M thiobarbituric acid in 0.5 M Na_2SO_4 (pH 7.0) and heated at 100 °C for 15 min. The samples were cooled and the pink color extracted into 4 mL of cyclohexanone. The aqueous and organic layers were separated by centrifugation (2000 x g, 15 min) and the absorbance of the organic layer measured at 549 nm (ε = 68000 L mol^{-1} cm^{-1}). One unit of DAHP synthase activity was defined as the formation of 1 μmol of DAHP per min at 37 °C.

Transketolase activity measurement

Transketolase activity was assayed using the method of Paoletti.[69a] Harvested cells were resuspended in 50 mM potassium phosphate (pH 7.5), 1 mM $MgCl_2$, and 0.2 mM DTT and subjected to lysis using a French press as described earlier. A dilute solution of E4P was concentrated to 10 mM and the pH adjusted to 7.0 with KOH. The assay mixture (1 mL) contained 200 mM triethanolamine (pH7.6), 5 mM $MgCl_2$, 0.1 mM thiamine pyrophosphate, 0.4 mM NADP, 0.4 mM β-hydroxypyruvate, 0.2 mM E4P, 8 units glucose-6-phosphate dehydrogenase, and 4 units phosphoglucose isomerase. The solution was allowed to equilibrate at room temperature for 5 min and the absorbance at 340 nm was monitored for several minutes. After all the unreacted D-glucose 6-

phosphate from the E4P synthesis had reacted, an aliquot of the diluted lysate was added

and the reaction monitored at 340 nm for 20-30 min. One unit of tranketolase activity is

defined as the formation of 1 μmol of NADP (ε = 6220 L mol^{-1} cm^{-1}) per min.

Bacterial Strains

E. coli DH5α [*F' endA1 hsdR17(r$_K^-$m$_K^+$) supE44 thi-1 recA1 gyrA relA1*

$\emptyset$80lacZΔM15 Δ(lacZYA-argF)$_{U169}$], RB791 (W3110 *lacL8I^q*) and JWF1 (RB791 *serA*)

were obtained previously in this laboratory. *E. coli* B was purchased from ATCC.

JP11123 (*thi-1 argE3 his-4 proA2 galK2 lacY1 tsk29 aroD362 shiA354*::Kan^R) was

obtained from the laboratory of Professor J Pittard. TP2811 (*F$^-$ xyl argH1 ΔlacX74 aroB*

ilvA Δ(ptsH ptsI crr)::Kan^R) was obtained from Sophie Lévy at the Institut Pasteur,

France. Plasmid pTC325 was obtained from Professor L. Ingram.

Storage of Bacterial Strains and Plasmids

All bacterial strains were stored at -78 °C in glycerol. Plasmids were transformed

into either DH5α or JWF1 for storage. Glycerol freezes were prepared by adding

0.75 mL of culture to 0.25 mL of sterile 80% (v/v) glycerol. The solutions were mixed,

allowed to stand at room temperature for 2 h, and then stored at -78 °C.

Culture Medium

All solutions were prepared in distilled, deionized water. LB medium contained (1

L) Bacto tryptone (10 g), Bacto yeast extract (5 g), and NaCl (10 g). M9 salts (1 L)

contained Na$_2$HPO$_4$ (6 g), KH$_2$PO$_4$ (3 g), NH$_4$Cl (1 g), and NaCl (0.5 g). M9 minimal

medium contained D-glucose (10 g), MgSO$_4$ (0.12 g), and thiamine hydrochloride (0.001 g) in 1 L of M9 salts. M9 medium (1 L) was supplemented where appropriate with L-phenylalanine, L-tyrosine, L-tryptophan, and L-serine to a final concentration of 40 μg/mL and with p-hydroxybenzoic acid, potassium p-aminobenzoate, and 2,3-dihydroxybenzoic acid to a final concentration of 10 μg/mL. Antibiotics were added where required to the following final concentrations: chloramphenicol (Cm), 20 μg/mL; ampicillin (Ap), 50 μg/mL; and kanamycin (Kan), 50 μg/mL. Inorganic salts, D-glucose, and MgSO$_4$ solutions were autoclaved separately while thiamine hydrochloride, amino acids, aromatic vitamins, casamino acids, and antibiotic stock solutions were sterilized through 0.22-μm membranes. Solid medium was prepared by addition of 1.5% (w/v) Difco agar to medium solution.

Fermentation medium (1L) contained K$_2$HPO$_4$ (7.5 g), citric acid monohydrate (2.1g), ammonium iron (III) citrate (0.3g), concentrated H$_2$SO$_4$ (1.2 mL), L-tyrosine (0.7 g), L-phenylalanine (0.7 g) and L-tryptophan (0.35g). The pH of the medium was adjusted to 7.0 with concentrated NH$_4$OH prior to autoclaving. The following supplements were added to the medium immediately prior to initiation of the fermentation: D-glucose (20 g or 30 g), MgSO$_4$ (0.24 g), p-hydroxybenzoic acid (0.01 g), 2,3-dihydroxybenzoic acid (0.01 g), potassium p-aminobenzoate (0.01 g) and trace minerals including (NH$_4$)$_6$(Mo$_7$O$_{24}$)·4H$_2$O (0.0037 g), ZnSO$_4$·7H$_2$O (0.0029 g), H$_3$BO$_3$ (0.0247 g), CuSO$_4$·5H$_2$O (0.0025 g) and MnCl$_2$·4H$_2$O (0.0158 g). Solutions of D-glucose and MgSO$_4$ were autoclaved separately while aromatic vitamins and trace minerals solutions were sterilized through 0.22 μm membranes.

General Fed-Batch Fermentor Conditions

Fermentations were conducted in a B. Braun M2 culture vessel with a 2 L working capacity. The vessel was modified using a stainless steel baffle cage containing four 1/4" x 4" baffles for all fermentations except those using KL3/pKL4.130B. Environmental conditions were supplied by a B. Braun Biostat MD controlled by a DCU-1. Data was acquired on a Dell Optiplex Gs+ 5166M personal computer utilizing B. Braun MFCS/Win software. PID control loops were used to control temperature, pH, and glucose addition. The temperature was maintained at 33 °C, and the pH was maintained at 7.0 by addition of NH_4OH or 2 N H_2SO_4. Glucose was added as a 60% (w/v) solution for all strains. Dissolved oxygen (D.O.) was monitored using a Mettler-Toledo 12 mm sterilizable O_2 sensor fitted with an Ingold A-type O_2 permeable membrane. D.O. was maintained at 10% air saturation throughout the course of the fermentations. Antifoam (Sigma 204) was pumped into the vessel manually as needed.

Each inoculant was initiated by introduction of a single colony into 5 mL of M9 medium and grown at 37 °C with agitation for 12-24 h until the culture was turbid. After this time, the starter culture was transferred to 100 mL of M9 medium and grown for an additional 12 to 24 h at 37 °C and 250 rpm. After an appropriate OD_{600} was reached (1.0-3.0), the inoculant was transferred to the fermentation vessel. The initial glucose concentration in the fermentation was 30 g/L for all fermentations discussed in Chapter 3, and 20 g/L for those described in Chapter 4. Three staged methods were used to maintain D.O. levels at 10% air saturation during the course of the run. With the airflow at an initial setting of 0.06 L/L/min, D.O. concentration was maintained by increasing the impeller speed from its initial set point of 50 rpm to its preset maximum of 750 rpm.

When the impeller reached its preset maximum, the mass flow controller then maintained D.O. levels by increasing the airflow rate from 0.06 L/L/min to a preset maximum of 1.0 L/L/min. Once the air flow rate leveled off at 1.0 L/L/min at a constant impeller speed of 750 rpm, glucose was manually pumped into the fermentor so as to maintain an average glucose concentration of 25 g/L throughout the run. At this stage, the D.O. level was maintained at 10% by allowing the impeller speed to vary from 750 rpm to 1600 rpm. Fermentations were typically run for 60 h.

The fermentations in Chapter 4 did not employ the baffle cage and were run under slightly different conditions. During the first two stages the stirrer was allowed to ramp up to 940 rpm and the air flow up to 1.0 L/L/min. At this stage dissolved oxygen levels were maintained for the duration of the fermentation at 10% by oxygen sensor-controlled glucose feeding. Under these conditions, at no stage during the fermentation was there any excess glucose present in the fermentation culture. Fermentations were typically run for 42-48 h.

Analysis of Fermentation broth

Samples (5 mL) of fermentation broth were taken at indicated intervals. Cell densities were determined by dilution of fermentation broth with water (1:100) followed by measurement of absorption at 600 nm (OD_{600}). Dry cell weight (g/L) was obtained using a conversion coefficient of 0.43 $g/L/OD_{600}$ for RB791-derived strains and 0.29 $g/L/OD_{600}$ for strains derived from *E. coli* B. The remaining fermentation broth was centrifuged using a Beckman microcentrifuge to obtain cell-free broth. Solute concentrations in the cell-free broth were determined by ^1H NMR (Figure 80). For ^1H

NMR quantitation of solute concentrations, solutions were concentrated to dryness under reduced pressure, concentrated to dryness on additional time from D_2O, and then redissolved in D_2O containing a known concentration of the sodium salt of 3-(trimethylsilyl)propionic-2,2,3,3-d_4 acid (TSP) purchased from Lancaster Synthesis Inc. Concentrations were determined by comparison of the integrals corresponding to each compound with the integral corresponding to TSP ($\delta = 0.00$ ppm) in the ^1H NMR. Compounds were quantified using the following resonances: shikimic acid (δ 4.4, m, 1 H) (Figure 81), DHS (δ 4.3, d, 1 H) (Figure 82), quinic acid (δ 4.2, m, 1 H) (Figure 83). Concentrations of shikimic acid and quinic acid derived from their respective ^1H NMR integral values tended to be overestimated and precise concentrations of shikimic acid and quinic acid were calculated by application of the following formulae: $[SA]_{actual} = 0.67523$ x $[SA]_{NMR} + 0.26658$; $[QA]_{actual} = 0.65887$ x $[QA]_{NMR} - 0.48161$. These equations were obtained by dissolving various known amounts of shikimic acid or quinic acid in 1 mL of D_2O containing 10 mM TSP and recording their ^1H NMR spectra. The concentration of SA or QA in each sample that was estimated from ^1H NMR, was plotted against the known concentration of shikimic acid or quinic acid for that sample resulting in the calibration curve. All ^1H NMR spectra were recorded on a Varian VXR-300 FT-NMR spectrometer (300 MHz).
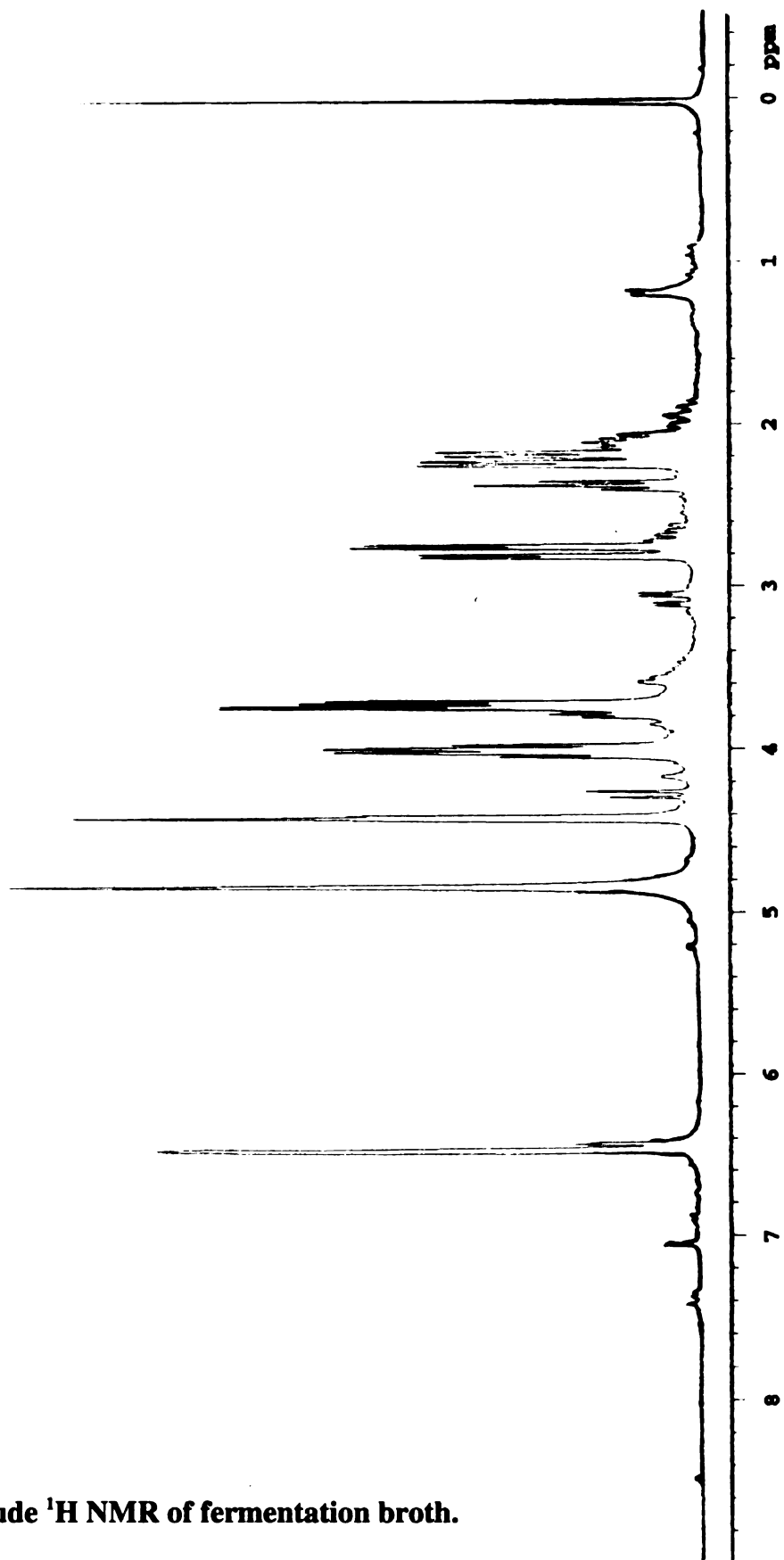
Figure 80. Crude ^{1}H NMR of fermentation broth.
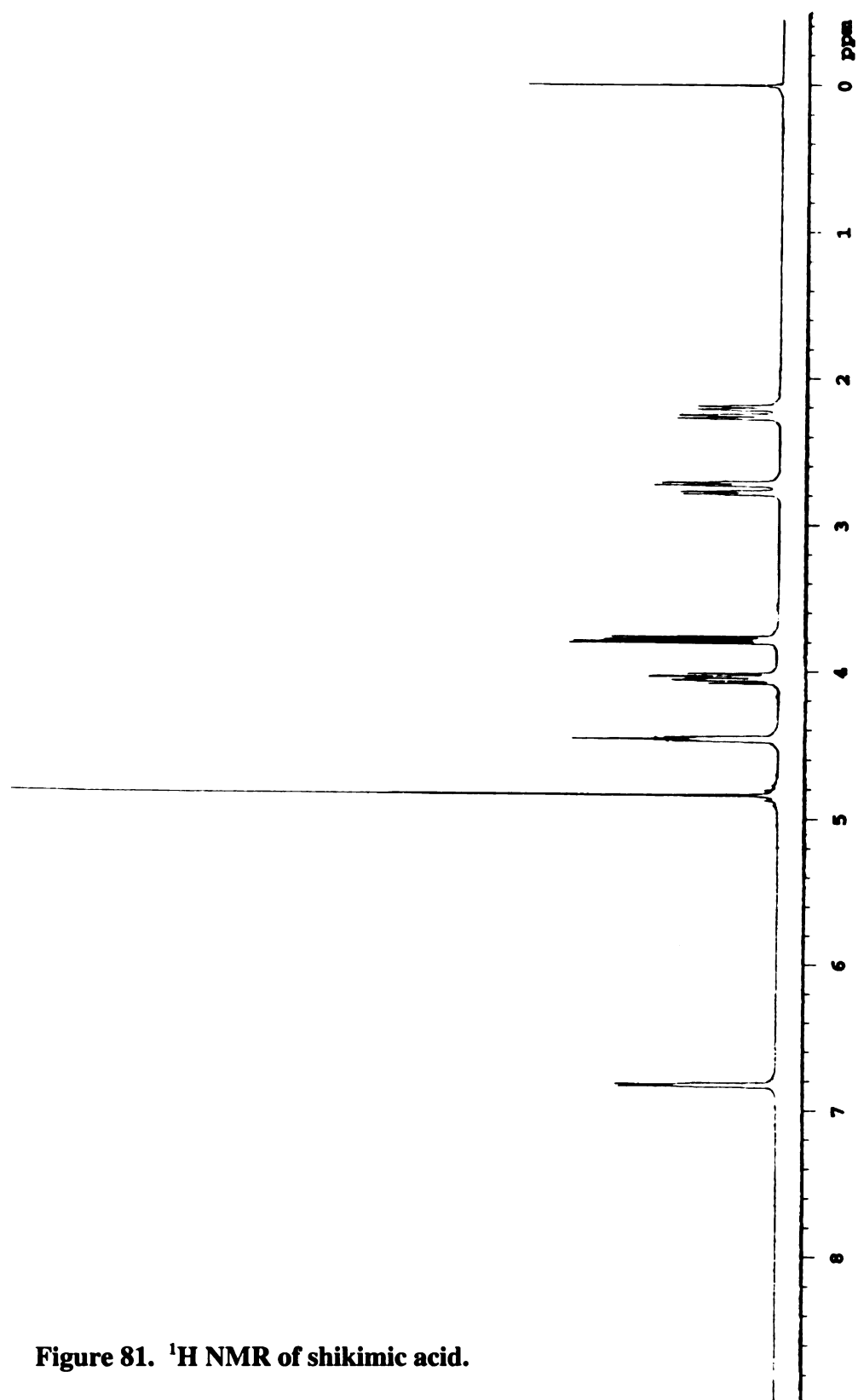
Figure 81. ¹H NMR of shikimic acid.
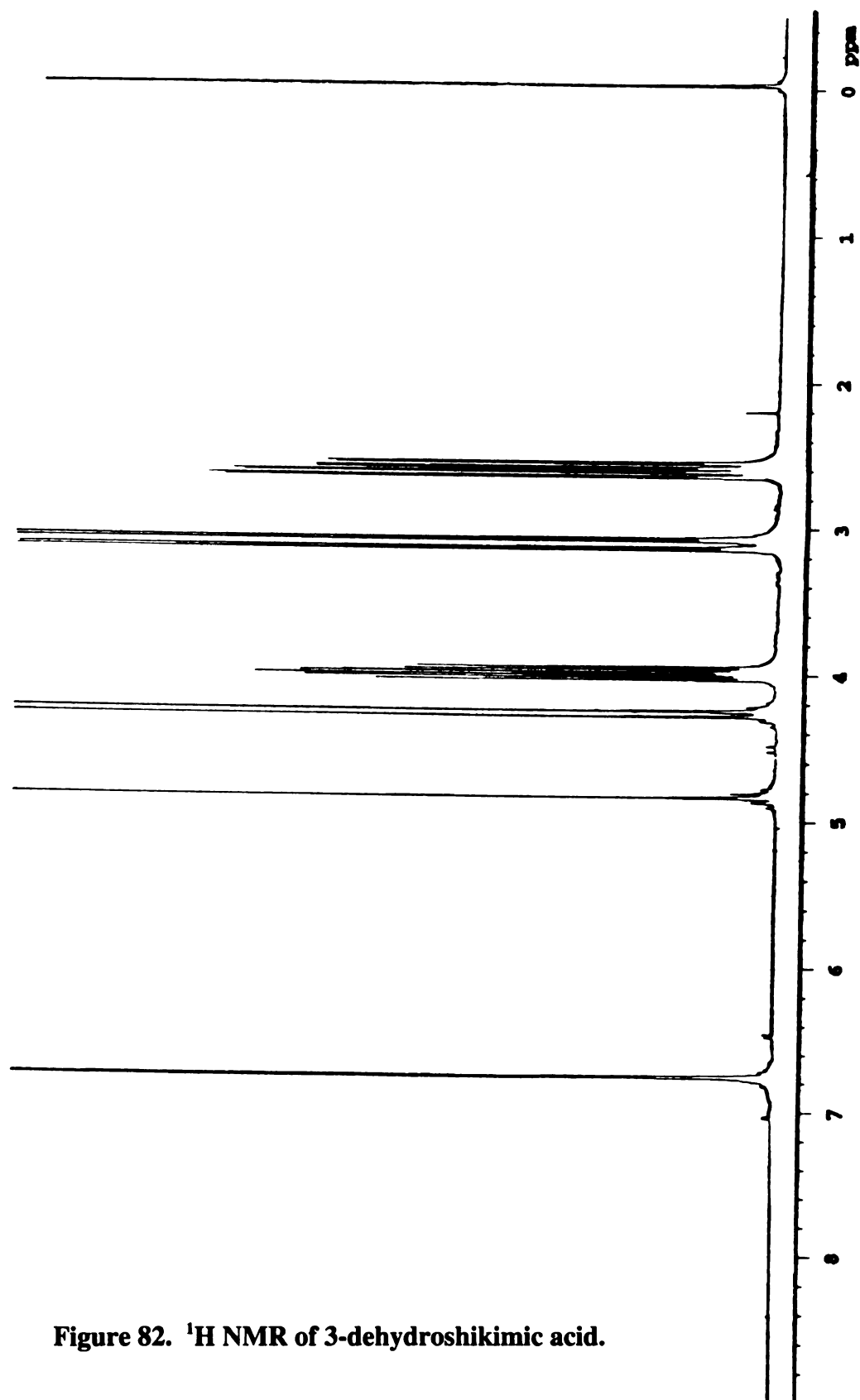
Figure 82. ^{1}H NMR of 3-dehydroshikimic acid.
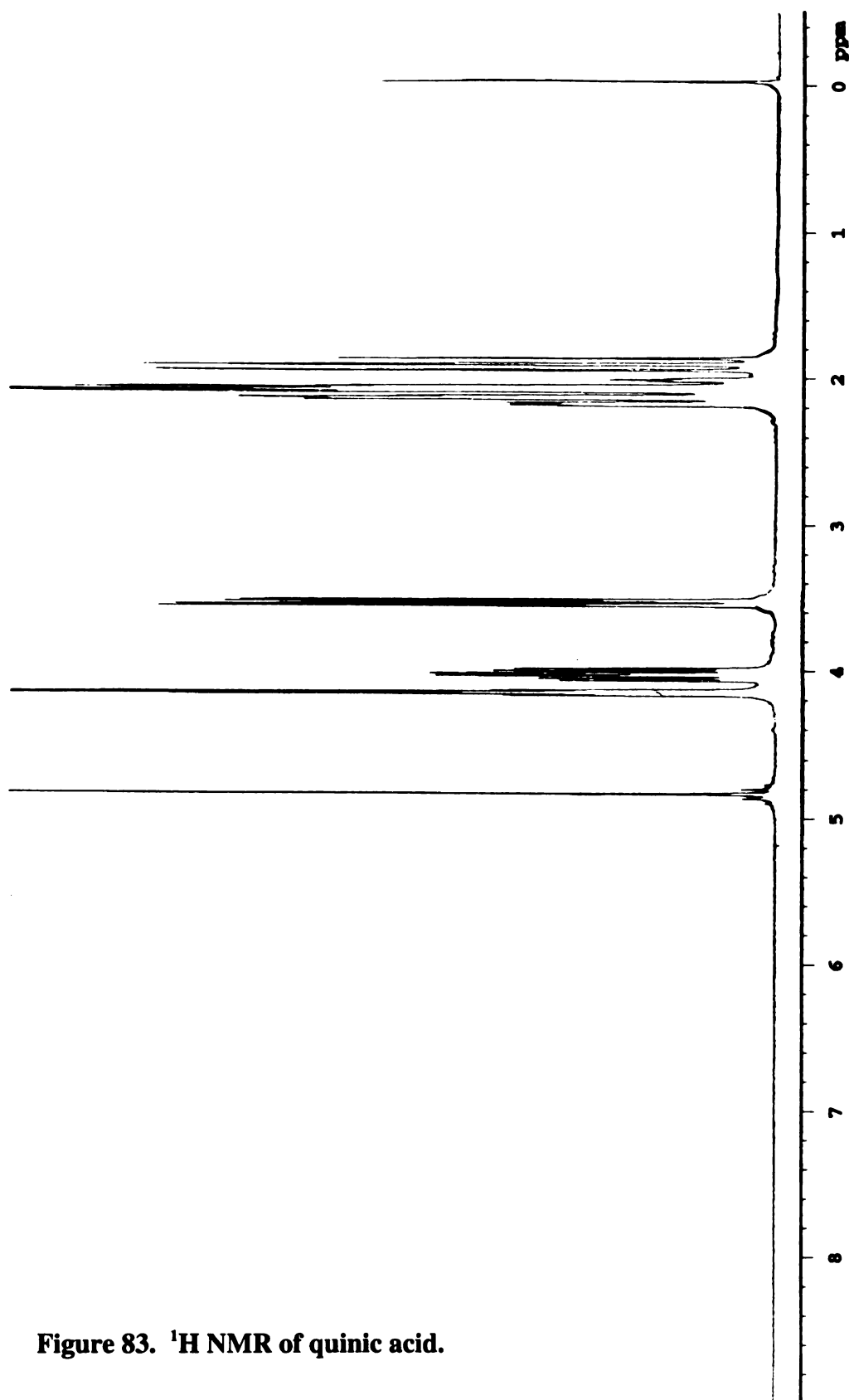
Figure 83. ^{1}H NMR of quinic acid.

Genetic Manipulations

General Information

Recombinant DNA manipulations were performed according to procedures outlined in Sambrook and co-workers.[116] Restriction endonucleases were purchased from Gibco BRL and New England Biolabs. T4 DNA ligase, Klenow fragment and dNTP's were purchased from Gibco BRL while calf intestinal alkaline phosphatase was purchased from Roche Molecular Biochemicals. Depending on the selection available, *E. coli* DH5α or JWF1 were used for all plasmid constructions. Electrophoresis grade agarose was purchased from Gibco BRL. Prior to use, phenol was distilled and mixed with 0.1% (w/v) 8-hydroxyquinoline. This was followed by extraction with 1 M Tris-HCl (pH 8.0) (twice) and finally extraction with 0.1 M Tris-HCl (pH 8.0) until the pH of the aqueous layer was greater than 7.6. Phenol was stored under an equal volume of 0.1 M Tris-HCl (pH 8.0) at 4 °C. SEVAG was prepared by mixing chloroform and isoamyl alcohol (24:1 v/v). TE buffer contained 10 mM Tris-HCl (pH 8.0) and 1mM Na_2EDTA (pH 8.0). Endostop solution (10X concentrated) was made up of 50% glycerol (v/v), 0.1 M Na_2EDTA, pH 7.5, 1% sodium dodecyl sulfate (SDS) (w/v), 0.1% bromophenol blue (w/v) and 0.1% xylene cyanole FF (w/v) and stored at 4 °C. Prior to use, 1 mL of 10X Endostop was mixed with 0.12 mL of DNAase-free RNAase. DNAase-free RNAase was prepared by dissolving 10 mg RNAase in 1mL of 10mM Tris-HCl (pH 7.5) and 15 mM NaCl. The solution was heated at 100 °C for 15 min to inactivate the DNAase and stored at -20 °C.

Large Scale Purification of Plasmid DNA

Purification of plasmid DNA on a large scale followed a modified alkaline alkaline lysis procedure described in Sambrook and co-workers.[116] A 2 L Erlenmeyer flask containing 500 mL of LB with appropriate antibiotics, was inoculated with a single colony and the culture was shaken (250 rpm) at 37 °C for 14 h. In cases where the plasmid did not possess an antibiotic marker, 500 mL of M9 minimal medium was used and the culture grown for 24 h under the conditions described earlier. The cells were harvested by centrifugation (4000 x g, 5 min, 4 °C) and resuspended in 10 mL of cold GETL solution [50 mM glucose, 20 mM Tris-HCl (pH 8.0), 10 mM Na_2EDTA (pH 8.0)] into which 50 mg of lysozyme had been added immediately prior to use. The suspension was kept at room temperature for 5 min after which it was treated with 20 mL of 1 % sodium dodecyl sulfate (w/v) in 0.2 N NaOH. The thick suspension was gently mixed, kept on ice for 15 min and then treated with 15 mL of cold 3 M KOAc (prepared by mixing 60 mL of 5 M KOAc, 11.5 mL of glacial acetic acid and 28.5 mL of water). The mixture was shaken vigorously resulting in a thick white precipitate. The sample was stored for 10 min on ice. The cellular debris was removed by centrifugation (48000 x g, 20 min, 4 °C) and the supernatant transferred equally to two clean centrifuge tubes. Isopropanol (0.6 volume) was added to each tube and they were kept at room temperature for 15 min. The precipitated DNA was recovered by centrifugation (20000 x g, 20 min, 4 °C), the supernatant discarded and the DNA pellet carefully rinsed with 70% ethanol.

The DNA pellet was dried, dissolved in 3 mL TE and transferred to a 15 mL Corex tube. To this solution was added 3 mL of cold 5 M LiCl and after thorough mixing, the high molecular weight RNA was removed by centrifugation (12000 x g, 10

min, 4 °C). The clear supernatant was transferred to a fresh Corex tube and treated with 6 mL of isopropanol followed by gentle mixing. The precipitated DNA was collected by centrifugation (12000 x g, 10 min, 4 °C), rinsed with 70% ethanol and dried. The dried DNA pellet was dissolved in 0.5 mL of TE containing 10 μg of DNAase-free RNAase, transferred to a 1.5 mL microcentrifuge tube and stored at room temperature for 30 min. To this solution was added 0.5 mL of 13% PEG-8000 (w/v) in 1.6 M NaCl. The solution was mixed well and centrifuged (microcentrifuge, 5 min, 4 °C) to recover the precipitated DNA. The supernatant was discarded and the pellet dissolved in 0.4 mL of TE. The sample was sequentially extracted with phenol (0.4 mL), phenol and SEVAG (0.4 mL each) and finally SEVAG (0.4 mL). After the extraction was complete, the aqueous portion was mixed with 0.1 mL of 10 M NH₄OAc followed by addition of 1 mL of 95% ethanol. The sample was mixed well and left at room temperature for 5 min resulting in precipitation of DNA. After recovery of the DNA by centrifugation (microcentrifuge, 5 min, 4 °C), the pellet was dissolved in 0.2-0.4 mL of TE.

In order to determine the DNA concentration, an aliquot (10 μL) of the DNA solution was diluted to 1 mL in TE and the absorbance at 260 nm was measured relative to TE. DNA concentration was then calculated based on the fact that the absorbance at 260 nm of 50 μg mL^{-1} of plasmid DNA is 1.0.

Small Scale Purification of Plasmid DNA

A single colony was inoculated into 5 mL of LB containing appropriate antibiotics and grown overnight at 37 °C. In cases where the plasmid did not possess an antibiotic marker, 5 mL of M9 minimal medium was used and the culture grown for 24 h.

Cells were harvested from 3 mL of culture in a 1.5 mL microcentrifuge tube by centrifugation. The cell pellet was resuspended in 0.1 mL of cold GETL solution into which lysozyme (5 mg mL^{-1}) was added immediately before use. The suspension was incubated on ice for 10 min and was then treated with 0.2 mL of 1 % sodium dodecyl sulfate (w/v) in 0.2 N NaOH. The mixture was shaken gently and kept on ice for 5-10 min. To this sample was added 0.15 mL of cold 3 M KOAc solution and the mixture shaken vigorously resulting in formation of a thick white precipitate. The sample was stored on ice for 5 min following which the precipitate was removed by centrifugation (microcentrifuge, 20 min, 4 °C). The supernatant was transferred to a fresh microcentrifuge tube and extracted with phenol and SEVAG (0.25 mL each). The aqueous layer was transferred to a fresh microfuge tube and mixed well with 1 mL of 95% ethanol. The mixture was kept at room temperature for 5 min and the precipitated DNA was centrifuged (15 min, room temperature) into a pellet. The DNA pellet was rinsed with 75% ethanol, dried well and redissolved in 50-100 μL of TE. No concentration determination was done and the sample was used directly for restriction endonuclease analysis.

Restriction Enzyme Digestion of DNA

Restriction enzyme digests were performed in buffers provided by Gibco BRL or New England Biolabs. A typical restriction enzyme digest contained 0.8 μg of DNA in 8 μL of TE, 2 μL of restriction enzyme buffer (10X concentration), 1 μL of bovine serum albumin, 1 μL of restriction enzyme and 8 μL TE. Reactions were incubated at 37 °C for 1 h, terminated by addition of 2.0 μL of 10X Endostop and analyzed by agarose gel

electrophoresis. For cloning experiments, the reaction was terminated by addition of 1 μL of 0.5 M Na$_2$EDTA (pH 8.0), followed by extraction with phenol and SEVAG (0.1 mL each). DNA was precipitated by addition of 0.1 volume of 3 M NaOAc (pH 5.2) followed by thorough mixing and addition of 3 volumes of 95% ethanol. Samples were mixed and kept at -78 °C for 3 h. Precipitated DNA was recovered by centrifugation (15 min, 4 °C), treated with 0.1 mL of 70% ethanol and again centrifuged (15 min, 4 °C). DNA was dried and redissolved in TE.

Agarose Gel Electrophoresis

Agarose gels were run in TAE buffer made up of 40 mM Tris-acetate and 2 mM EDTA (pH 8.0). Gels typically contained 0.7% agarose (w/v) in TAE buffer. Addition of ethidium bromide (0.5 μg mL^{-1}) to the agarose allowed for visualization of DNA under ultra-violet exposure. Two standards were used to determine the size of DNA fragments: λ DNA digested with *Hind*III resulted in bands at 23.1-kb, 9.4-kb, 6.6-kb, 4.4-kb, 2.3-kb, 2.0-kb, and 0.6-kb; while λ DNA digested with *Hind*III and *Eco*RI gave fragments at 21.2-kb, 5.1-kb, 5.0-kb, 4.3-kb, 3.5-kb, 2.0-kb, 1.9-kb, 1.6-kb, 1.4-kb, 0.9-kb, and 0.8-kb.

Isolation of DNA from Agarose

Two methods were used for isolating DNA from agarose gels. The first method involved cutting out the band of agarose containing the required DNA from the gel and chopping it thoroughly with a razor. The agarose was then transferred to a 0.5 mL microfuge tube packed tightly with glass wool and having an 18 gauge hole at the bottom. The tube was centrifuged for 5 min using a Beckman microfuge to extrude the

DNA solution from the agarose into a 1.5 mL microfuge tube. The DNA was precipitated out using 3 M NaOAc and 95% ethanol as previously described.

The second method involved use of the Zymoclean DNA isolation kit purchased from Zymogen.

Treatment of DNA with Klenow fragment

DNA fragments with recessed 3' termini were modified to blunt end fragments by treatment with the Klenow fragment of *E. coli* DNA polymerase I. Digested DNA (4-6 μg) in 120 μL of TE was treated with 6 μL of a solution containing 25 mM of each of the desired dNTP's, followed by addition of 6 units of the Klenow fragment. The reaction was incubated at room temperature for 30 min. Klenow reactions were quenched by addition of 15 μL of 10X Endostop in cases where the DNA fragment needed to be purified by agarose gel electrophoresis, or in case of vector plasmid was taken forward directly for treatment with calf intestinal alkaline phosphatase.

Treatment of Vector DNA with Calf Intestinal Alkaline Phosphatase

Linearized plasmid vectors were dephosphorylated to prevent self-ligation. The plasmid (4-6 μg) after digestion was dissolved in TE (120-140 μL) and treated with 14 μL of dephosphorylation buffer and 3 μL of calf intestinal alkaline phosphatase (3 units). The reaction was incubated at 37 °C for 1 h and quenched with 1 μL of 0.5 M Na$_2$EDTA (pH 8.0) followed by heating at 75 °C for 15 min. The DNA was extracted with phenol and SEVAG (0.1 mL each), precipitated out as described previously and redissolved in TE.

Ligation of DNA

Molar ratios of insert to vector were typically maintained at 3 to 1 during ligations. A typical ligation reaction contained 0.1 μg vector DNA, 0.05 to 0.2 μg insert in a total volume of 7 μL. To this was added 2 μL of T4 ligation buffer (5X concentration) and 1 μL of T4 DNA ligase (2 units). The reaction was incubated at 16 °C for at least 10 h and then used to transform competent cells.

Preparation and Transformation of Competent Cells

Competent cells were prepared using a procedure modified from Sambrook and co-workers.[117] A single colony was inoculated into 5 mL LB containing the necessary antibiotics. After overnight growth 1 mL of the culture was transferred to a 500 mL Erlenmeyer flask containing 100 mL LB with the necessary antibiotics. The cells were cultured in a gyratory shaker (250 rpm, 37 °C) until an absorbance of 0.4-0.6 was observed at 600 nm. The entire culture was transferred to a sterile centrifuge bottle and the cells were collected by centrifugation (4000 x g, 5 min, 4 °C). The cells were washed with 100 mL of cold 0.9% NaCl (w/v) and then resuspended gently in 50 mL of cold 100 mM CaCl$_2$. The suspension was kept on ice for 30 min and then centrifuged (4000 x g, 5 min, 4 °C). The cells were slowly resuspended in 4 mL of cold 100 mM CaCl$_2$ containing 15% glycerol (v/v). Aliquots (0.25 mL) were transferred to microfuge tubes and immediately frozen with liquid nitrogen. Competent cells were stored at -78 °C and used over a period of at least six months without any noticeable loss in transformation efficiency.

In order to perform a transformation, frozen competent cells were allowed to thaw on ice for 5 min immediately prior to use. Either 10 μL of a ligation reaction or 1-2 μL of 0.1 mg mL^{-1} plasmid solution was added to 0.1 mL of cold competent cells. The solution was gently mixed and kept on ice for 30 min. The cells were then heat shocked at 42 °C for 2 min and kept on ice briefly (1-2 min). LB (0.5 mL) was added to the cells and the sample incubated (no agitation) at 37 °C for 1 h. Cells were pelleted in a microcentrifuge. If the cells were to be plated onto LB, then the cell pellet was resuspended in 0.1 mL of LB and the entire volume spread out onto the LB plate containing the appropriate antibiotics. If the cells were to be plated out onto M9 minimal medium plates, then the cell pellet was washed once with 0.5 mL of M9 minimal medium. The cells were resuspended in fresh M9 minimal medium (0.1 mL) and spread onto the plate. Competent cells which were not transformed with any DNA were also subjected to the same transformation protocol. These cells were used to confirm the viability of the competent cells and also to confirm absence of growth on the selective medium without the required DNA.

Transformation was also performed by electroporation using electrocompetent cells. In order to prepare electrocompetent cells, instead of the 100 mL culture grown for normal competent cells, a 500 mL culture was grown. Once an absorbance between 0.5-0.7 was observed at 600 nm, the cells were kept on ice for 15 min and harvested. The cells were gently washed twice with cold water (350 mL and 150 mL) and then resuspended in 20 mL of cold aqueous 10% glycerol (v/v). The cells were centrifuged (4000 x g, 5 min, 4 °C) and the cell pellet was slowly resuspended with 5 mL of cold

aqueous 10% glycerol. The cells were transferred into microfuge tubes in 0.25 mL aliquots, immediately frozen using liquid nitrogen and stored at -78 °C.

The electroporation was performed in Bio-Rad gene pulser cuvettes with an electrode gap of 0.2 cm. The cuvettes were chilled on ice for 5 min prior to use. Electrocompetent cells were thawed on ice for 5 min and 0.1 mL of thawed cells was added to the chilled cuvette. To this was added 1-2 μL of plasmid DNA (0.1 mg mL^{-1}) and the mixture was gently shaken. The Bio-Rad gene pulser was set at 2.5 Kvolts, 25 μF and 200-400 Ohms. The outside surface of the cuvette was wiped clean and it was placed in the sample chamber. A single pulse was applied, the cuvette was removed and 0.5 mL of LB was added to it. The contents of the cuvette were transferred to a 1.5 mL microfuge tube. The cells were incubated at 37 °C for 1 h. The transformed cells were plated in the same manner as in a normal transformation with the same controls.

CHAPTER 2

Synthetic Procedures

Synthesis of PCA phosphonate 4 and PCA homophosphonate 5

Methyl 3,4-dimethoxy benzoate 10. To a solution of 3,4-dimethoxy benzoic acid (100 g, 552.5 mmol) in methanol (1000 mL) was added 5 mL of conc. H$_2$SO$_4$. The reaction mixture was refluxed for 24 h, to rt and neutralized with saturated aqueous NaHCO3. The solution was concentrated to dryness and the solid obtained was partitioned between EtOAc and water. The organic layer was dried and concentrated to afford the ester **10** as a pink solid (106 g, 98 %): ^{1}H NMR (CDCl$_3$) δ 3.90 (s, 3H), 3.94

(s, 6H), 6.89 (d, J= 8 Hz, 1H), 7.55 (d, J= 2 Hz, 1H), 7.68 (dd, J= 8, 2 Hz, 1H); ^{13}C NMR (CDCl$_3$) δ 166.7, 152.8, 148.4, 123.4, 122.5, 111.7, 110.1, 58.4, 55.8, 51.8. Anal. Calcd for C$_{10}$H$_{12}$O$_4$: C, 61.25; H, 6.17. Found: C, 61.21; H, 6.10.

5-bromo-3,4-dimethoxy methybenzoate 11. A solution of methyl 3,4-dimethoxy benzoate **10** (25 g, 127 mmol) and NaOAc (15.2 g, 190.5 mmol) in AcOH (300 mL) at rt was treated slowly with a solution of Br$_2$ (54 g, 337 mmol) in AcOH (100 mL) over a period of 30 min. After the addition was complete, the reaction mixture was stirred at 70 ° C for 24 h. The reaction mixture was then poured into 1 L of ice water and kept at 4 °C for 6 h. The brown solid which had precipitated was filtered and crystallized from EtOAc/hexane to give 34 g of the bromide **11** in 97% yield: ^{1}H NMR (CDCl$_3$) δ 3.90 (s, 6H), 3.92 (s, 3H), 7.10 (s, 1H), 7.42 (s, 3H); ^{13}C NMR (CDCl$_3$) δ 165.8, 151.9, 147.7, 122.7, 116.8, 114.1, 113.8, 56.2, 56.1, 52.2. Anal. Calcd for C$_{10}$H$_{11}$BrO$_4$: C, 43.84; H, 4.05. Found: C, 43.94; H, 4.07.

5-vinyl-3,4-dimethoxy methyl benzoate 12. The bromide **11** (10.5 g, 38.2 mmol) and tetrakis(triphenylphosphine)palladium (0) (0.882 g, 0.764 mmol) were dissolved in dry HMPA (260 mL) and stirred for 10 min at rt. The reaction mixture was then heated up to 65 °C and treated with tributyl vinyltin (13.9 g, 43.9 mmol). After 18 h, the reaction was quenched by the addition of saturated aqueous KF, stirred for 15 min and filtered through celite. The filtrate was concentrated to a minimum volume and the liquid loaded onto a silica gel column. Purification by flash chromatography (hexane, EtOAc/hexane, 1:4 v/v) afforded the vinylic ester **12** as white crystals (5.3 g, 63%): ^{1}H NMR (CDCl$_3$) δ 3.90 (s, 3H), 3.92 (s, 3H), 3.96 (s, 3H), 5.30 (dd, J= 1, 11 Hz, 1H), 5.57 (dd, J= 1, 17 Hz, 1H), 7.03 (s, 1H), 7.43 (s, 1H), 7.54 (dd, J= 11, 17 Hz, 1H);

^{13}C NMR (CDCl$_3$) δ 167.1, 151.8, 147.8, 135.8, 134.2, 120.2, 114.9, 112.6, 109.2, 55.8, 55.7, 51.8. Anal. Calcd for C$_{12}$H$_{14}$O$_4$: C, 64.86; H, 6.35. Found: C, 64.79; H, 6.33.

3-formyl-4,5-dimethoxy methyl benzoate 13. Alkene **12** (5.33 g, 24 mmol) was dissolved in CH$_2$Cl$_2$ and cooled the solution to −78 °C. Ozone was then passed through the reaction flask until the reaction was complete as indicated by TLC. Addition of 50 mL Et$_3$N followed by concentration of the reaction mixture in vacuo gave a colorless oil. The oil was treated with 300 mL of water and the flask kept at 4 °C for 3 h. White crystals were obtained which were filtered off to give 4.9 g of the required formyl ester **13** in 91% yield: ^{1}H NMR (CDCl$_3$) δ 3.97 (s, 3H), 3.99 (s, 3H), 4.01 (s, 3H), 7.47 (s, 1H), 7.51 (s, 1H), 10.65 (s, 1H); ^{13}C NMR (CDCl$_3$) δ 191.2, 166.2, 152.3, 151.9, 131.2, 125.9, 112.5, 109.5, 56.3, 56.2, 52.6. Anal. Calcd for C$_{11}$H$_{12}$O$_5$: C, 58.96; H, 5.40. Found: C, 58.57; H, 5.49.

Phosphonate Intermediate 15. Formyl ester **13** (1 g, 4.5 mmol) and NaI (1.35 g, 9 mmol) were dissolved in dry AcCN under Ar at rt and TMSCl was added. After stirring for 10 min the reaction mixture was cooled to 0 °C and tetramethyl disilazane was added dropwise. After the addition was complete the reaction was stirred at 0 °C for 10 min and then refluxed for 2 h. The solution was then partitioned between EtOAc and water. The organic layer was dried and concentrated to get a red oil containing the required iodide **14**: ^{1}H NMR (CDCl$_3$) δ 3.92 (s, 3H), 3.93 (s, 3H), 3.94 (s, 3H), 4.96 (s, 2H), 6.86 (s, 1H), 7.48 (s, 1H); ^{13}C NMR (CDCl$_3$) δ 166.4, 152.0, 148.0, 135.4, 120.0, 113.7, 113.3, 56.02, 52.03, 5.2.

The iodide **14** without any purification was dissolved in toluene (20 mL) at rt. Triisopropyl phosphite (5.5 g, 26.2 mmol) was added and the reaction mixture refluxed

for 24 h. The solution was concentrated to ~ 2 mL and then treated with 50 mL hexane. The mixture was kept at –20 °C and the white crystals formed were filtered off to get the phosphonate intermediate **15** (0.39 g, 23%): ^{1}H NMR (CDCl$_3$) δ 1.17 (d, J= 6 Hz, 6H), 1.27 (d, J= 6 Hz, 6H), 3.77 (d, J= 23 Hz, 2H), 3.89 (s, 3H), 3.91 (s, 3H), 3.93 (s, 3H), 4.61 (m, 2H), 6.95 (d, J= 2.4 Hz, 1H), 7.46 (s, 1H); ^{13}C NMR (CDCl$_3$) δ 167.2, 151.3, 146.9, 127.8, 121.6, 114.3, 113.2, 70.2 (d, J= 7.0 Hz), 55.8, 51.7, 31.4 (d, J= 138 Hz), 24.0, 23.8, 23.7, 23.6. Anal. Calcd for C$_{17}$H$_{27}$O$_7$P: C, 54.54; H, 7.27. Found: C, 54.40; H, 7.34.

Protocatechuic phosphonate 4. A solution of protected phosphonate **15** (0.39 g, 1.04 mmol) in dry CH$_2$Cl$_2$ (10 mL) was cooled to –78 °C and treated with BBr$_3$ (9.5 g, 38.1 mmol). The reaction was allowed to warm to rt and stirred for 12 h. The reaction mixture was cooled to 0 °C and slowly treated with conc. HCl (10 mL). After stirring for 1 h at rt CHCl$_3$ (20 mL) was added, and the aqueous layer separated out and concentrated to dryness. The residue was dissolved in water, neutralized to pH 7.5 and loaded onto a DEAE-52 cellulose anion exchange column (25 mL). Washed the column with 50 mL water followed by 250 mL of 200 mM Et$_3$NH$^+$HCO$_3^-$ (pH 7.5). The fractions containing phosphorous were identified by the methods of Avila and Ames and the buffer removed by azeotropic distillation of three additions of 2-propanol. The resulting white residue was dissolved in water and passed down a short column of Dowex 50 (H$^+$). The filtrate was concentrated to get protocatechuic phosphonate **4** (0.161 g, 62%): ^{1}H NMR (D$_2$O) δ 3.5 (d, J= 22 Hz, 2H), 6.85 (s, 1H), 7.38 (s, 1H); ^{13}C NMR (D$_2$O) δ 174.4, 150.8, 145.1, 130.9 (d, J= 10 Hz), 124.8 (d, J= 6 Hz), 121.9, 121.4, 34.9 (d, J= 130 Hz); HRMS (FAB) calcd for C$_8$H$_8$PO$_7$ 247.0008, found 246.9998.

Homophosphonate Intermediate 16. A solution of *n*-BuLi in hexane (1.6M, 6 mL, 8.9 mmol) was added to a solution of tetraisopropyl methylenediphosphonate (2.9 g, 8.9 mmol) in dry THF (20 mL) at –78 °C. The mixture was stirred for 10 min and a solution of the formyl ester **13** (2 g, 8.9 mmol) was added via cannula. The reaction was stirred at –78 °C for 10 min and then at rt for 12 h. Saturated aqueous NH_4Cl and EtOAc were added, the aqueous layer extracted with EtOAc (2x) and the combined organic layers dried and concentrated. Recrystallization from EtOAc/hexane afforded white crystals of the homophosphonate intermediate **16** (1.17 g, 34%): ^1H NMR ($CDCl_3$) δ 1.38 (s, 12H), 3.91 (s, 3H), 3.95 (s, 3H), 3.96 (s, 3H), 4.76 (m, 2H), 6.12 (dd, J= 17, 18 Hz), 7.03 (s, 1H), 7.46 (s, 1H), 8.23 (dd, J= 17, 22 Hz, 1H); ^{13}C NMR ($CDCl_3$) δ 166.6, 151.8, 149.3, 146.0 (d, J= 8 Hz, 1H), 131.0 (d, J= 25 Hz), 122.0, 117.2 (d, J= 191 Hz), 112.8, 109.3, 70.6 (d, J= 6 Hz), 70.5, 56.0, 52.1, 24.1, 24.0, 23.9, 23.8. Anal. Calcd for $C_{18}H_{27}O_7P$: C, 55.95; H, 7.05. Found: C, 55.40; H, 6.83.

Homophosphonate Intermediate 17. Ethenyl phosphonate **16** (0.5 g, 1.3 mmol) was dissolved in MeOH (20 mL) and hydrogenated over 10% Pd over C (0.25 g) at 50 psi H_2 pressure for 12 h. The mixture was filtered through celite, and the filtrate concentrated in vacuo. Homophosphonate intermediate **17** was obtained as white crystals (0.376 g, 76%): ^1H NMR ($CDCl_3$) δ 1.34 (s, 12H), 2.06 (m, 2H), 3.20 (m, 2H), 3.89 (s, 3H), 3.91 (s, 3H), 3.93 (s, 3H), 4.72 (m, 2H), 6.78 (s, 1H), 7.48 (s, 1H); ^{13}C NMR ($CDCl_3$) δ 166.9, 151.9, 146.8, 137.7 (d, J= 18 Hz), 120.4, 113.5, 113.4, 69.9 (d, J= 6 Hz), 28.8 (d, J= 123 Hz), 27.8 (d, J= 11 Hz), 23.9. Anal. Calcd for $C_{18}H_{29}O_7P$: C, 55.66; H, 7.53. Found: C, 55.03; H, 7.50.

Protocatechuic homophosphonate 5. Homophosphonate intermediate **17** (0.466 g, 1.2 mmol) was deprotected and purified as described for phosphonate intermediate **15** to afford protocatechuic homophosphonate **5** as a white powder (0.277 g, 88%): ^{1}H NMR (D$_2$O) δ 2.00 (m, 2H), 3.02 (m, 2H), 6.76 (s, 1H), 7.37 (s, 1H); ^{13}C NMR (D$_2$O) δ 172.9, 151.3, 144.7, 140.3 (d, J= 19 Hz), 122.3, 121.7, 120.6, 31.1 (d, J= 131 Hz), 29.9; HRMS (FAB) calcd for C$_9$H$_{10}$PO$_7$ 261.0164, found 261.0158.

Synthesis of catechol homophosphonate 6

Catechol Homophosphonate Intermediate 19. A solution of tetraisopropyl methylenediphosphonate in dry THF was cooled to −78 °C and treated with n-BuLi in hexane (1.6M, 37 mL, 54.2 mmol). The mixture was stirred for10 min and a solution of 2,3-dimethoxy benzaldehyde **18** (9 g, 54.2 mmol) in dry THF was added via cannula. The reaction mixture was stirred at −78 °C for 10 min and then at rt for 18 h. The reaction was by addition of cold water and the product extracted out with EtOAc (3x). The combined organic layers were dried and concentrated to get a colorless oil. Purification by flash chromatography (hexane, EtOAc/hexane, 1:2, 1:1 v/v) gave catechol homophosphonate intermediate **19** as a colorless oil (11.8 g, 95%): ^{1}H NMR (CDCl$_3$) δ 1.33 (s, 3H), 1.35 (s, 3H), 1.37 (s, 3H), 1.39 (s, 3H), 3.86 (s, 3H), 3.87 (s, 3H), 4.72 (m, 2H), 6.35 (dd, J= 18, 19 Hz, 1H), 6.93 (dd, J= 2, 8Hz, 1H), 7.06 (dd, J= 8, 8 Hz, 1H), 7.13 (dd, J= 2, 8 Hz, 1H), 7.78 (dd, J= 18, 23 Hz, 1H); ^{13}C NMR (CDCl$_3$) δ 153.0, 148.0, 142.1 (d, J= 8 Hz), 129.1 (d, J= 23 Hz), 124.0, 118.8, 117.1 (d, J= 190 Hz), 113.5, 70.3

(d, J= 6 Hz), 61.1, 55.8, 24.1, 24.0, 23.9, 23.8. Anal. Calcd for $C_{16}H_{25}O_5P$: C, 58.53; H, 7.68. Found: C, 57.91; H, 7.70.

Catechol Homophosphonate Intermediate 20. A solution of catechol homophosphonate intermediate **19** (0.87 g, 2.7 mmol) was hydrogenated over 10% Pd over C (0.5 g) at 50 psi H_2 pressure for 12 h. The reaction mixture was filtered through celite and the filtrate concentrated in vacuo. Purification by radial chromatography (2 mm thickness, hexane, EtOAc/hexane 1:2, 1:1 v/v) afforded catechol homophosphonate intermediate **20** as a colorless oil (0.66 g, 75%): ^{1}H NMR (CDCl₃) δ 1.32 (s, 3H), 1.33 (s, 3H), 1.34 (s, 3H), 1.35 (s, 3H), 2.01 (m, 2H), 2.90 (m, 2H), 3.84 (s, 3H) 3.85 (s, 3H), 4.72 (m, 2H), 6.79 (m, 2H), 6.99 (dd, J= 8, 8 Hz, 1H); ^{13}C NMR (CDCl₃) δ 152.6, 146.9, 135.0 (d, J= 18 Hz), 123.9, 121.4, 110.6, 69.9 (d, J= 6 Hz), 60.5, 55.6, 27.9 (d, J= 138 Hz), 23.9, 23.6 (d, J= 4 Hz). Anal. Calcd for $C_{16}H_{27}O_5P$: C, 58.17; H, 8.24. Found: C, 57.56; H, 8.24.

Catechol Homophosphonate 6. Catechol homophosphonate intermediate **20** was deprotected and purified in exactly the same manner as described for phosphonate intermediate **15** to yield catechol homophosphonate **6** as a brown oil (0.643 g, 97%). ^{1}H NMR (D₂O) δ 2.10 (m, 2 H), 2.90 (m, 2H), 6.82 (m, 3H); ^{13}C NMR δ 147.2, 144.6, 132.2 (d, J= 17 Hz), 123.8 (d, J= 27 Hz), 117.0, 29.5 (d, J= 132 Hz), 25.768; HRMS (FAB) calcd for $C_8H_{12}PO_5$ 219.0422, found 219.0416.

Enzyme Kinetics

Determination of Inhibition Constants (K_i) for Inhibitors of DHQ synthase

DHQ synthase activity was assayed in a 1.0 mL solution of 3-(N-morpholino)propanesulfonate (MOPS) buffer (50 mM, pH 7.5) containing either 50 μM CoCl$_2$ or 75 μM ZnSO$_4$ depending on the form of enzyme being studied, NAD$^+$ (10 μM), DHQ dehydratase (1 unit), and varying concentrations of DAHP and inhibitor. After equilibration at rt, purified DHQ synthase (0.024 units) was added, and the increase in absorbance at 234 nM was monitored over time. Initial rates were determined by linear square fits of the progress curves and were used to determine inhibition constants.

CHAPTER 3

Strain Constructions

Strain SP1.1

Construction of SP1.1 began with the homologous recombination of the *aroB* gene into the *serA* locus of *E. coli* RB791 resulting in RB791 *serA::aroB*. Construction of plasmid pKL3.82A which was used for the homologous recombination was described previously.[48] The procedure used for the homologous recombination was based on methods described elsewhere.[48,95b] Competent *E. coli* RB791 was transformed with pKL3.82A and plated out onto LB plates containing Cm. Colonies were observed after incubation of the plates at 44 °C for 12 h. The resulting cointegrates were inoculated into 5 mL LB and grown at 30 °C for 12 h to allow excision of the plasmid from the genome. Cultures were diluted (1:20,000) in LB and two more growth cycles were performed at 30 °C for 12 h to enrich the cultures for more rapidly growing cells that had lost the

temperature-sensitive replicon. Cultures were then diluted (1:20,000) into LB and grown at 44 °C for 12 h to promote plasmid loss from the cells. Serial dilutions of each culture were spread onto LB plates and incubated at 30 °C for 12 h. The resulting colonies were screened on multiple plates to select the desired recombination product. RB791 *serA::aroB* was isolated based on the following growth characteristics: growth on M9 containing serine; no growth on M9; growth on LB; and no growth on LB containing Cm.

RB791 *serA::aroB* was then subjected to two successive P1 phage-mediated transductions to transfer the *aroL478*::Tn*10* and *aroK*::Cm^R loci of ALO807 onto the genome and eliminating shikimate kinase activity. P1 phage was propagated from *E. coli*. ALO807, which was generously provided by Professor M. G. Marinus.[11] Transductions were carried out using protocols described by Miller.[117] RB791 *serA::aroB* *aroL*::Tn*10* *aroK*::Cm^R was selected based on the following growth characteristics: growth on M9 containing aromatic amino acids, aromatic vitamins and serine; no growth on M9 containing aromatic amino acids and aromatic vitamins; no growth on M9 containing serine; and growth on LB containing Tc and Cm. RB791 *serA::aroB* *aroL*::Tn*10* *aroK*::Cm^R was renamed SP1.1.

Strain EB1.1

Construction of EB1.1 followed the same protocols as used for the generation of SP1.1 except that *E. coli* B (ATCC11303) was used as the starting strain instead of the *E. coli* K12 strain RB791.

Strain SP1.1*pts*

Strain SP1.1 was subjected to P1 phage mediated transduction to transfer the

$\Delta(ptsHptsIcrr)$::Kan^R locus of TP2811 onto the SP1.1 genome. P1 phage was propagated

from TP2811, which was generously provided by Professor Sophie Lévy.[94]

Transductions were carried out using protocols described by Miller.[117] Following the

transduction, cells were plated out onto LB medium containing only Kan, since no

colonies were obtained when transductions were plated out onto LB medium containing

Kan, Tc, and Cm. Colonies growing on the Kan plates were subsequently screened for

resistance to Tc and Cm. SP1.1*pts* possessed the following growth characteristics:

growth on LB containing Tc. Cm and Kan; no growth on M9 containing aromatic amino

acids, aromatic vitamins, and serine; and light pink colonies on MacConkey agar

supplemented with 1% glucose. One candidate possessing these growth characteristics

was made competent. Transformation of the candidate with pSC5.112B afforded

colonies, which were incapable of growth on M9 medium containing aromatic amino

acids, aromatic vitamins, and serine, while transformation of the candidate with

pSC6.090B afforded colonies which grew on M9 medium containing aromatic amino

acids, aromatic vitamins, and serine.

Plasmid pKD12.036A

Construction of this 4.8-kb plasmid started with the PCR amplification of the

P$_{tac}$*aroE* fragment from pIA321,[98] followed by digestion of the PCR product with *Kpn*I.

Plasmid pKL4.20B was linearized by treatment with *Kpn*I and the two DNA fragments

were ligated to generate pKD12.036A. Orientation of the $P_{tac}aroE$ locus was in the opposite direction to that of the $aroF^{FBR}$ gene.

Plasmid pKD12.047A

This 6.7-kb plasmid was constructed by ligation of the *serA* gene into pKD12.036A. The *serA* locus was excised from pD2625[95b] by digestion with *Sma*I and subsequently treated with Klenow fragment. Plasmid pKD12.047A was digested with *Sma*I and treated with Klenow fragment. Ligation of the purified fragments resulted in pKD12.047A in which the *serA* gene is transcribed in the same orientation as $P_{tac}aroE$.

Plasmid pKD12.112A

This 7.7-kb plasmid was created by insertion of the *β-lac* gene into pKD12.047A. PCR amplification of the *β-lac* gene was accomplished from pUC18 followed by digestion of the 1.0-kb fragment with *Nco*I. Plasmid pKD12.047A was linearized by digestion with *Nco*I and the two DNA fragments were ligated to afford pKD12.112A.

Plasmid pKD12.138A

This 9.9-kb plasmid was constructed by inserting the 2.2-kb *tktA* fragment from pMF51A[72a] into pKD12.112A. Digestion of pMF51A with *Bam*HI followed by treatment with Klenow fragment yielded the *tktA* gene with blunt ends. Plasmid pKD12.112A was linearized with *Hind*III and treated with Klenow fragment. Subsequent ligation of the *tktA* fragment to pKD12.112A resulted in pKD12.138A. The *tktA* gene is transcribed in the same orientation as the *serA* gene.

Plasmid pKD15.071B

This 11.9-kb plasmid was assembled by replacing the 1.0-kb *β-lac* gene of pKD12.138A with the *pps* fragment from pKL1.87B.[99] Plasmid pKL1.87B was digested with *Bam*HI and *Hind*III and the resulting 3.0-kb *pps* fragment was treated with Klenow fragment. Following digestion of pKD12.138A with *Nco*I, the 8.9-kb fragment was modified to blunt ends using Klenow fragment. Ligation of these two purified fragments yielded pKD15.071A. The *pps* gene is transcribed in the opposite orientation relative to the *tktA* gene.

Plasmid pSC5.112B

This 11.1-kb plasmid was created by replacing the 1.0-kb *β-lac* gene of pKD12.138A with the *glf* fragment from pTC325.[73c,d] A 2.2-kb fragment containing the *glf* locus behind P$_{tac}$ was excised from pTC325 by digestion with *Bam*HI, *Hind*III and *Xba*I followed by treatment with Klenow fragment. Plasmid pKD12.138A was digested with *Nco*I and the resulting 8.9-kb fragment was treated with Klenow fragment. The two purified fragments were ligated to generate pSC5.112B. The P$_{tac}$*glf* gene is transcribed in the opposite orientation relative to *tktA*.

Plasmid pSC6.090B

This 12.8-kb plasmid was constructed by ligation of the P$_{tac}$*glfglk* cassette into pKD12.138A. The P$_{tac}$*glfglk* cassette was excised from pTC325 by digestion with *Bam*HI and *Xba*I and subsequently treated with Klenow fragment. Plasmid pKD12.138A was digested with *Nco*I and the 8.9-kb fragment was treated with Klenow fragment.

Ligation of the purified fragments resulted in pSC6.090B in which the $P_{tac}glfglk$ cassette is transcribed in the same orientation as the *tktA* gene.

Plasmid pSC6.142B

This 7.5-kb plasmid was assembled by inserting the *glf* gene into pKL1.87A. Plasmid pTC325 was digested with *Bam*HI, *Hind*III and *Xba*I and the resulting 2.2-kb $P_{tac}glf$ fragment was treated with Klenow fragment. Plasmid pKL1.87A was linearized by digestion with *Sal*I subsequently treated with Klenow fragment. Ligation of the $P_{tac}glf$ fragment into pKL1.87A afforded pSC6.142B in which the $P_{tac}glf$ gene is transcribed in the opposite orientation relative to the *pps* gene.

Plasmid pSC6.162A

This 14.1-kb plasmid was constructed by inserting the 5.2-kb $ppsP_{tac}glf$ cassette from pSC6.142B into pKD12.138A. Plasmid pSC6.142B was digested with *Bam*HI and *Hind*III to liberate the $ppsP_{tac}glf$ fragment, which was then treated with Klenow fragment. The 1.0-kb *β-lac* gene was excised from pKD12.138A by digestion with *Nco*I and the resulting 8.9-kb fragment was treated with Klenow fragment. Ligation of the two purified DNA fragments afforded pSC6.162A. The $P_{tac}glf$ fragment was transcribed in the same orientation and the *pps* gene in the opposite orientation relative to the *tktA* gene.

Plasmid pSC6.301A

This 15.8-kb plasmid was created by inserting the *pps* gene into pSC6.090B. Plasmid pKL1.87B was digested with *Bam*HI and *Hind*III and the resulting 3.0-kb *pps* fragment was treated with Klenow fragment. Plasmid pSC6.090B was linearized by digestion with *Xba*I and then treated with Klenow fragment. Ligation of the *pps* fragment into pSC6.090B afforded pSC6.301A. The *pps* gene is transcribed in the same orientation relative to the *tktA* gene.

CHAPTER 4

Strains Constructions

Strain SC1.0

Construction of SC1.0 started with the P1 phage-mediated transductions of *aroL478*::Tn*10* and *aroK*::Cm^R into JWF1 thereby knocking out the *aroL* and *aroK* encoded isozymes of shikimate kinase. This strain was designated as SC1.1 and it was selected based on the following growth characteristics: growth on M9 containing aromatic amino acids, aromatic vitamins and serine; no growth on M9 containing aromatic amino acids and aromatic vitamins; no growth on M9 containing serine, and growth on LB containing Tc and Cm.

The construction of SC1.0 was completed by the P1 phage-mediated transduction of *aroB*::Tn*5* into SC1.1. P1 phage was propagated from JB5, which was already available in the Frost laboratory.[95b] Selection of SC1.0 was based on the following growth characteristics: growth on M9 containing aromatic amino acids, aromatic vitamins, and serine; no growth on M9 containing aromatic amino acids and aromatic

vitamins; no growth on M9 containing serine and; growth on LB containing Tc and Cm, Kan

Strain SP1.1shiA

E. coli SP1.1shiA was constructed by transduction of the *shiA*::Kan^R locus from JP11123 into SP1.1. The preparation of strain JP11123 has been previously reported by Pittard and co-workers.[111] Transduction of the *shiA*::Kan^R locus via P1 phage from JP11123 into SP1.1 followed the procedure described by Miller.[117] Following the transduction, cells were spread onto LB plates containing Kan. Plates were incubated at 37 °C for 16 h before colonies appeared. SP1.1shiA was identified based on growth on LB plates containing Tc, Cm, and Kan.

Plasmid pSC5.214A

Plasmid pSC5.214A was constructed via disruption of the *aroF*^{FBR} gene in plasmid pKD12.138A. This was achieved by utilizing the unique *Bgl*II restriction site present at 0.623-kb within *aroF*^{FBR}. Plasmid pKD12.138A was linearized by digestion with *Bgl*II followed by treatment with Klenow fragment. Subsequent ligation afforded the 9.9-kb plasmid pSC5.214A.

BIBLIOGRAPHY

[1]   Srinivasan, P. R.; Rothchschild, J.; Sprinson, D. B. *J. Biol. Chem.* **1963**, *238*, 3176.

[2]   Frey, P. A. In *Pyridine Nucleotide Coenzymes*; Wiley: New York, 1987; part B, Chapter 13.

[3]   Loewus, F. A.; Kelly, S. *Biochem. Biophys. Res. Commun.* **1962**, *7*, 204.

[4]   Palmer, J. L.; Abeles, R. H. *J. Biol. Chem.* **1976**, *251*, 5817.

[5]   Duerre, J. A.; Walker, R. D. In *The Biochemistry of Adenosylmethionine*; Salvatore, F.; Borek, E.; Zappia, V.; Williams-Ashman, H.; Schlenk, F., Eds.; Columbia: New York, 1977; p 43.

[6]   Maxwell, E. S. *J. Biol. Chem.* **1957**, *229*, 139.

[7]   (a) Haslam, E. *The Shikimate Pathway*; John Wiley and Sons: New York, 1974. (b) Bentley, R. *Crit. Rev. Biochem. Mol. Biol.* **1990**, *25*, 307. (c) Herrman, K. M. In *Amino Acids: Biosynthesis and Genetic Regulation*; Herrmann, K. M.; Somerville, R. L., Eds.; Addison-Wesley: Reading, 1983: p. 301.

[8]   (a) Haslem, E.; Smith, B. W.; Turner, M. J. *J. Chem. Soc., Perkin Trans. 1* **1995**, 52. (b) Duncan, K.; Chaudhuri, S.; Campbell, M. S.; Coggins, J. R. *Biochem. J.* **1986**, *238*, 475.

[9]   (a) Anton, I. A.; Cogins, J. R. *Biochem. J.* **1988**, *249*, 319. (d) Chaudhuri, S.; Coggins, J. R. *Biochem. J.* **1985**, *226*, 217.

[10]   (a) Defeyter, R. C.; Pittard, J. *J. Bacteriol.* **1986**, *165*, 226. (b) Defeyter, R. C.; Pittard, J. *J. Bacteriol.* **1986**, *165*, 231. (c) Defeyter, R. C.; Pittard, J. *J. Bacteriol.* **1986**, *165*, 233.

[11]   Løbner-Olesen, A.; Marinus, M. G. *J. Bacteriol.* **1992**, *174*, 525.

[12]   Duncan, K.; Coggins, J. R. *Biochem. J.* **1986**, *234*, 49. (b) Duncan, K.; Lewendon, A.; Coggins, J. R. *FEBS Lett.* **1984**, *165*, 121.

[13]   White, P. J.; Millar, G.; Coggins, J. R. *Biochem. J.* **1988**, *251*, 313.

[14]   (a) Callaghan, D.; Maskell, D.; Liew, F. Y.; Easmon, C. S. F.; Dougan, G. *Infect. Immun.* **1988**, *56*, 419. (b) Dougan G.; Chatfield, S.; Pickard, D.; Bester, J.; O'Callaghan, D.; Maskell, D. *J. Infect. Dis.* **1988**, *158*, 1329. (c) Miller, I.; Maskell, D.; Hormaeche, C.; Johnson, K.; Pickard, D.; Dougan, G. *Infect. Immun.* **1989**, *57*, 2758.

[15]   Gunel-Ozcan, A.; Brown, K. A.; Allen, A. G.; Maskell, D. J. *Microbial Pathogen.* **1997**, *23*, 311.

[16]   (a) Miller, I. A.; Chatfield, S.; Dougan, G.; Desilva, L.; Joysey, H. S.; Hormaeche, C. *Mol. Gen. Genet.* **1989**, *215*, 312. (b) Hoiseth, S. K.; Stocker, B. A. *Nature* **1981**, *291*, 38. (c) Maskell, D. J.; Sweeney, K. J.; O'Callaghan, D.; Hormaeche, C. E.; Liew, F. Y.; Dougan, C. *Microbial Pathogen.* **1987**, *2*, 211.

[17]   (a) Davies, G. M.; Barrett-Bee, K. J.; Jude, D. A.; Lehan, M.; Nichols, W. W.; Pinder, P. E.; Thain, J. L.; Watkins, W. J.; Wison, R. G. *Antimicrob. Agents Chemother.* **1994**, *38*, 403. (b) Ewart, C. D. C.; Jude, D. A.; Thain, J. L.; Nichols, W. W. *Antimicrob. Agents Chemother.* **1995**, *39*, 87.

[18]   (a) Grossbard, E.; Alkinson, D., Eds.; *The Herbicide Glyphosate*; Butterworths: Boston, 1985. (b) Devine, M. E.; Duke, S. O.; Fedlke, C. F. In *Physiology of Herbicide Action*; Prentice Hall: New Jersey, 1993; Chapter 13. (c) Franz, J. E.; Mao, M. K.; Sikorski, J. A. In *Glyphosate: An Extraordinary Global Herbicide*; American Chemical Society Monograph, Washington, DC, 1996.

[19]   Roberts, F.; Roberts, C. W.; Johnson, J. J.; Kyle, D. E.; Krell, T.; Coggins, J. R.; Coombs, G.; Milhous, W.; Tzipori, D. V. M.; Ferguson, D.; Chakrabarti, D.; McLeod, R. *Nature* **1998**, *393*, 801.

[20]   (a) Bender, S. L.; Mehdi, S.; Knowles, J. R. *Biochemistry* **1989**, *28*, 7555. (b) Rotenberg, S. L.; Sprinson, D. D. *J. Biol. Chem.* **1978**, *253*, 2210. (c) LeMarechal, P.; Azerad, R. *Biochimie* **1976**, *58*, 1123. (d) Maitra, U. S.; Sprinson, D. B. *J. Biol. Chem.* **1978**, *253*, 5426. (e) Bender, S. L.; Widlanski, T.; Knowles, J. R. *Biochemistry* **1989**, *28*, 7560. (f) Widlanski, T.; Bender, S. L.; Knowles, J. R. *Biochemistry* **1989**, *28*, 7572.

[21]   (a) Widlanski, T.; Bender, S. L.; Knowles, J. R. *J. Am. Chem. Soc.* **1987**, *109*, 1873. (b) Widlanski, T.; Bender, S. L.; Knowles, J. R. *J. Am. Chem. Soc.* **1989**, *111*, 2299. (c) Montchamp, J.-L.; Peng, J.; Frost, J. W. *J. Org. Chem.* **1994**, *59*, 6999. (d) Bartlett, P. A.; Satake, K. *J. Am. Chem. Soc.* **1988**, *110*, 1628.

[22]   (a) Bartlett, P. A.; McLaren, K. L.; Marx, M. A. *J. Org. Chem.* **1994**, *59*, 2082. (b) Parker, E. J.; Coggins, J. R.; Abell, C. *J. Org. Chem.* **1997**, *62*, 8582. (c) Montchamp, J.-L.; Frost, J. W. *J. Am. Chem. Soc.* **1997**, *119*, 7645.

[23]   Carpenter, E. P.; Hawkins, A. R.; Frost, J. W.; Brown, K. A. *Nature* **1998**, *394*, 299.

[24]   Weissermel, K.; Arpe, H. J., Eds.; *Industrial Organic Chemicals*; BCH: New York, 1997; p 303.

[25]   (a) Yamada, H.; Ryuno, K.; Nagasawa, T.; Enomoto, K.; Watanabe, I. *Agric. Biol. Chem.* **1986**, *50*, 2859. (b) Nagasawa, T.; Ryuno, K.; Yamada, H. *Experientia*, **1989**, *45*, 1066.

[26]   (a) Raber, L. R. *Chem. Eng. News* **1998**, *76*, 25. (b) Datta, R.; Tsai, S. P.; Bonsignore, P.; Moon, S. H.; Frank, J. R. *FEMS Microbiol. Rev.* **1995**, *16*, 221. (c) Kascak, J. S.; Kominek, J.; Roehr, M. In *Biotechnology*; Rehm, H. J.; Reed, G..; Puhler, A.; Stadler, P., Ed.; VCH: Weinheim, 1996, p. 293.

[27]   Weissermel, K.; Arpe, H. J., Eds.; *Industrial Organic Chemicals*; BCH: New York, 1997; p 309.

[28]   Skory, C. D. *Appl. Environ. Microbiol.* **2000**, *66*, 2343.

[29]   Eggeling, L.; Sahm, H. *Appl. Microbiol. Biotech.* **1999**, *52*, 146.

[30]   (a) Thayer, A. M. *Chem. Eng. News* **1991**, *69*, 9. (b) Oyama, K.; Irino, S.; Hagi, N. *Methods Enzymol.* **1987**, *136*, 503.

[31]   Hodgson, J. *Biotechnology* **1994**, *12*, 152.

[32]   della-Cioppa, G.; Garger, S. J.; Sverlow, G. G.; Turpen, T. H.; Grill, L. K. *Biotechnology* **1990**, *8*, 634.

[33]   Murdock, D.; Ensley, B. D.; Serdar, C.; Thalen, M. *Biotechnology* **1993**, *11*, 381.

[34]   (a) Farris, R. E. In *Kirk-Othmer Encycolpedia of Chemical Technology*, 3rd ed.; Grayson, M., Eds.; Wiley: New York, 1979; Vol. 8, p 364. (b) Szmant, H. H. In *Organic Building Blocks of the Chemical Industry*; Wiley: New York, 1989; p 585.

[35]   Clark, G. S. *Perfum. Flavor.* **1990**, *15*, 45.

[36]   (a) Esposito, L.; Formanek, K.; Kientz, G.; Mauger, F.; Maureaux, V.; Robert, G.; Truchet, F. In *Kirk-Othmer Encycolpedia of Chemical Technology*, 4th ed.; Kroschwitz, J. I.; Howe-Frant, M., Eds.; Wiley: New York, 1997; Vol. 24, p 812. (b) van Ness, J. H. In *Kirk-Othmer Encycolpedia of Chemical Technology*, 3rd ed.; Grayson, M., Ed.; Wiley: New York, 1983; Vol. 23, p 704.

[37]   Li, K.; Frost, J. W. *J. Am. Chem. Soc.* **1998**, *120*, 10545.

[38]   (a) Kirsch, M. A.; Williams, D. J. *CHEMTECH* **1994**, *24*, 40. (b) Szmant, H. H. In *Organic Building Blocks of the Chemical Industry*; Wiley: New York, 1989; p 467.

[39]   Siebert, M.; Berchthold, A.; Melxer, M.; May, U.; Berger, U. *FEBS Lett.* **1992**, *307*, 347.

[40]   Barker, J. L.; Frost, J. W. Unpublished results.

[41]   Szmant, H. H. In *Organic Building Blocks of the Chemical Industry*; Wiley: New York, 1989; p 465.

[42]   (a) Goncharoff, P.; Nichols, B. P. *J. Bacteriol.* **1984**, *159*, 57. (b) Green, J. M.; Merkel, W. K.; Nichols, B. P. *J. Bacteriol.* **1992**, *174*, 5317. (c) Kaplan, J. B.; Nicols, B. P. *J. Mol. Biol.* **1983**, *168*, 451.

[43]   (a) Draths, K. M.; Ward, T. L.; Frost, J. W. *J. Am. Chem. Soc.* **1992**, *114*, 9725. (b) Hanessian, S.; Beaulieu, P.; Dube, D. *Tetrahedron Lett.* **1986**, *27*, 2332. (c) Flack, J. R.; Yadagiri, P. *J. Org. Chem.* **1989**, *54*, 5851. (d) Molin, H.; Pring, B. G. *Tetrahedron Lett.* **1985**, *26*, 677.

[44]   Knop, D. R.; Frost, J. W. Unpublished result.

[45]   (a) Krumenacker, L.; Constantini, M.; Pontal, P.; Sentrnac, J. In *Kirk-Othmer Encycolpedia of Chemical Technology*, 4th ed.; Kroschwitz, J. I.; Howe-Frant, M., Eds.; Wiley: New York, 1995; Vol. 13, p 996. (b) Shearson, W. H.; Davy, L. G.; von Bramer, H. *Ind. Eng. Chem.* **1952**, *44*, 1730. (c) Varagnat, J. In *Kirk-Othmer Encycolpedia of Chemical Technology*, 3rd ed.; Grayson, M., Ed.; Wiley: New York, 1981; Vol. 13, p 39. (d) Finley, K. T. In *Kirk-Othmer Encycolpedia of Chemical Technology*, 3rd ed.; Grayson, M., Ed.; Wiley: New York, 1982; Vol. 19, p 572. (e) Szmant, H. H. In *Organic Building Blocks of the Chemical Industry*; Wiley: New York, 1989; p 512.

[46]   Varagnat, J. In *Kirk-Othmer Encycolpedia of Chemical Technology*, 3rd ed.; Grayson, M., Ed.; Wiley: New York, 1981; Vol. 13, p 47.

[47] Ningqing, R.; Frost, J. W. Unpublished result.

[48]   Li, K.; Mikola, M. R.; Draths, K. M.; Worden, R. M.; Frost, J. W. *Biotechnol. Bioeng.* **1999**, *64*, 61.

[49]   Richman, J. E.; Chang, Y.-C.; Kambourakis, S.; Draths, K. M.; Almy, E.; Snell, K. D.; Strasburg, G. M.; Frost, J. W. *J. Am. Chem. Soc.* **1996**, *118*, 11587.

[50]   Yi, J.; Frost, J. W. Unpublished result.

[51]   Leston, G. In *Kirk-Othmer Encycolpedia of Chemical Technology*, 4th ed.; Kroschwitz, J. I.; Howe-Frant, M., Eds.; Wiley: New York, 1996; Vol. 19, p 778.

[52]   Szmant, H. H. In *Organic Building Blocks of the Chemical Industry*; Wiley: New York, 1989; p 519.

[53]   Kambourakis, S.; Draths, K. M.; Frost, J. W. *J. Am. Chem. Soc.* **2000**, *122*, 9042.

[54] (a) Entsch, B.; Palfey, B. A.; Ballou, D. P.; Massey, J. Biol. Chem. **1991**, 266, 17341. (b) Eschrich, K.; van der Bolt, F. J. T.; de Kok, A.; van Berkel, W. J. H. Eur. J. Biochem. **1993**, 216, 137.

[55] Kambourakis, S.; Frost, J. W. Unpublished result.

[56] (a) Draths, K. M.; Frost, J. W. J. Am. Chem. Soc. **1994**, 116, 399. (b) Draths, K. M.; Frost, J. W. J. Am. Chem. Soc. **1995**, 117, 2395.

[57] Franck, H.-G.; Stadelhofer, J. W. Industrial Aromatic Chemistry; Springer-Verlag: New York, 1988; p 183.

[58] (a) Davis, D. D.; Kemp, D. R. In Kirk-Othmer Encycolpedia of Chemical Technology, 4th ed.; Kroschwitz, J. I.; Howe-Frant, M., Eds.; Wiley: New York, 1991, Vol. 1, p 466. (b) Thiemens, M. H.; Trogler, W. C. Science **1991**, 251, 932.

[59] Dickinson, R. E.; Cicerone, R. J. Nature **1986**, 319, 109.

[60] Neidle, E. L.; Ornston, L. N. J. Bacteriol. **1986**, 168, 815.

[61] (a) Draths, K. M.; Pompliano, D. L.; Conley, D. L.; Frost, J. W.; Berry, A.; Disbrow, G. L.; Staversky, R. J.; Lievense, J. C. J. Am. Chem. Soc. **1992**, 114, 3956. (b) Gubler, M.; Jetten, M.; Lee, S. H.; Sinskey, A. J. Appl. Environ. Microbiol. **1994**, 60, 2494. (c) Miller, J. E.; Backman, K. C.; O'Connor, M. J.; Hatch, R. T. J. Ind. Microbiol. **1987**, 2, 143. (d) Patnaik, R.; Liao, J. C. Appl. Environ. Microbiol. **1994**, 60, 3903. (e) Patnaik, R.; Spitzer, R. G.; Liao, J. C. Biotechnol. Bioeng. **1995**, 46, 361.

[62] Pitard, A. J. In Escherichia coli and Salmonella Typhimurium; Neidhardt, F. C., Ed.; American Society for Microbiology: Washington, DC, 1987; Vol. 1, p 368.

[63] Takasi, O.; Garner, C.; Markley, J. L.; Herrmann, K. M. Proc. Natl. Acad. Sci. USA **1982**, 79, 5828.

[64] (a) Weaver, L. M.; Herrmann, K. M. J. Bacteriol. **1990**, 172, 6581. (b) Ray, J. M.; Yanofsky, C.; Bauerle, R. J. Bacteriol. **1988**, 170, 5500.

[65] Mikola, M. R.; Widman, M. T.; Worden, R. M. Appl. Biochem. Biotechnol. **1997**, 70, 905.

[66] Mori, M.; Yokota, A.; Sugitomo, S.; Kawamura, K. Patent JP 62,205,782, 1987.

[67] Backman, K. C. U.S. Patent 5,169,768, 1992.

[68] Draths, K. M.; Frost, J. W. J. Am. Chem. Soc. **1990**, 112, 1657.

[69]   (a) Paoletti, F.; Williams, J. F.; Horecker, B. L. *Anal. Biochem.* **1979**, *95*, 250. (b) William, J. F.; Blackmore, P. F.; Duke, C. C.; Macleod, J. F. *Int. J. Biochem.* **1980**, *12*, 339.

[70]   (a) Blackmore, P. F.; William, J. F.; Macleod, J. F. *FEBS Lett.* **1976**, *64*, 222. (b) Duke, C. C.; Macleod, J. F.; Williams, J. F. *Carbohydr Res.* 1981, 95, 1.

[71]   Postma, P. W.; Lengeler, J. W.; Jacobson, G. R. In *Escherichia coli and Salmonella Typhimurium*; Neidhardt, F. C., Ed.; American Society for Microbiology: Washington, DC, 1996; Vol. 1, p 1149.

[72]   (a) Farabaugh, M. M. S. Thesis, Michigan State University, April 1996. (b) Lu, J.-L.; Liao, J. C. *Biotechnol.* **1997**, *53*, 132.

[73]   (a) Belaich, J. P.; Senez, J.; Murgier, M. *J. Bacteriol.* **1968**, *95*, 1750. (b) DiMarco, A. A.; Romano, A. *Appl. Environ. Microbiol.* **1985**, *49*, 151. (c) Snoep, J. L.; Arfman, N.; Yomano, L. P.; Fliege, R. K.; Conway, T.; Ingram, L. O. *J. Bacteriol.* **1994**, *176*, 2133. (d) Parker, C.; Barnell, W. O.; Snoep, J. L.; Conway, T.; Ingram, L. O. *Mol. Microbiol.* **1995**, *15*, 795. (e) Weisser, P.; Kramer, R.; Sahm, H.; Sprenger, G. A. *J. Bacteriol.* **1995**, *177*, 3351.

[74]   (a) Barnell, W. O.; Yi, K. C.; Conway, T. *J. Bacteriol.* **1990**, *172*, 7227. (b)Barnell, W. O.; Liu, J.; Hesman, T. L.; O'Neill, M. C.; Conway, T. *J. Bacteriol.* **1992**, *174*, 2816.

[75]   (a) Griffith, J. K.; Baker, M. E.; Rouch, D. A.; Page, M. G. P.; Skurray, R. A.; Paulsen, I.; Chater, K. F.; Baldwin, S. A.; Henderson, P. J. F. *Curr. Opin. Cell Biol.* **1992**, *4*, 684. (b) Henderson, P. J. F.; Roberts, P. E.; Martin, G. E. M.; Seamon, K. B.; Walmsley, A. R.; Rutherford, N. G.; Varela, M. F.; Griffith, J. K. *Biochem. Soc. Trans.* **1993**, *21*, 1002. (c) Marger, M. D.; Saier, M. H. *Trends Biochem. Sci.* **1993**, *18*, 13.

[76]   Li, K.; Frost, J. W. *Biotechnol. Prog.* **1999**, *15*, 876.

[77]   Lambert, J. M.; Boocock, M. R.; Coggins, J. R. *Biochem. J.* **1985**, *226*, 817.

[78]   (a) Vallee, B. L.; Auld, A. S. *Biochemistry* **1990**, *29*, 5647. (b) Vallee, B. L.; Auld, A. S. *Acc. Chem. Res.* **1993**, *26*, 543. (c) Auld, A. S. *Struct. Bond.* **1997**, *89*, 29.

[79]   (a) Lipscomb, W. N.; Sträter, N. *Chem. Rev.* **1996**, *96*, 2375. (b) Vallee, B. L. In *Zinc Enzyme*; Spiro, T. G., Eds; John Wiley and Sons: New York, 1983; p 1. (c) Prasad, A. S. *Biochemistry of Zinc*; Plenum: New York, 1993.

[80]   (a) Ondetti, M. A.; Rubin, B.; Cushman, D. W. *Science* **1977**, *196*, 441. (b) Ondetti, M. A.; Cushman, D. W. *CRC Crit. Rev. Biochem.* **1984**, *16*, 381.

[81]   Gordon, E. M.; Godfrey, J. D.; Pluscec, J.; von Langen, D.; Natrajan, S. *Biochem. Biophys. Res. Commun.* **1985**, *126*, 419.

[82]   Tian, F.; Montchamp, J.-L.; Frost, J. W. *J. Org. Chem.* **1996**, *61*, 7373.

[83]   (a) Montchamp, J.-L.; Frost. J. W. *J. Org. Chem.* **1994**, *59*, 7596.   (b) Montchamp, J.-L.; Piehler, L. T.; Tolbert, T. J.; Frost. J. W. *Bioorg. Med. Chem. Lett.* **1993**, *3*, 1403.

[84]   Shepherd, J. A.; Poon, W. W.; Myles, D. C.; Clarke, C. F. *Tetrahedron Lett.* **1996**, *37*, 2395.

[85]   Aizpura, J. M.; Palomo, C. *Tetrahedron Lett.* **1984**, *25*, 1103.

[86]   Chaudhuri, S.; Duncan, K.; Coggins, J. R. *Methods Enzymol.* **1987**, *142*, 320.

[87]   Segel, I. H. *Biochemical Calculations*, 2nd ed.; Wiley: New York, 1976, Chapter 4.

[88]   More, J. D.; Skinner, M. A.; Swatman, D. R.; Hawkins, A. R.; Brown, K. A. *J. Am. Chem. Soc.* **1998**, *120*, 7105.

[89]   (a) Haslam, E. Shikimic Acid: Metabolism and Metabolites; Wiley: New York, 1993. (b) Pitard, A. J. In *Escherichia coli and Salmonella Typhimurium*; Neidhardt, F. C., Ed.; American Society for Microbiology: Washington, DC, 1996; Chapter 28.

[90]   Tan, D. S.; Foley, M. A.; Shair, M. D.; Schreiber, S. L. *J. Am. Chem. Soc.* **1998**, *120*, 8565.

[91]   Haslam, E. *Shikimic Acid: Metabolism and Metabolites*; Wiley: New York, 1993; p 40.

[92]   (a) Federspiel, M.; Fischer, R.; Hennig, M.; Mair, H.-J.; Oberhauser, T.; Rimmler, G.; Albiez, T.; Bruhin, J.; Estermann, H.; Gandert, C.; Göckel, V.; Götzö, S.; Hoffmann, U.; Huber, G.; Janatsch, G.; Lauper, S.; Odette, R.-S.; Trussardi, R.; Zwahlen, A. G. *Org. Process Res. Dev.* **1999**, *3*, 266. (b) Kim, C. U.; Lew, W.; Williams, M. A.; Liu, H.; Zhang, L.; Swaminathan, S.; Bischofberger, N.; Chen, M. S.; Mendel, D. B.; Tai, C. Y.; Laver, W. G.; Stevens, R. C. *J. Am. Chem. Soc.* **1997**, *119*, 681. (c) Rohloff, J. C.; Kent, K. M.; Postich, M. J.; Becker, M. W.; Chapman, H. H.; Kelly, D. E.; Lew, W.; Louie, M. S.; McGee, L. R.; Prisbe, E. J.; Schultze, L. M.; Yu, R. H.; Zhang, L. *J. Org. Chem.* **1998**, *63*, 4545.

[93]   (a) Studier, F. W.; Rosenberg, A. H.; Dunn, J.; Dubendorff, J. W. *Methods Enzymol.* **1990**, *185*, 60 (b) Studier, F. W.; Moffatt, B. A. *J. Mol. Biol.* **1986**, *113*, 189.

(c) Grodberg, J.; Dunn, J. J. *J. Bacteriol.* **1988**, *170*, 1245. (d) Neidhardt, F. C.; van Bogelen, R. A.; Phillips, T. A. *J. Bacteriol.* **1984**, *166*, 283.

[94]   Lévy, S.; Zeng, G. Q.; Danchin, A. *Gene*, **1990**, *86*, 27.

[95]   (a) Snell, K. D.; Frost, J. W. *J. Am. Chem. Soc.* **1993**, *115*, 11581. (b) Snell, K. D.; Draths, K. M.; Frost, J. W. *J. Am. Chem. Soc.* **1996**, *118*, 5605.

[96]   Tobey, K. L.; Grant, G. A. *J. Biol. Chem.* **1986**, *261*, 12179.

[97]   Bartolome, B.; Jubete, Y.; Martines, E.; de la Cruz, F. *Gene* **1991**, *102*, 75.

[98]   Anton, I. A.; Coggins, J. R. *Biochem. J.* **1988**, *249*, 319.

[99]   Li, K.; Frost, J. W. Unpublished result.

[100]   van de Walle, Michele, Shiloach, J. *Biotechnol. Bioeng.* **1998**, *57*, 71.

[101]   (a) Skjerdal, O. T.; Sletta, H.; Flenstad, S. G.; Josefsen, K. D.; Levine, D. W.; Ellingsen, T. E. *Appl. Microbiol. Biotechnol.* **1995**, *43*, 1099. (b) Skjerdal, O. T.; Sletta, H.; Flenstad, S. G.; Josefsen, K. D.; Levine, D. W.; Ellingsen, T. E. *Appl. Microbiol. Biotechnol.* **1996**, *44*, 635.

[102]   Epstein, W.; Csonka, L. N. In *Escherichia coli and Salmonella Typhimurium*; Neidhardt, F. C., Ed.; American Society for Microbiology: Washington, DC, 1996; p 1210.

[103]   Swartz, J. R. In *Escherichia coli and Salmonella Typhimurium*; Neidhardt, F. C., Ed.; American Society for Microbiology: Washington, DC, 1996; p 1699.

[104]   Draths, K. D.; Knop, D. R.; Frost, J. W. *J. Am. Chem. Soc.* **1999**, *121*, 1603.

[105]   Wallace, J. In *Kirk-Othmer Encycolpedia of Chemical Technology*, 4th ed.; Kroschwitz, J. I.; Howe-Frant, M., Eds.; Wiley: New York, 1996; Vol. 18, p 592.

[106]   Draths, K. M.; Frost, J. W. Unpublished result.

[107]   Draths, K. M.; Knop, D. R.; Frost, J. W. Unpublished result.

[108]   (a) Pittard, J.; Wallace, B. J. *J. Bacteriol.* **1966**, *92*, 1070. (b) Brown, K. D.; Doy, C. H. *Biochim. Biophys. Acta.* **1976**, *428*, 550.

[109]   (a) Postma, P. W.; Lengeler, J. W.; Jacobson, G. R. *Microbiol. Rev.* **1993**, *57*, 543. (b) Saier, M. H.; Ramseier, T. M.; Reizer, J. In *Escherichia coli and Salmonella*

Typhimurium; Neidhardt, F. C., Ed.; American Society for Microbiology: Washington, DC, 1996; p 1325.

[110]   Postma, P. W.; Lengeler, J. W.; Jacobson, G. R. *Microbiol. Rev.* **1985,** *49,* 232.

[111]   Pittard, A. J.; Camarakis, H.; Whipp, M. J. *Gene* **1998,** *209,* 185.

[112]   Frost, J. W.; Knowles, J. R. *Biochemistry* **1984,** *23,* 4465.

[113]   Frost, J. W.; Bender, J. L.; Kadonaga, J. T.; Knowles, J. R. *Biochemistry* **1984,** *23,* 4470.

[114]   (a) Ames, B. N. *Methods Enzymol.* **1966,** *8,* 115.   (b) Avila, L. Z. Ph. D. Dissertation, Stanford University, 1990.

[115]   Schoner, R.; Herrmann, K. M. *J. Biol. Chem.* **1976,** *251,* 5440.

[116]   Sambrook, J.; Fritsch, E. F.; Maniatis, T. Molecular Cloning: A Laboratory Manual; Cold Spring Harbor Laboratory: Plainview, NY, 1990.

[117]   Miller, J. H. Experiments in Molecular Genetics; Cold Spring Harbor Laboratory: Plainview, NY, 1972.